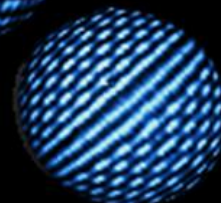
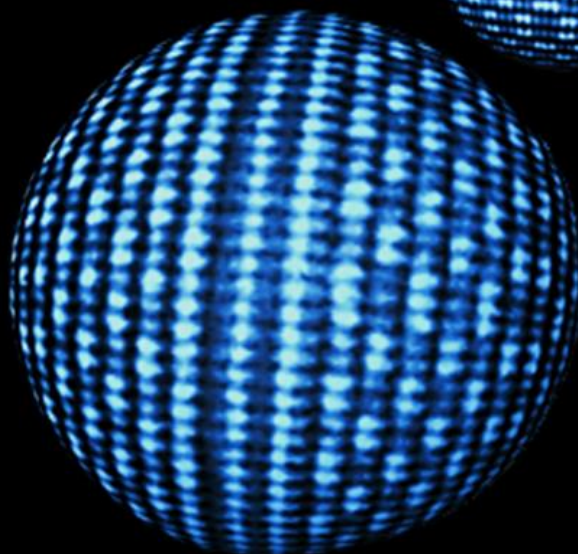
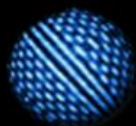


RESEARCH REPORT

Imaging and Analysis Center
PRISM



2020



iac.princeton.edu

A MESSAGE FROM THE DIRECTORS

Dear Friends of the PRISM Imaging and Analysis Center,

The PRISM Imaging and Analysis Center (IAC) offers high-end, state-of-the-art instrumentation and expertise for characterization of hard, soft, and biological materials to stimulate research and education at Princeton University and beyond. The IAC houses and operates a full range of instruments employing visible photons, electrons, ions, X-rays, and scanning probe microscopy for the physical examination and analysis of complex materials. With 25 years of continuous support from Princeton University, as well as the National Science Foundation, the Air Force Office of Scientific Research, the Office of Naval Research, the State of New Jersey, Industrial Companies, etc., the IAC has become the largest central facility at Princeton and a world-leader in advanced materials characterization.

A central mission of the IAC is the education, research, and training of students at Princeton University. The IAC supports more than ten regular courses annually. The award-winning course, MSE505-Characterization of Materials is conducted at the IAC for both graduate and undergraduate students. The IAC also offers a full range of training courses, which involve direct experimental demonstrations and hands-on instruction ranging from basic sample preparation, to the operation of high-end electron microscopes. The IAC's short courses have drawn over 3,500 student enrollments. Additionally, over 700 industrial scientists from more than 120 companies and 40 institutions have utilized instruments in the IAC. Our efforts have helped build bridges between Princeton and Industry that have fostered many innovations and new product developments.

Recent IAC internal users include over 300 students and researchers from more than 90 research groups. The IAC supports ~230 current research contracts worth a total of ~\$440M. In the IAC, undergraduate students are provided with the opportunity to operate various electron microscopes during class and later utilize these instruments in research for their senior thesis. The research experience provided by the IAC has helped students win many national awards including the Fannie and John Hertz Foundation Fellowship, Rhode Scholarship, the Barry M. Goldwater National Scholarship, Fulbright Scholarship, National Science Foundation Fellowship, etc.

In this report, we highlight many recent research projects conducted by our internal users, which were enabled by the IAC's facilities and expertise. These topics cover a wide range of scientific disciplines, reflecting the great diversity in research conducted at Princeton. We hope this report will encourage learning from our students and stimulate research and education in the years to come.

Thank you for your continued support and please enjoy learning about the IAC and the exciting research being carried out here at Princeton University.



Nan Yao, Director of the Imaging and Analysis Center



Craig B. Arnold, Director of PRISM

Imaging and Analysis Center

Recent IAC users include over 300 students and researchers from 18 departments and centers on campus. Undergraduates, graduate students, and post-docs are each provided with a unique opportunity to conduct research using the IAC's state-of-the-art instrumentation. Their research covers a diverse spectrum of topics including: improving photovoltaics, batteries, circuit-design, and cements; elucidating biochemical pathways, understanding the structures of biomolecular machines; and characterizing samples from aerodynamic wing models, pharmaceutical drug crystals, catalytic nanoparticles, and biofilms.



Nanomaterials

topological 2D materials, cathode coating for battery cells, lead free solder, catalysts etc.



Biomaterials

biofilms, hydrogel, dental implants, contact lenses, surgical mesh, etc.



Electronic Materials

light-emitting diodes, transistors, solar cells, etc.



Ceramics and Glasses

cement, rock, anti-corrosion coating, display panel, anti-reflection coating, etc.



Polymers

bolck copolymer, food wrap, adhesives, paints, etc.



Metal Alloys

corrosion resistance supports, turbine blades, automobile chassis, etc.

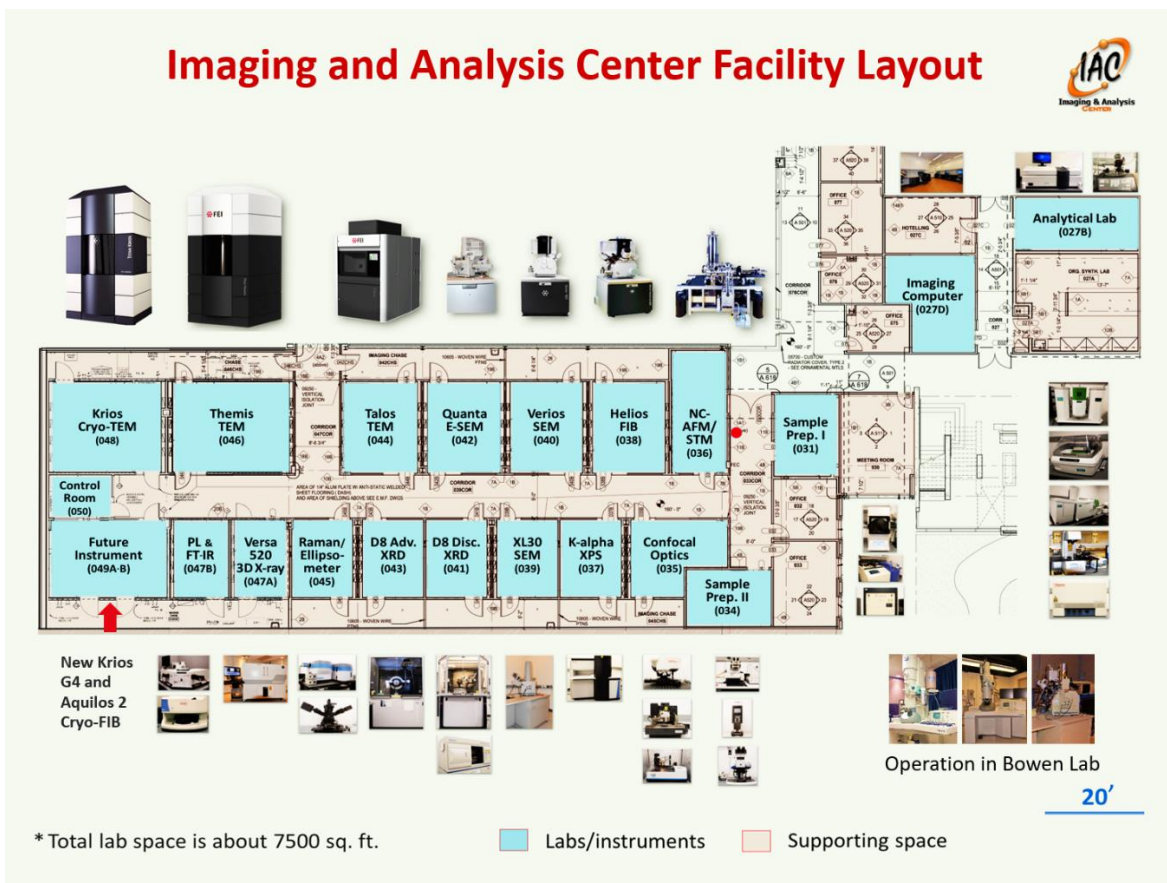
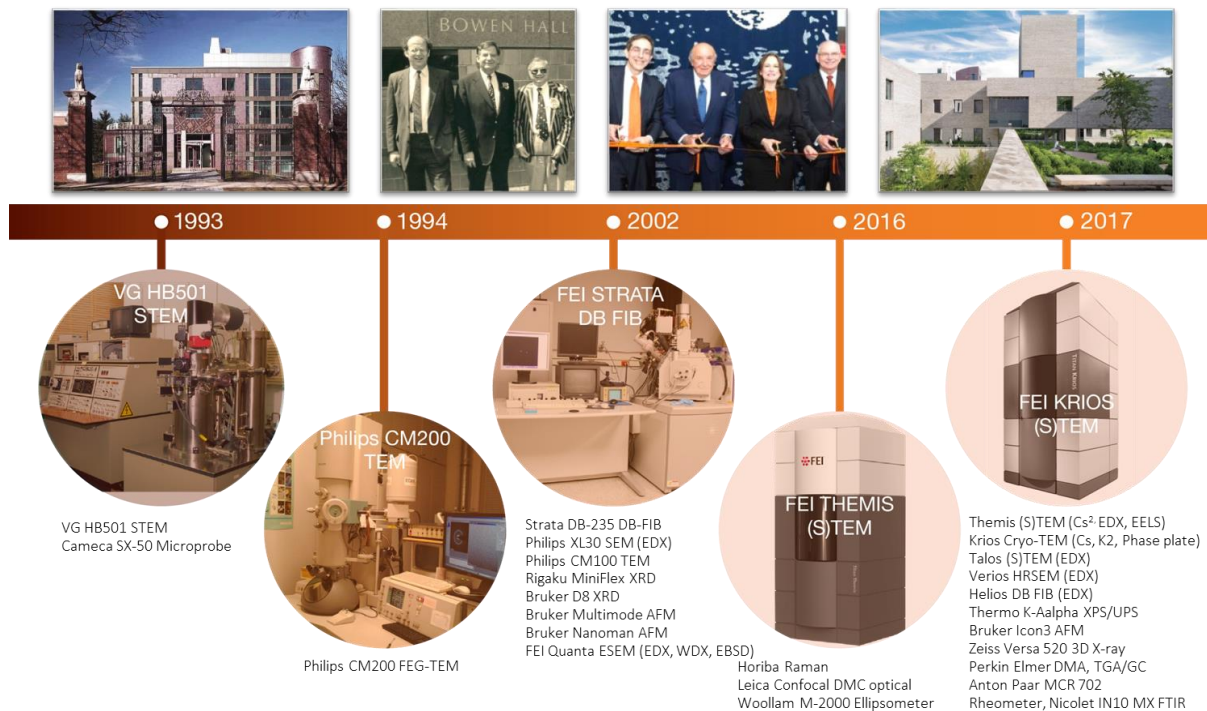


Pharmaceutical Materials

drug coating, toothpaste, molecular crystals, etc.

PRISM Imaging and Analysis Center (IAC)

IAC Background: Started in 1993 with one person, one microscope, and today it has grown to have seven staff and become a world-leading microscopy facility for the physical and life sciences.



IAC team members:



Nan Yao



John Schreiber



Paul Shao



Daniel Gregory



Denis Potapenko



Dan McNesby



Kevin Lamb

IAC faculty users from Princeton:

Architecture

Forrest Meggers

Civil & Environmental Eng.

Catherine Peters

Claire White

Ian Bourg

Zhiyong (Jason) Ren

Computer Science

Sebastian Seung

Electrical Engineering

Andrew Houck

Antoine Kahn

Barry Rand

Claire Gmachl

James Sturm

Jeff Thompson

Nathalie De Leon

Paul Prucnal

Steve Chou

Steve Lyon

Molecular Biology

Alexei Korennykh

Bonnie Bassler

Fred Hughson

Martin Jonikas

Nieng Yan

Sabine Petry

Zemer Gitai

Chemical & Biological Eng.

Bruce E. Koel

Celeste Nelson

Lynn Loo

Michele Sarazen

Pierre-Thomas Brun

Rick Register

Robert Prud'homme

Rodney Priestley

Ecology and Evolutionary Biology

Sarah Kocher

Geosciences

Adam Maloof

Bess Ward

Blair Schoene

Tullis Onstott

Satish Myneni

Thomas Duffy

Physics

Ali Yazdani

Chris Tully

Frank Calaprice

Jason Petta

Joshua Shaevitz

Phuan Ong

Sanfeng Wu

Zahid Hasan

Chemistry

Andrew Bocarsly

Bob Cava

Erik Sorensen

Greg Scholes

Haw Yang

Jeff Schwartz

Leslie M. Schoop

Mohammad Seyedsayamdost

Paul Chirik

Tom Muir

Library-Rare Books & Special Collections

Alan Stahl

Mechanical and Aerospace Eng.

Craig Arnold

Daniel Steingart

Edgar Choueiri

Howard Stone

Jeremy Kasdin

Yiguang Ju

Plasma Physics

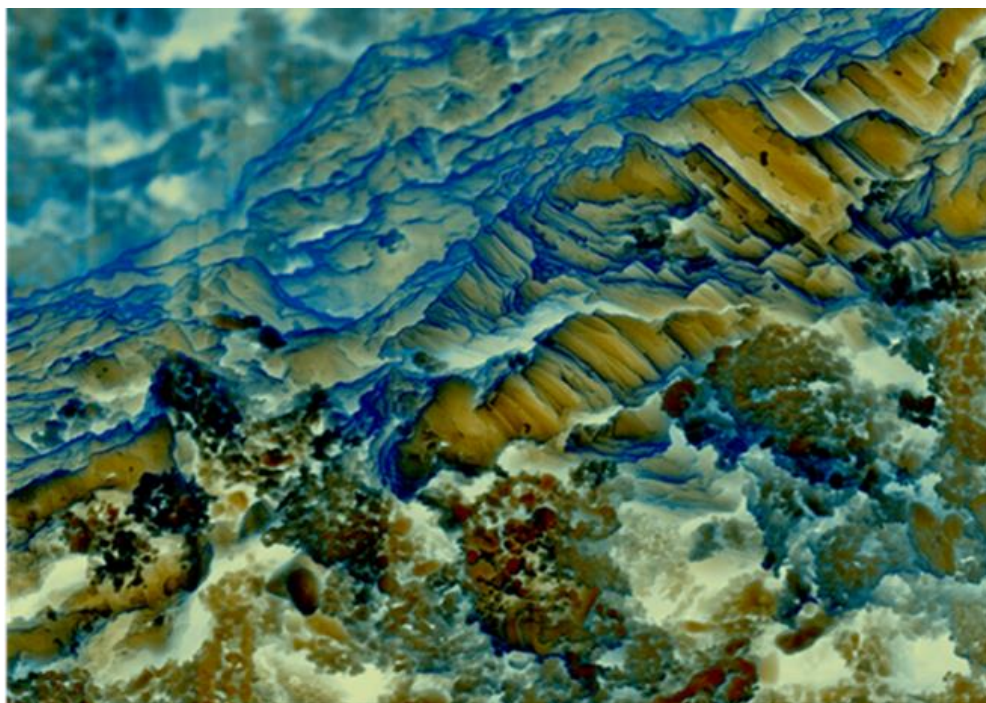
Mojtaba Safabakhsh

Yevgeny Raitses

PRISM

Nan Yao

IAC outside users from industry and other universities:



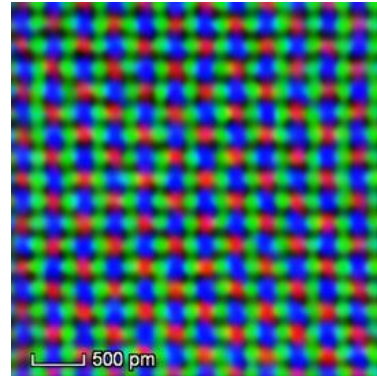
Secondary electron image showing surface morphology of SmCoS_2 material collected using a field-emission environmental scanning electron microscope operated at 20 keV. Field of view: 80 μm . (Image courtesy of Gerald Poirier and Nan Yao)

Acknowledgement:

The Imaging and Analysis Center acknowledges partial support from the National Science Foundation through the Princeton University Materials Research Science and Engineering Center (PCCM), DMR-2011750.

IAC new instrumentation highlights:

(1) Titan Themis Double Cs-corrected Scanning/Transmission Electron Microscope



(2) Titan Krios G3 Cryo-Transmission Electron Microscope

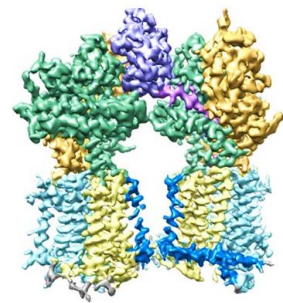
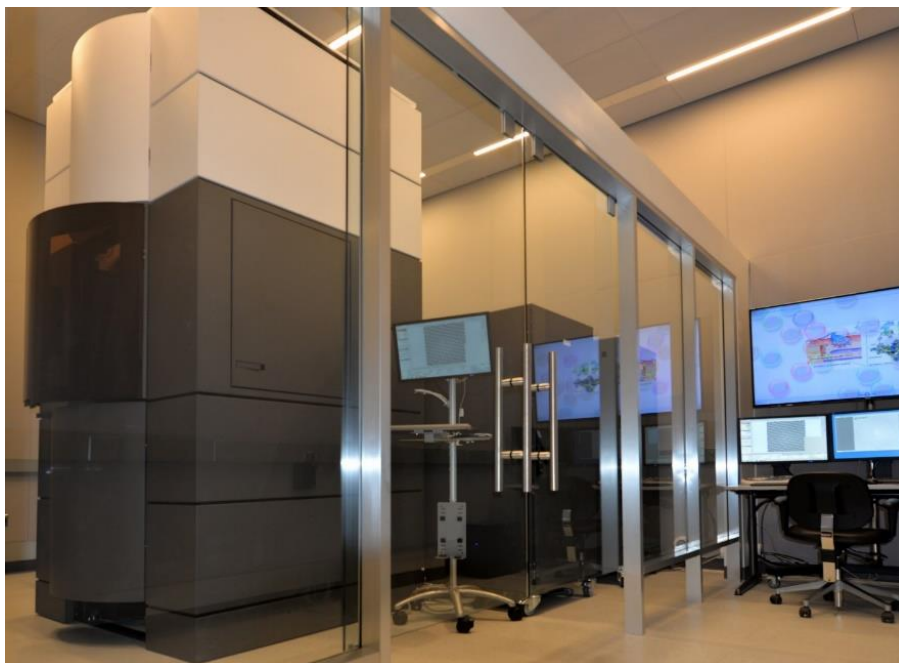


Table of Contents

School of Architecture	14
Teitelbaum, <i>et al.</i> Membrane-assisted radiant cooling for expanding thermal comfort zones globally without air conditioning	15
Department of Chemical and Biological Engineering	16
Markwalter, <i>et al.</i> Polymeric Nanocarrier Formulations of Biologics Using Inverse Flash NanoPrecipitation	17
Nerger, <i>et al.</i> Microextrusion Printing Cell-Laden Networks of Type I Collagen with Patterned Fiber Alignment and Geometry	18
Sezen-Edmonds, <i>et al.</i> Humidity and Strain Rate Determine the Extent of Phase Shift in the Piezoresistive Response of PEDOT:PSS	19
Yang, <i>et al.</i> Nitrogen-plasma treated hafnium oxyhydroxide as an efficient acid-stable electrocatalyst for hydrogen evolution and oxidation reactions	20
Buzi, <i>et al.</i> Deuterium and helium ion irradiation of nanograined tungsten and tungsten–titanium alloys	21
Zhao, <i>et al.</i> Extending the Photovoltaic Response of Perovskite Solar Cells into the Near-Infrared with a Narrow-Bandgap Organic Semiconductor	22
Hamill, <i>et al.</i> Influence of Solvent Coordination on Hybrid Organic–Inorganic Perovskite Formation	23
Hamill, <i>et al.</i> Acid-Catalyzed Reactions Activate DMSO as a Reagent in Perovskite Precursor Inks	24
Hamill, <i>et al.</i> Sulfur-Donor Solvents Strongly Coordinate Pb ²⁺ in Hybrid Organic–Inorganic Perovskite Precursor Solutions	25
Khlyabich, <i>et al.</i> Precursor Solution Annealing Forms Cubic-Phase Perovskite and Improves Humidity Resistance of Solar Cells	26
Khlyabich, <i>et al.</i> Crystalline Intermediates and Their Transformation Kinetics during the Formation of Methylammonium Lead Halide Perovskite Thin Films	27
Zhao, <i>et al.</i> A hole-transport material that also passivates perovskite surface defects for solar cells with improved efficiency and stability	28
Zhao, <i>et al.</i> Accessing Highly Oriented Two-Dimensional Perovskite Films via Solvent-Vapor Annealing for Efficient and Stable Solar Cells	29

Department of Chemistry.....	30
Ferrenti, <i>et al.</i> Change in Magnetic Properties upon Chemical Exfoliation of FeOCl.....	31
Guerra, <i>et al.</i> Single-Particle Dynamic Light Scattering: Shapes of Individual Nanoparticles	32
Lei, <i>et al.</i> Charge Density Waves and Magnetism in Topological Semimetal Candidates $GdSb_xTe_{2-x-\delta}$	33
Lei, <i>et al.</i> High mobility in a van der Waals layered antiferromagnetic metal	34
Song, <i>et al.</i> Soft Chemical Synthesis of H_xCrS_2 : An Antiferromagnetic Material with Alternating Amorphous and Crystalline Layers	35
DelPo, <i>et al.</i> Polariton Transitions in Femtosecond Transient Absorption Studies of Ultrastrong Light–Molecule Coupling.....	36
Jin, <i>et al.</i> $Sn_{0.24}WO_3$ hexagonal tungsten bronze prepared via the metal chloride route	37
Kirby, <i>et al.</i> Transient Drude Response Dominates Near-Infrared Pump–Probe Reflectivity in Nodal-Line Semimetals ZrSiS and ZrSiSe.....	38
Frick, <i>et al.</i> Observation of $[V_{Cu}^{1-} In_i^{2+} V_{Cu}^{1-}]$ Defect Triplets in Cu-Deficient $CuInS_2$	39
Foster, <i>et al.</i> Catalytic Mismatching of $CuInSe_2$ and Ni_3Al Demonstrates Selective Photoelectrochemical CO_2 Reduction to Methanol.....	40
Department of Civil and Environmental Engineering	41
Spokas, <i>et al.</i> Collapse of Reacted Fracture Surface Decreases Permeability and Frictional Strength.....	42
Hunter, <i>et al.</i> Metals Coprecipitation with Barite: Nano-XRF Observation of Enhanced Strontium Incorporation	43
Gong, <i>et al.</i> In situ quasi-elastic neutron scattering study on the water dynamics and reaction mechanisms in alkali- activated slags	44
Department of Electrical Engineering	45
Kerner, <i>et al.</i> Electrochemical and Thermal Etching of Indium Tin Oxide by Solid-State Hybrid Organic-Inorganic Perovskites	46
Noel, <i>et al.</i> Interfacial charge-transfer doping of metal halide perovskites for high performance photovoltaics	47
Phenicie, <i>et al.</i> Narrow Optical Line Widths in Erbium Implanted in TiO_2	48
Zang, <i>et al.</i> Ultrasensitive Ebola Virus Antigen Sensing via 3D Nanoantenna Arrays	49

Zhao, <i>et al.</i> Thermal Management Enables Bright and Stable Perovskite Light-Emitting Diodes.....	50
Mundada, <i>et al.</i> Suppression of Qubit Crosstalk in a Tunable Coupling Superconducting Circuit.....	51
Raha, <i>et al.</i> Optical quantum nondemolition measurement of a single rare earth ion qubit	52
Smith, <i>et al.</i> n-Doping of a Low-Electron-Affinity Polymer Used as an Electron-Transport Layer in Organic Light-Emitting Diodes	53
Chung, <i>et al.</i> Heterostructure design to achieve high quality, high density GaAs 2D electron system with g-factor tending to zero.....	54
Patlatiuk, <i>et al.</i> Edge State Wave Functions from Momentum-Conserving Tunneling Spectroscopy	55
Hossain, <i>et al.</i> Bloch Ferromagnetism of Composite Fermions	56
Yoo, <i>et al.</i> Demonstration of a tunable antenna-coupled intersubband terahertz (TACIT) mixer	57
Hatke, <i>et al.</i> Wigner solid pinning modes tuned by fractional quantum Hall states of a nearby layer.....	58
Du, <i>et al.</i> Observation of new plasmons in the fractional quantum Hall effect: Interplay of topological and nematic orders	59
Caputo, <i>et al.</i> Josephson vortices induced by phase twisting a polariton superfluid.....	60
Drichko, <i>et al.</i> Electronic band structure in n-type GaAs/AlGaAs wide quantum wells in tilted magnetic field.....	61
Chung, <i>et al.</i> Spatial Mapping of Local Density Variations in Two-dimensional Electron Systems Using Scanning Photoluminescence	62
Huang, <i>et al.</i> Discontinuity in the transport of strongly correlated two-dimensional hole systems in zero magnetic field	63
Pieczarka, <i>et al.</i> Effect of optically-induced potential on the energy of trapped exciton-polaritons below the condensation threshold.....	64
Deng, <i>et al.</i> Probing the Melting of a Two-Dimensional Quantum Wigner Crystal via its Screening Efficiency	65
Huang, <i>et al.</i> Resymmetrizing Broken Symmetry with Hydraulic Pressure	66
Ro, <i>et al.</i> Stability of multielectron bubbles in high Landau levels.....	67

Ro, <i>et al.</i> Electron bubbles and the structure of the orbital wave function.....	68
Sammon, <i>et al.</i> Resistivity anisotropy of quantum Hall stripe phases	69
Hossain, <i>et al.</i> Geometric resonance of four-flux composite fermions	70
Mi, <i>et al.</i> Quantum oscillations in a two-dimensional electron system under low-frequency microwave irradiation	71
Mukherjee, <i>et al.</i> Observation of nonequilibrium motion and equilibration in polariton rings	72
Wang, <i>et al.</i> Surface acoustic wave detection of robust zero-resistance states under microwaves	73
Pan, <i>et al.</i> Particle-Hole Symmetry and the Fractional Quantum Hall Effect in the Lowest Landau Level.....	74
Ma, <i>et al.</i> Thermal and Quantum Melting Phase Diagrams for a Magnetic-Field-Induced Wigner Solid	75
Hossain, <i>et al.</i> Precise Experimental Test of the Luttinger Theorem and Particle-Hole Symmetry for a Strongly Correlated Fermionic System.....	76
Murotani, <i>et al.</i> Light-Driven Electron-Hole Bardeen-Cooper-Schrieffer-Like State in Bulk GaAs.....	77
Eisenstein, <i>et al.</i> Precursors to Exciton Condensation in Quantum Hall Bilayers	78
Fu, <i>et al.</i> Anomalous Nematic States in High Half-Filled Landau Levels.....	79
Chung, <i>et al.</i> Working principles of doping-well structures for high-mobility two-dimensional electron systems.....	80
Yuan, <i>et al.</i> Charge state dynamics and optically detected electron spin resonance contrast of shallow nitrogen-vacancy centers in diamond	81
Xu, <i>et al.</i> Negative longitudinal magnetoresistance in gallium arsenide quantum wells	82
Fu, <i>et al.</i> 3/2 fractional quantum Hall plateau in confined two-dimensional electron gas.....	83
Place, <i>et al.</i> New material platform for superconducting transmon qubits with coherence times exceeding 0.3 milliseconds	84
Kerner, <i>et al.</i> Low Threshold Voltages Electrochemically Drive Gold Migration in Halide Perovskite Devices	85
Zhang, <i>et al.</i> Ultraviolet Photoemission Spectroscopy and Kelvin Probe Measurements on Metal Halide Perovskites: Advantages and Pitfalls.....	86

Zhang, <i>et al.</i> Gap States in Methylammonium Lead Halides: The Link to Dimethylsulfoxide?.....	87
Lewis-Sigler Institute for Integrative Genomics	88
Copenhagen, <i>et al.</i> Topological defects promote layer formation in <i>Myxococcus xanthus</i> colonies	89
Princeton Institute for the Science and Technology of Materials (PRISM)	90
Dutta, <i>et al.</i> Understanding solution processing of inorganic materials using cryo-EM	91
Noel, <i>et al.</i> Elucidating the Role of a Tetrafluoroborate-Based Ionic Liquid at the n-Type Oxide/Perovskite Interface	92
Chen, <i>et al.</i> Petroleum pitch: Exploring a 50-year structure puzzle with real-space molecular imaging.....	93
Xu, <i>et al.</i> Liquid-involved synthesis and processing of sulfide-based solid electrolytes, electrodes, and all-solid- state batteries.....	94
Dutta, <i>et al.</i> Crystalline Nature of Colloids in Methylammonium Lead Halide Perovskite Precursor Inks Revealed by Cryo-Electron Microscopy.....	95
Pieczarka, <i>et al.</i> Observation of quantum depletion in a non-equilibrium exciton-polariton condensate	96
Gianfrate, <i>et al.</i> Measurement of the quantum geometric tensor and of the anomalous Hall drift	97
Gregory, <i>et al.</i> Recent Advances in Colloid Characterization.....	98
Estrecho, <i>et al.</i> Direct measurement of polariton-polariton interaction strength in the Thomas-Fermi regime of exciton- polariton condensation	99
Ballarini, <i>et al.</i> Self-Trapping of Exciton-Polariton Condensates in GaAs Microcavities	100
Suárez-Forero, <i>et al.</i> Quantum hydrodynamics of a single particle	101
Ballarini, <i>et al.</i> Directional Goldstone waves in polariton condensates close to equilibrium.....	102
Chen, <i>et al.</i> Conformational Analysis of Nonplanar Archipelago Structures on a Cu (111) Surface by Molecular Imaging	103
Liang, <i>et al.</i> Scaling of deterministic lateral displacement devices to a single column of bumping obstacles	104
Department of Mechanical and Aerospace Engineering	105
Bommier, <i>et al.</i> In Operando Acoustic Detection of Lithium Metal Plating in Commercial LiCoO ₂ /Graphite Pouch Cells	106

Bommier, <i>et al.</i> Operando Acoustic Monitoring of SEI Formation and Long-Term Cycling in NMC/SiGr Composite Pouch Cells	107
Chang, <i>et al.</i> Morphological and Chemical Mapping of Columnar Lithium Metal	108
Chang, <i>et al.</i> Understanding Adverse Effects of Temperature Shifts on Li-Ion Batteries: An Operando Acoustic Study	109
Dutta, <i>et al.</i> Effects of disorder on two-photon absorption in amorphous semiconductors.....	110
Chang, <i>et al.</i> Measuring effective stiffness of Li-ion batteries via acoustic signal processing.....	111
Yan, <i>et al.</i> Controlled Dy-doping to nickel-rich cathode materials in high temperature aerosol synthesis	112
Zhong, <i>et al.</i> Kinetic study of plasma-assisted n-dodecane/O ₂ /N ₂ pyrolysis and oxidation in a nanosecond-pulsed discharge	113
Department of Molecular Biology	114
Gao, <i>et al.</i> Employing NaChBac for cryo-EM analysis of toxin action on voltage-gated Na ⁺ channels in nanodisc	115
Han, <i>et al.</i> High-yield monolayer graphene grids for near-atomic resolution cryoelectron microscopy	116
Qian, <i>et al.</i> Structural Basis of Low-pH-Dependent Lysosomal Cholesterol Egress by NPC1 and NPC2.....	117
Qian, <i>et al.</i> Structural basis for catalysis and substrate specificity of human ACAT1	118
Qian, <i>et al.</i> Inhibition of tetrameric Patched1 by Sonic Hedgehog through an asymmetric paradigm	119
Wang, <i>et al.</i> Structural and mechanism of human diacylglycerol <i>O</i> -acyltransferase 1.....	120
Qin, <i>et al.</i> Cell position fates and collective fountain flow in bacterial biofilms revealed by light-sheet microscopy	121
Department of Physics	122
Sigillito, <i>et al.</i> Site-Selective Quantum Control in an Isotopically Enriched ²⁸ Si/Si _{0.7} Ge _{0.3} Quadruple Quantum Dot. 123	123
Sigillito, <i>et al.</i> Coherent transfer of quantum information in a silicon double quantum dot using resonant SWAP gates	124
Suerfu, <i>et al.</i> Pyrolytic carbon coating of fused quartz by vacuum vapor transport.....	125

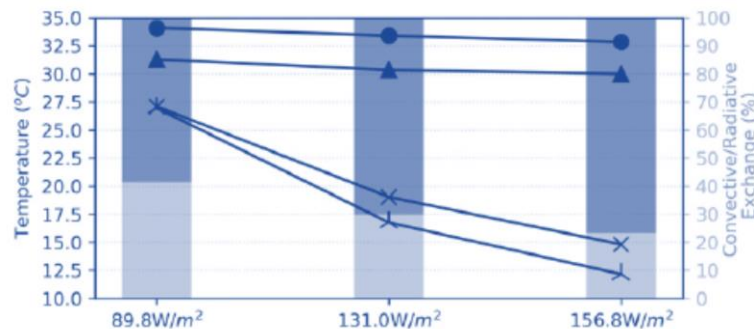
<i>Xie, et al.</i> Spectroscopic signatures of many-body correlations in magic-angle twisted bilayer graphene.....	126
<i>Yin, et al.</i> Giant and anisotropic many-body spin-orbit tunability in a strongly correlated kagome magnet	127
<i>Yin, et al.</i> Negative flat band magnetism in a spin-orbit-coupled correlated kagome magnet	128
<i>Yin, et al.</i> Quantum-limit Chern topological magnetism in TbMn ₆ Sn ₆	129
<i>Borjans, et al.</i> Split-Gate Cavity Coupler for Silicon Circuit Quantum Electrodynamics	130
<i>Borjans, et al.</i> Resonant microwave-mediated interactions between distant electron spins	131
<i>Burkard, et al.</i> Superconductor–semiconductor hybrid-circuit quantum electrodynamics	132
<i>Mills, et al.</i> Shuttling a single charge across a one-dimensional array of silicon quantum dots	133
<i>Wong, et al.</i> Cascade of electronic transitions in magic-angle twisted bilayer graphene.....	134

School of Architecture

Membrane-assisted radiant cooling for expanding thermal comfort zones globally without air conditioning

Eric Teitelbaum,^{1,2,3} Kian Wee Chen,³ Dorit Aviv,^{2,4} Kipp Bradford,² Lea Ruefenacht,¹ Denon Sheppard,⁵ Megan Teitelbaum,⁶ Forrest Meggers,^{2,3} Jovan Pantelic,^{6,7} and Adam Rysanek.⁵

¹Singapore-ETH Centre, ETH Zurich, Singapore 318602, Singapore; ²School of Architecture, Princeton University, Princeton, NJ 08544, USA; ³Andlinger Center for Energy and the Environment, Princeton University, Princeton, NJ 08544, USA; ⁴Weitzman School of Design, University of Pennsylvania, Philadelphia, PA 19104, USA; ⁵School of Architecture and Landscape Architecture, University of British Columbia, Vancouver, BC V6T 1Z4, Canada; ⁶Berkeley Education Alliance for Research in Singapore, 138602, Singapore; ⁷Center for the Built Environment, University of California, Berkeley, CA 94720, USA



We present results of a radiant cooling system that made the hot and humid tropical climate of Singapore feel cool and comfortable. Thermal radiation exchange between occupants and surfaces in the built environment can augment thermal comfort. The lack of widespread commercial adoption of radiant-cooling technologies is due to two widely held views: 1) The low temperature required for radiant cooling in humid environments will form condensation; and 2) cold surfaces will still cool adjacent air via convection, limiting overall radiant-cooling effectiveness. This work directly challenges these views and provides proof-of-concept solutions examined for a transient thermal-comfort scenario. We constructed an outdoor radiant-cooling pavilion in Singapore that used an infrared-transparent, low density polyethylene membrane to provide radiant cooling. Test subjects in the pavilion ($n = 37$) reported a “satisfactory” thermal sensation 79% of the time, despite experiencing 29.6 ± 0.9 °C air at $66.5 \pm 5\%$ relative humidity and with low air movement of 0.26 ± 0.18 $m \cdot s^{-1}$. Comfort was achieved with a coincident mean radiant temperature of 23.9 ± 0.8 °C, requiring a chilled water-supply temperature of 17.0 ± 1.8 °C. The pavilion operated successfully without any observed condensation on exposed surfaces, despite an observed dew-point temperature of 23.7 ± 0.7 °C.

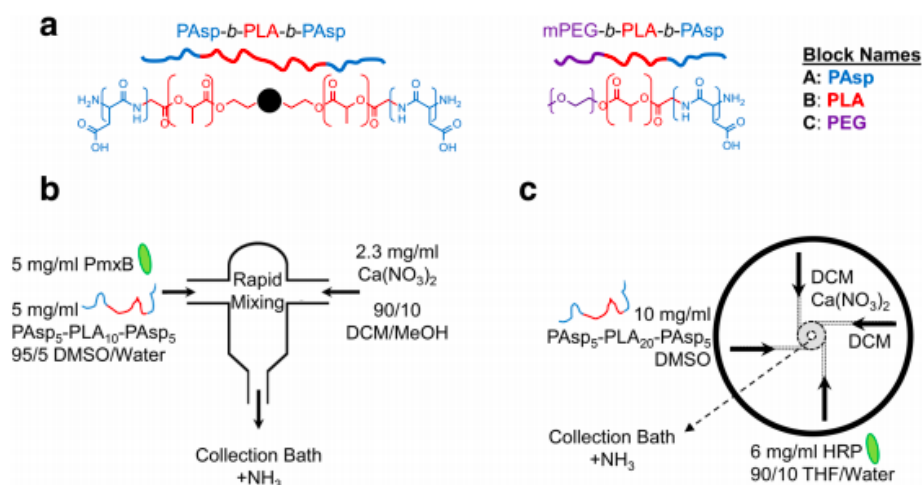
Status: published work in Proc. Natl. Acad. Sci. U.S.A. 2020, **117**, 21162–21169

Department of Chemical and Biological Engineering

Polymeric Nanocarrier Formulations of Biologics Using Inverse Flash NanoPrecipitation

Chester E. Markwalter,¹ Robert F. Pagels,^{1,2} Ava N. Hejazi,^{1,3} Akiva G. R. Gordon,^{1,4} Alexandra L. Thompson,^{1,5} and Robert K. Prud'homme¹

¹Department of Chemical and Biological Engineering, Princeton University, A301 Engineering Quad, Olden St., Princeton, New Jersey 08544, USA. ²Optimeos Life Sciences, Princeton, New Jersey, USA. ³Department of Chemistry, University of California, Berkeley, Berkeley, California, USA. ⁴Department of Chemical Engineering, Massachusetts Institute of Technology, Cambridge, Massachusetts, USA. ⁵Cardiothoracic Surgery, Children's Hospital Los Angeles, Los Angeles, California, USA.



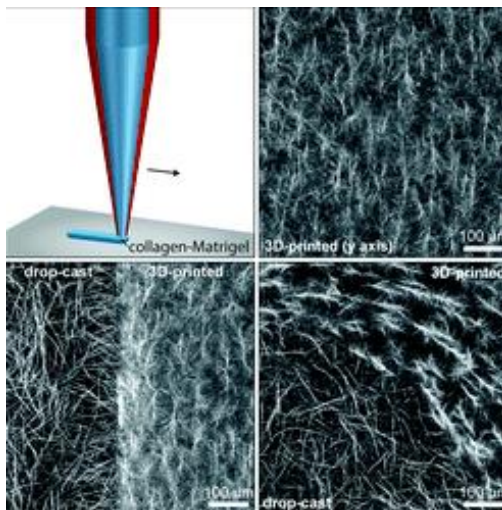
The encapsulation of water-soluble therapeutics and biologics into nanocarriers to produce novel therapeutics has been envisioned for decades, but clinical translation has been hampered by complex synthesis strategies. To address this unmet need, we introduce a solubility-driven self-assembly process to form polymeric nanocarriers comprising a biologic in a hydrophilic core, encapsulated by a poly(lactic acid) shell, and stabilized by a poly(ethylene glycol) brush. Called “inverse Flash NanoPrecipitation (iFNP),” the technique achieves biologic loadings (wt% of total formulation) that are 5–15× higher than typical values. We sequentially assemble the polymer layers to form the final nanocarrier. Installation of the poly(lactic acid) shell before water exposure sequesters the biologic in the core and results in the improved loadings that are achieved. We demonstrate the broad applicability of the process and illustrate its implementation by formulating over a dozen different oligosaccharides, antibiotics, peptides, proteins, and RNA into nanocarriers with narrow size distributions, at high loadings, and with high reproducibility. Lysozyme and horseradish peroxidase are shown to retain 99% activity after processing. These results demonstrate the potential for commercial implementation of this technology, enabling the translation of novel treatments in immunology, oncology, or enzyme therapies.

Status: published work at The AAPS Journal 2020, **22**, 18

Microextrusion Printing Cell-Laden Networks of Type I Collagen with Patterned Fiber Alignment and Geometry

Bryan A. Nerger,¹ P.-T. Brun,¹ and Celeste M. Nelson^{1,2}

¹Department of Chemical and Biological Engineering, Princeton University, Princeton, NJ 08544 and ²Department of Molecular Biology, Princeton University, Princeton, NJ 08544



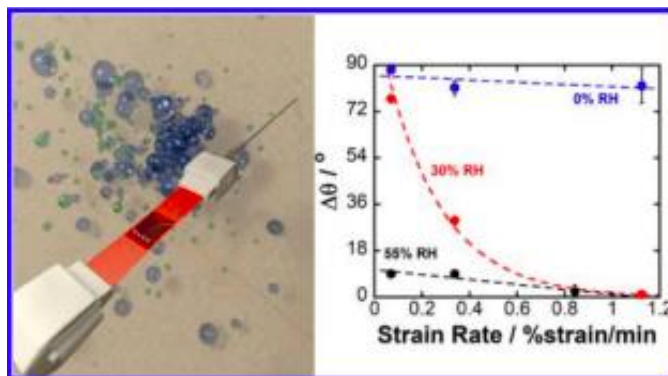
Type I collagen self-assembles into three-dimensional (3D) fibrous networks. These dynamic viscoelastic materials can be remodeled in response to mechanical and chemical signals to form anisotropic networks, the structure of which influences tissue development, homeostasis, and disease progression. Conventional approaches for fabricating anisotropic networks of type I collagen are often limited to unidirectional fiber alignment over small areas. Here, we describe a new approach for engineering cell-laden networks of aligned type I collagen fibers using 3D microextrusion printing of a collagen-Matrigel ink. We demonstrate hierarchical control of 3D-printed collagen with the ability to spatially pattern collagen fiber alignment and geometry. Our data suggest that collagen alignment results from a combination of molecular crowding in the ink and shear and extensional flows present during 3D printing. We demonstrate that human breast cancer cells cultured on 3D-printed collagen constructs orient along the direction of collagen fiber alignment. We also demonstrate the ability to simultaneously bioprint epithelial cell clusters and control the alignment and geometry of collagen fibers surrounding cells in the bioink. The resulting cell-laden constructs consist of epithelial cell clusters fully embedded in aligned networks of collagen fibers. Such 3D-printed constructs can be used for studies of developmental biology, tissue engineering, and regenerative medicine.

Status: published work at Soft Matter 2019, **15**, 5728-5738

Humidity and Strain Rate Determine the Extent of Phase Shift in the Piezoresistive Response of PEDOT:PSS

Melda Sezen-Edmonds,¹ Yao-Wen Yeh,² Nan Yao,² and Yueh-Lin Loo^{1,2,3}

¹Department of Chemical and Biological Engineering, Princeton University, Princeton, New Jersey 08544, United States; ²Princeton Institute for Science and Technology of Materials, Princeton University, Princeton, New Jersey 08544, United States; ³Andlinger Center for Energy and the Environment, Princeton University, Princeton, New Jersey 08544, United States



The piezoresistive response of PEDOT:PSS is sensitive to changes in its morphology when exposed to humidity and in response to different strain rates. The piezoresistive response of as-cast PEDOT:PSS transitions from being in-phase to being out-of-phase with applied strain when the relative humidity is reduced from >50% to near zero. At >50% relative humidity, the PSS matrix swells and interrupts the connectivity of electrically conducting PEDOT domains. Stretching PEDOT:PSS at such conditions leads to an increase in resistance with strain. Under dry conditions, PEDOT domains are connected; stretching PEDOT:PSS instead leads to preferential alignment of the conducting domains and a concomitant decrease in resistance. At intermediate humidity, the piezoresistive response of PEDOT:PSS is phase shifted relative to applied strain, with it being out-of-phase at low strain rates (0.34%/min) and in-phase at high strain rates (1.12%/min). We interpret this peculiar and surprising observation as a competition between strain-induced domain separation and alignment, each having a different response time to applied strain. Postdeposition treatment of PEDOT:PSS with dichloroacetic acid removes excess PSS; PEDOT:PSS's piezoresistive response is then invariant with humidity and strain rate. Stabilizing its piezoresistive response can ensure accuracy of PEDOT:PSS-based flexible resistive sensors whose response to small strains is used to monitor environmental and human-health.

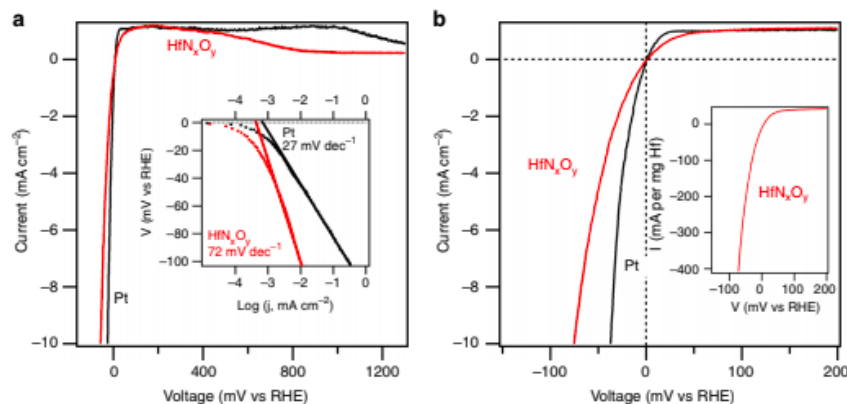
Status: published work at ACS Appl. Mater. Interfaces 2019, **11**, 16888-16895

Nitrogen-plasma treated hafnium oxyhydroxide as an efficient acid-stable electrocatalyst for hydrogen evolution and oxidation reactions

Xiaofang Yang¹, Fang Zhao², Yao-Wen Yeh³, Rachel S. Selinsky¹, Zhu Chen¹, Nan Yao³, Christopher G. Tully², Yiguang Ju⁴ & Bruce E. Koel¹

¹Department of Chemical and Biological Engineering, Princeton University, Princeton, NJ 08544, USA.

²Department of Physics, Princeton University, Princeton, NJ 08544, USA. ³Princeton Institute for Science and Technology of Materials (PRISM), Princeton University, Princeton, NJ 08544, USA. ⁴Department of Mechanical and Aerospace Engineering, Princeton University, Princeton, NJ 08544, USA.



Development of earth-abundant electrocatalysts for hydrogen evolution and oxidation reactions in strong acids represents a great challenge for developing high efficiency, durable, and cost effective electrolyzers and fuel cells. We report herein that hafnium oxyhydroxide with incorporated nitrogen by treatment using an atmospheric nitrogen plasma demonstrates high catalytic activity and stability for both hydrogen evolution and oxidation reactions in strong acidic media using earth-abundant materials. The observed properties are especially important for unitized regenerative fuel cells using polymer electrolyte membranes. Our results indicate that nitrogen-modified hafnium oxyhydroxide could be a true alternative for platinum as an active and stable electrocatalyst, and furthermore that nitrogen plasma treatment may be useful in activating other non-conductive materials to form new active electrocatalysts.

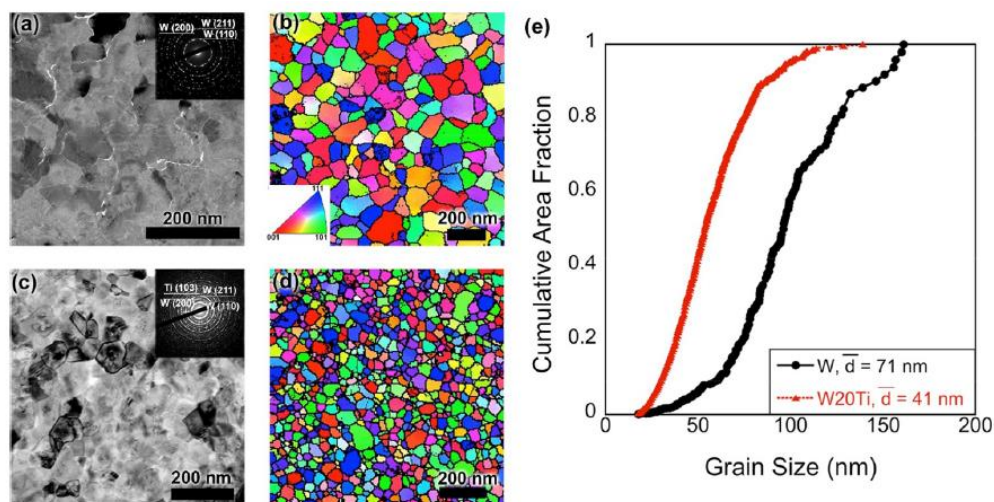
The VCR IBS/TM200S ion beam sputter was used to deposit the Hf thin film on Au foil. A ThermoFisher K-Alpha X-ray Photoelectron Spectrometer was used to analyze the HfO_x samples. Verios 460 Extreme High Resolution SEM (XHR-SEM) was used to characterize the thin film samples. A Bruker NanoMan AFM was used for topographical imaging of the N-modified HfO_x samples.

Status: published work at Nature Communications 2019, **10**, 1543

Deuterium and helium ion irradiation of nanograined tungsten and tungsten–titanium alloys

L. Buzi,¹ M. Yeh,¹ Y-W. Yeh,² O.K. Donaldson,³ M.I. Patino,⁴ J.R. Trelewicz,^{3,5} N. Yao,² R. Doerner,⁴ B.E. Koel¹

¹Department of Chemical and Biological Engineering, Princeton University, Princeton, NJ 08544, USA; ²Princeton Institute for the Science and Technology of Materials (PRISM), Princeton University, Princeton, NJ 08544, USA; ³Department of Materials Science and Chemical Engineering, Stony Brook University, Stony Brook, NY 11794, USA; ⁴Center for Energy Research, UCSD, La Jolla, CA 92093-0417, USA; ⁵Institute for Advanced Computational Science, Stony Brook University, Stony Brook, NY 11794, USA



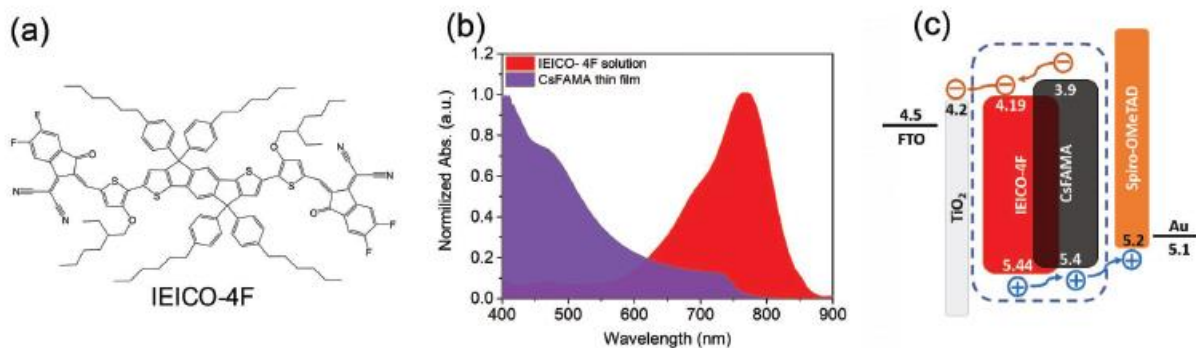
Tungsten (W), a primary candidate for the plasma-facing components of nuclear fusion reactors (e.g. the divertor region in ITER) is susceptible to cracks, blisters, bubbles, and other morphological changes when irradiated with energetic particles. This work investigated two new materials, nanograined W and a nanograined W–Ti alloy, for potential use as plasma-facing materials. Their retention properties and morphological changes after exposure to deuterium (D) and helium (He) plasma at 50 eV and surface temperatures of 500 and 1000 K were analyzed. Nanograined W was found to have smaller blisters and be less prone to fuzz formation than commonly-utilized micro-grain polycrystalline W. Additionally, the nanograined W–Ti alloy exhibited a lower concentration of blisters on its surface than pure W, including nanograined W.

Status: published work at Nuclear Materials and Energy 2019, **21**, 100713

Extending the Photovoltaic Response of Perovskite Solar Cells into the Near-Infrared with a Narrow-Bandgap Organic Semiconductor

Xiaoming Zhao,¹ Chao Yao,^{1,2} Tianran Liu,¹ J. Clay Hamill, Jr.,¹ Guy Olivier Ngongang Ndjawa,¹ Guangming Cheng,³ Nan Yao,³ Hong Meng,² and Yueh-Lin Loo^{1,4}

¹Department of Chemical and Biological Engineering, Princeton University, Princeton, NJ 08544, USA; ²School of Advanced Materials, Peking University Shenzhen Graduate School, Shenzhen 518055, China; ³Princeton Institute for Science and Technology of Materials, Princeton University, Princeton, NJ 08544, USA; ⁴Andlinger Center for Energy and the Environment, Princeton University, Princeton, NJ 08544, USA



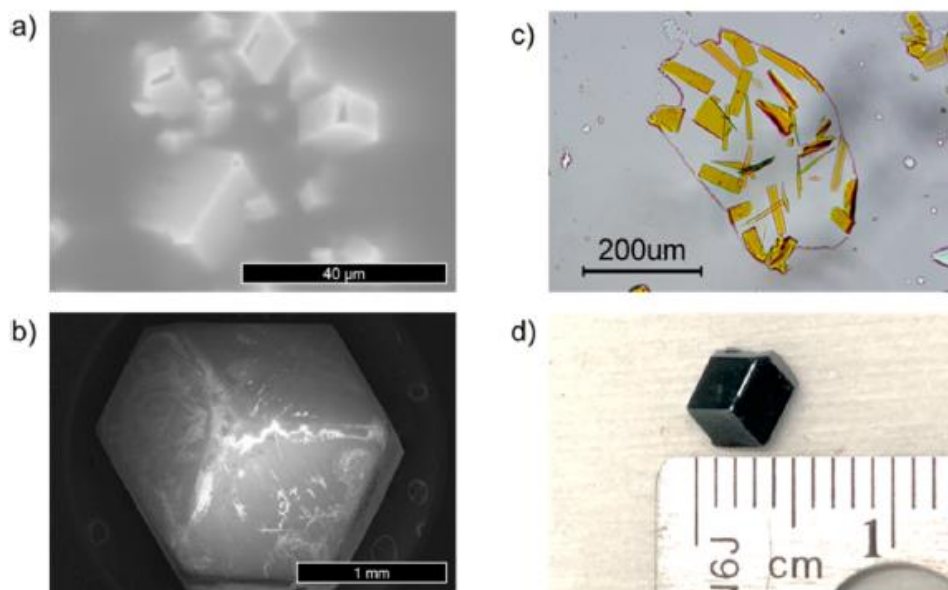
Typical lead-based perovskites solar cells show an onset of photogeneration around 800 nm, leaving plenty of spectral loss in the near-infrared (NIR). Extending light absorption beyond 800 nm into the NIR should increase photocurrent generation and further improve photovoltaic efficiency of perovskite solar cells (PSCs). Here, a simple and facile approach is reported to incorporate a NIR-chromophore that is also a Lewis-base into perovskite absorbers to broaden their photoresponse and increase their photovoltaic efficiency. Compared with pristine PSCs, these solar cells generate photocurrent in the NIR beyond the band edge of the perovskite active layer alone. Given the Lewis-basic nature of the organic semiconductor, its addition to the photoactive layer also effectively passivates perovskite defects. These films thus exhibit significantly reduced trap densities, enhanced hole and electron mobilities, and suppressed illumination-induced ion migration. As a consequence, perovskite solar cells with organic chromophore exhibit an enhanced efficiency of 21.6%, and substantively improved operational stability under continuous one-sun illumination. The results demonstrate the potential generalizability of directly incorporating a multifunctional organic semiconductor that both extends light absorption and passivates surface traps in perovskite active layers to yield highly efficient and stable NIR-harvesting PSCs.

Status: published work at *Advanced Materials* 2019, **31**, 1904494

Influence of Solvent Coordination on Hybrid Organic–Inorganic Perovskite Formation

J. Clay Hamill, Jr.,¹ Jeffrey Schwartz,² and Yueh-Lin Loo^{1,3}

¹Department of Chemical and Biological Engineering, Princeton University, Princeton, NJ 08544, USA; ²Department of Chemistry, Princeton University, Princeton, NJ 08544, USA; ³Andlinger Center for Energy and the Environment, Princeton University, Princeton, NJ 08544, USA



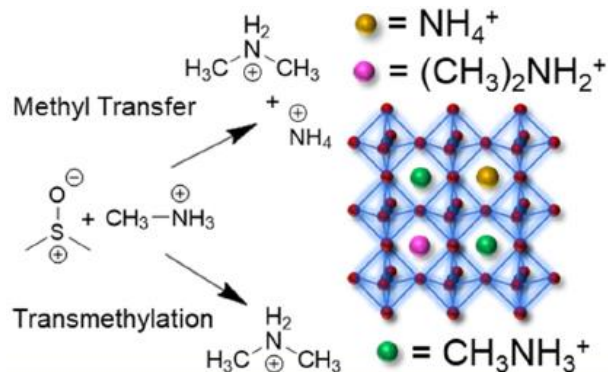
Solution-processed hybrid organic–inorganic perovskites (HOIPs) from organoammonium halide and lead halide precursors form efficacious active layers for photovoltaics, light-emitting diodes, and flexible electronics. Though solvent–solute coordination plays a critical role in HOIP crystallization, the influence of solvent choice on such interactions is poorly understood. We demonstrate Gutmann’s donor number, D_N , as a parameter that indicates the coordinating ability of the processing solvent with the Pb^{2+} center of the lead halide precursor. Low D_N solvents interact weakly with the Pb^{2+} center, favoring instead complexation between Pb^{2+} and iodide and subsequent crystallization of perovskite. High D_N solvents coordinate more strongly with the Pb^{2+} center, which in turn inhibits iodide coordination and stalls perovskite crystallization. Varying the concentration of high- D_N additives in precursor solutions tunes the strength of lead–solvent interactions, allowing finer control over the crystallization and the resulting morphology of HOIP active layers.

Status: published work at ACS Energy Letters 2018, **3**, 92-97

Acid-Catalyzed Reactions Activate DMSO as a Reagent in Perovskite Precursor Inks

J. Clay Hamill, Jr.,¹ Jeni C. Sorli,¹ István Pelczar,² Jeffrey Schwartz,² and Yueh-Lin Loo^{1,3}

¹Department of Chemical and Biological Engineering, ²Department of Chemistry, and ³Andlinger Center for Energy and the Environment, Princeton University, Princeton, New Jersey 08544, United States



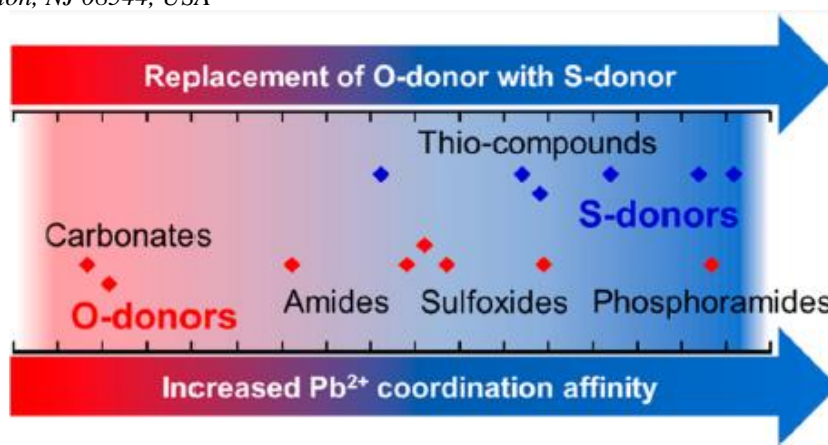
Proton transfer from methylammonium (CH_3NH_3^+) to dimethylsulfoxide (DMSO), a common Lewis-base solvent, initiates the production of ammonium (NH_4^+) and dimethylammonium ($(\text{CH}_3)_2\text{NH}_2^+$). We propose two parallel reaction pathways initiated by this proton transfer. Using DMSO-d_6 to elucidate reaction schemes, we demonstrate that protonation is followed either by methyl group transfer between the resulting CH_3NH_2 and residual CH_3NH_3^+ , or by transmethylation to CH_3NH_2 from DMSOH^+ . The former reaction yields NH_4^+ and $(\text{CH}_3)_2\text{NH}_2^+$ and is the dominant pathway at processing relevant temperatures; the latter yields $(\text{CH}_3)_2\text{NH}_2^+$ in addition to methylsulfonic acid and dimethylsulfide. In the preparation of hybrid organic–inorganic perovskite (HOIP) thin films for photovoltaic applications, the substitution of CH_3NH_3^+ with NH_4^+ and $(\text{CH}_3)_2\text{NH}_2^+$ in the HOIP crystal results in deviations from the tetragonal structure expected of phase-pure $\text{CH}_3\text{NH}_3\text{PbI}_3$, with a deleterious effect on the absorptivity of the resulting films. These results emphasize the importance of elucidating the under-appreciated precursor/solvent reactivity, the products of which, when incorporated into the solid state, can have profound effects on HOIP composition and structure, with a commensurate impact on macroscopic properties and device performance.

Status: published work at Chemistry of Materials 2019, **31**, 2114-2120

Sulfur-Donor Solvents Strongly Coordinate Pb^{2+} in Hybrid Organic–Inorganic Perovskite Precursor Solutions

J. Clay Hamill, Jr.,¹ Oluwaseun Romiluyi,² Sara A. Thomas,³ Jacquelyn Cetola,^{1,4} Jeffrey Schwartz,⁵ Michael F. Toney,⁶ Paulette Clancy,² and Yueh-Lin Loo^{1,7}

¹Department of Chemical and Biological Engineering, Princeton University, Princeton, NJ 08544, USA; ²Department of Chemical and Biomolecular Engineering, Johns Hopkins University, Baltimore, MD 21218, USA; ³Department of Geosciences and Andlinger Center for Energy and the Environment, Princeton University, Princeton, NJ 08544, USA; ⁴Department of Materials Science and Engineering, University of Florida, Gainesville, FL 32603, USA; ⁵Department of Chemistry, Princeton University, Princeton, NJ 08544, USA; ⁶Materials Science Division, Stanford Synchrotron Radiation Lightsource, Menlo Park, CA 94025, USA; ⁷Andlinger Center for Energy and the Environment, Princeton University, Princeton, NJ 08544, USA



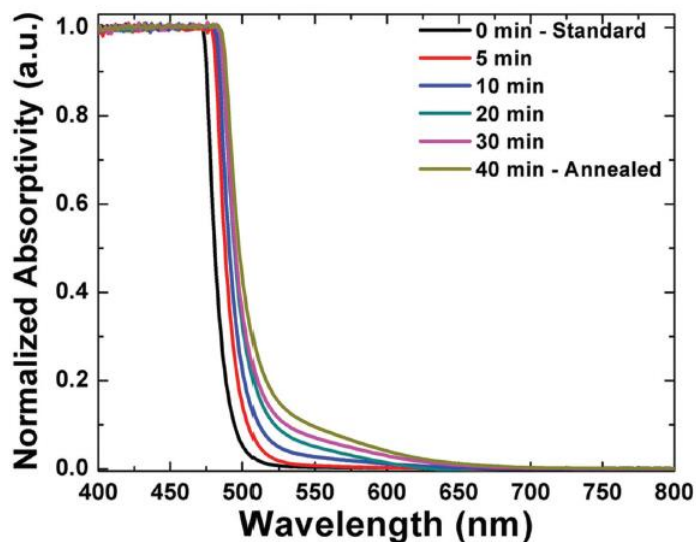
Strong coordination between Lewis-basic processing additives and the Lewis-acidic lead halide in hybrid organic–inorganic perovskite (HOIP) precursor solutions is required to solubilize the lead halide, and subsequently access the appropriate crystallization kinetics and attain the desired morphology of perovskite active layers. While oxygen-donor solvents and additives, such as dimethylformamide and dimethyl sulfoxide, are widely used for perovskite processing, we demonstrate that “soft” sulfur-donor solvents exhibit stronger coordination to the “borderline soft” Lewis acid Pb^{2+} center of PbI_2 relative to “hard” O-donor solvents in the precursor solution. The stronger coordination of S-donor solvents compared to O-donor solvents to Pb^{2+} implies that such compounds can be useful additives to HOIP precursor solutions. Density-functional calculations of the enthalpy change resulting from the coordination of solvents to Pb^{2+} provide direct numerical comparison of the strength of O-donor and S-donor coordination with Pb^{2+} and expands the library of candidate S-donor compounds. Our results provide a roadmap for processing additive selection and expand the previously limited choice of perovskite processing additives to include strongly coordinating S-donor compounds.

Status: published work at Journal of Physical Chemistry C 2020, **124**, 14496-14502

Precursor Solution Annealing Forms Cubic-Phase Perovskite and Improves Humidity Resistance of Solar Cells

Petr P. Khlyabich,¹ J. Clay Hamill Jr.,¹ and Yueh-Lin Loo^{1,2}

¹Department of Chemical and Biological Engineering, Princeton University, Princeton, NJ 08544, USA; ²Andlinger Center for Energy and the Environment, Princeton University, Princeton, NJ 08544, USA



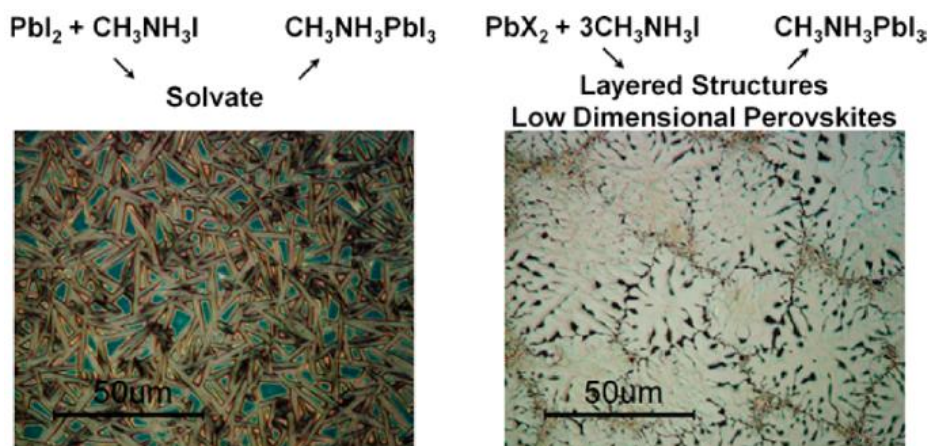
Solar cells with light-absorbing layers comprising organometal halide perovskites have recently exceeded 22% efficiency. Despite high power-conversion efficiencies, the stability of these devices, particularly when exposed to humidity and oxygen, remains poor. In the current study, a pathway to increase the stability of methylammonium lead iodide ($\text{CH}_3\text{NH}_3\text{PbI}_3$) based solar cells towards humidity is demonstrated, while maintaining the simplicity and solution-processability of the active layers. Thermal annealing of the precursor solution prior to deposition induces the formation of cubic-phase perovskite films in the solid state at room temperature. The experiments demonstrate that this improved ambient stability is correlated with the presence of the cubic phase at device operating temperatures, with the cubic phase resisting the formation of perovskite monohydrate—a pathway of degradation in conventionally processed perovskite thin films—on exposure to humidity.

Status: published work at *Advanced Functional Materials* 2018, **28**, 1801508

Crystalline Intermediates and Their Transformation Kinetics during the Formation of Methylammonium Lead Halide Perovskite Thin Films

Petr P. Khlyabich¹ and Yueh-Lin Loo²

¹Department of Chemical and Biological Engineering, Princeton University, Princeton, New Jersey 08544, United States; ²Andlinger Center for Energy and the Environment, Princeton University, Princeton, New Jersey 08544, United States



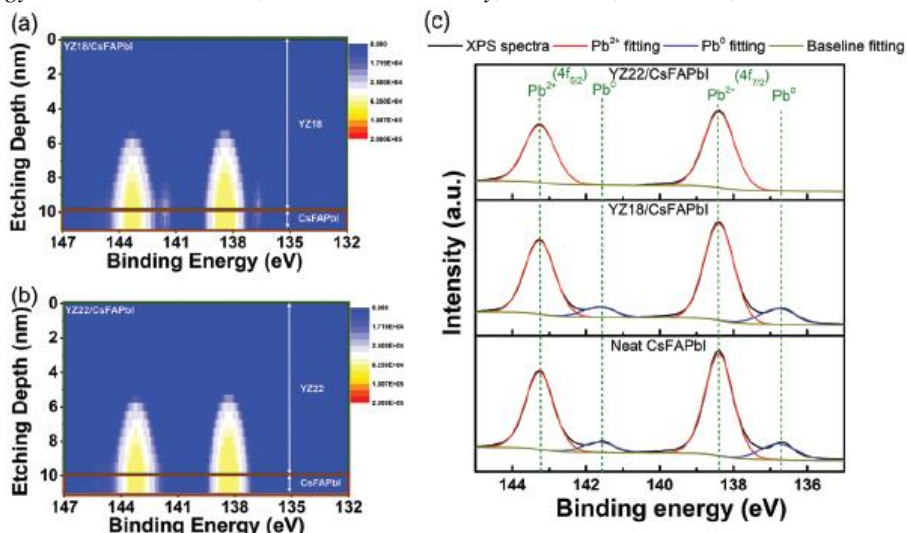
The morphology of methylammonium lead halide perovskite thin films significantly affects the performance of opto-electronic devices that comprise them. Using X-ray diffraction studies, we elucidated the mechanisms of thin-film formation to complete the complex picture of structural development of perovskites under an inert atmosphere. The presence of excess methylammonium iodide during perovskite crystallization leads to the formation of layered intermediates and low-dimensional perovskites; these intermediates are correlated with the formation of large and continuous grains in the final films. When the precursors are present in stoichiometric equivalence, initial stages of crystallization instead involve the formation of solvates; the fully crystallized films have poor surface coverage and comprise needle-like structures. The activation energy of crystallization in films with stoichiometric excess methylammonium iodide is higher than that for films comprising stoichiometrically equivalent precursors; the higher energy barrier is consistent with the need to sublime excess methylammonium iodide during film formation. Replacing lead iodide with lead chloride does not qualitatively alter the crystallization process or the final morphology; it lowers the activation energy for crystallization, presumably because sublimation of methylammonium chloride is less energetic than that of methylammonium iodide. Our study suggests the necessity of layered structures and low-dimensional perovskites for the formation of technologically relevant continuous thin films.

Status: published work at Chemistry of Materials 2016, **28**, 9041-9048

A hole-transport material that also passivates perovskite surface defects for solar cells with improved efficiency and stability

Xiaoming Zhao,¹ Chao Yao,¹ Kaichen Gu,¹ Tianran Liu,¹ Yu Xia,¹ and Yueh-Lin Loo.^{1,2}

¹Department of Chemical and Biological Engineering, Princeton University, Princeton, NJ 08544, USA. ²Andlinger Center for Energy and the Environment, Princeton University, Princeton, NJ 08544, USA



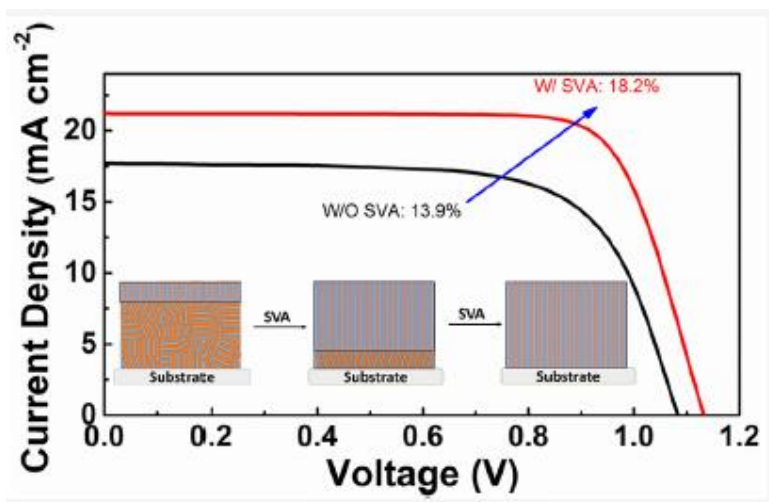
While typical perovskite solar cells (PSCs) with doped Spiro-OMeTAD as a hole transport material (HTM) have shown rapid increase in their power-conversion efficiencies (PCEs), their poor stability remains a big concern as the dopants and additives used with Spiro-OMeTAD have a strong tendency to diffuse into and degrade the perovskite active layer under normal operating conditions. Here, we report a facile design concept to functionalize HTMs so that they can passivate perovskite surface defects and enable perovskite active layers with lower density of surface trap states and more efficient charge transfer to the hole transport layer. As a consequence, perovskite solar cells with a functionalized HTM exhibit a champion PCE of 22.4%, the highest value for PSCs using dopant-free small molecular HTMs to date, and substantively improved operational stability under continuous illumination. With a T_{80} of (1617 ± 7) h for encapsulated cells tested at 30°C in air, the PSCs containing the functionalized HTM are among the most stable PSCs using dopant-free small-molecular HTMs. The effectiveness of our strategy is demonstrated in PSCs comprising both a state-of-the-art MA-free perovskite and MAPbI, a system having more surface defects, and implies the potential generality of our strategy for a broad class of perovskite systems, to further advance highly efficient and stable solar cells.

Status: published work at Energy & Environmental Science 2020, **13**, 4334-4343

Accessing Highly Oriented Two-Dimensional Perovskite Films via Solvent-Vapor Annealing for Efficient and Stable Solar Cells

Xiaoming Zhao,¹ Tianran Liu,² Alan B. Kaplan,² Chao Yao,¹ and Yueh-Lin Loo^{1,3}

¹Department of Chemical and Biological Engineering, Princeton University, Princeton, NJ 08544, USA; ²Department of Electrical Engineering, Princeton University, Princeton, NJ 08544, USA; ³Andlinger Center for Energy and the Environment, Princeton University, Princeton, NJ 08544, USA



Accessing vertical orientation of two-dimensional (2D) perovskite films is key to achieving high-performance solar cells with these materials. Herein, we report on solvent-vapor annealing (SVA) as a general postdeposition strategy to induce strong vertical orientation across broad classes of 2D perovskite films. We do not observe any local compositional drifts that would result in impure phases during SVA. Instead, our experiments point to solvent vapor plasticizing 2D perovskite films and facilitating their surface-induced reorientation and concomitant grain growth, which enhance out-of-plane charge transport. Solar cells with SVA 2D perovskites exhibit superior efficiency and stability compared to their untreated analogs. With a certified efficiency of $(18.00 \pm 0.30) \%$, our SVA (BDA)(Cs_{0.1}FA_{0.9})₄Pb₅I₁₆ solar cell boasts the highest efficiency among all solar cells with 2D perovskites ($n \leq 5$) reported so far.

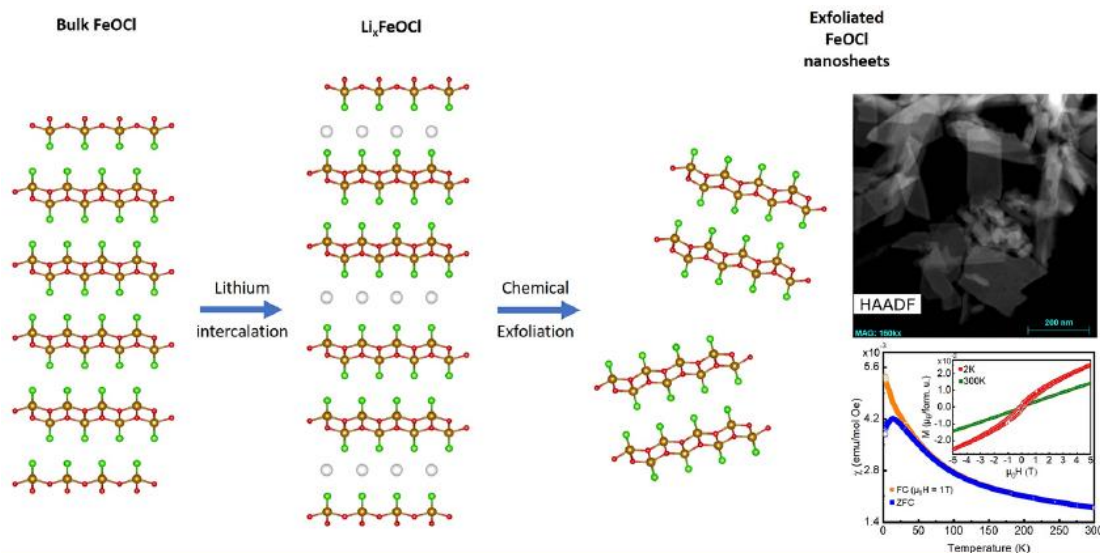
Status: published work at Nano Letters 2020

Department of Chemistry

Change in Magnetic Properties upon Chemical Exfoliation of FeOCl

Austin M. Ferrenti,¹ Sebastian Klemenz,¹ Shiming Lei,¹ Xiaoyu Song,¹ Pirmin Ganter,² Bettina V. Lotsch,² and Leslie M. Schoop¹

¹Department of Chemistry, Princeton University, Princeton, New Jersey 08544, United States; ²Max Planck Institute for Solid State Research, Heisenbergstraße 1, 70569 Stuttgart, Germany



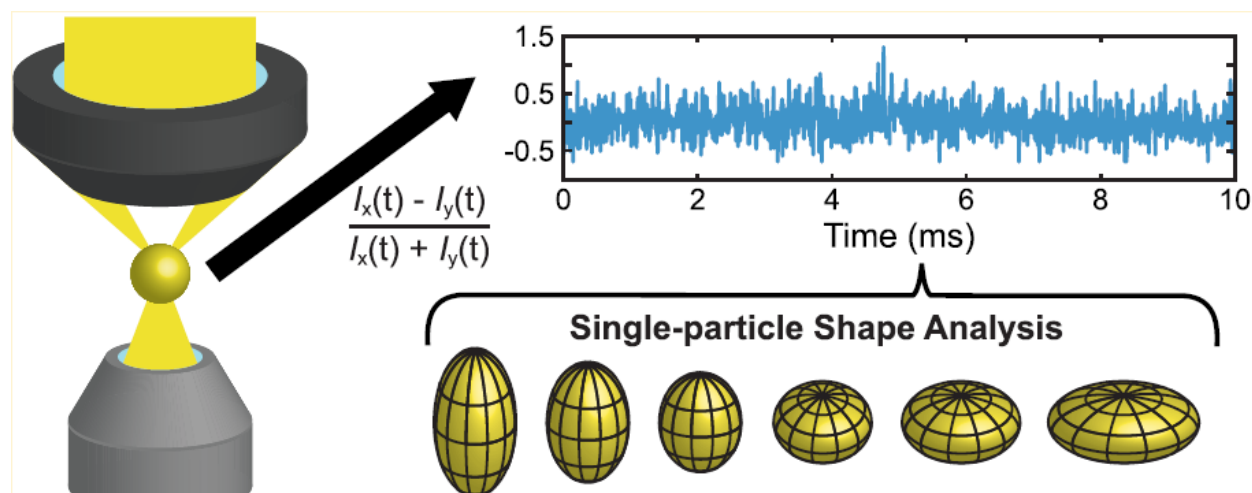
The development of novel, intrinsic two-dimensional (2D) antiferromagnets presents the opportunity to vastly improve the efficiency of spintronic devices and sensors. The strong intrinsic antiferromagnetism and van der Waals layered structure exhibited by the bulk transition-metal oxychlorides provide a convenient system for the synthesis of such materials. In this work, we report the exfoliation of bulk FeOCl into and subsequent characterization of intrinsically antiferromagnetic thin-layer FeOCl nanosheets. The magnetic properties of bulk FeOCl, its lithium intercalate, and its nanosheet pellet are measured to determine the evolution of magnetic properties from the three-dimensional to the quasi-two-dimensional system. This work establishes FeOCl and isostructural compounds as a source for the development of two-dimensional intrinsic antiferromagnets.

Status: published work at Inorg. Chem. 2020, **59**, 1176-1182

Single-Particle Dynamic Light Scattering: Shapes of Individual Nanoparticles

Luis F. Guerra, Tom W. Muir, and Haw Yang

Department of Chemistry, Princeton University, Frick Laboratory, Princeton, New Jersey 08544, United States



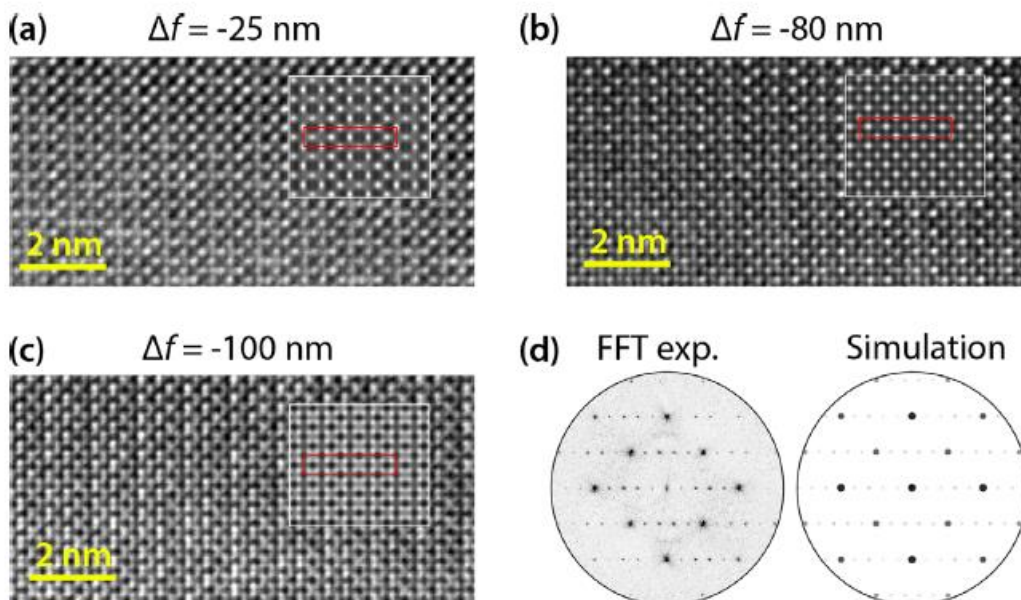
Metallic nanoparticles (MNPs) are prevalent in modern nanotechnologies due to their unique optical properties, chemical and photostability, and ease of manipulation. In particular, many recent advances have highlighted the importance of fundamentally understanding dynamic reconfiguration in MNP morphologies and compositions. Techniques to measure the shape of a single particle are lacking, however, often requiring immobilization, extensive numerical simulations, and irreversible alterations of the particle or its environment. In this work, we introduce “single-particle dynamic light scattering” (SP-DLS) as a far-field technique capable of analyzing the shape of individual, freely diffusing MNPs. Assuming symmetric-top rotors for MNPs and passively confining them to the focal volume of a dark-field microscope for long-term observation, we directly relate polarization dynamic fluctuations in the scattered light to the relative difference between the nondegenerate axes of individual particles. Our results show remarkable agreement with transmission electron microscopy analyses of the same population and allow for unprecedented measurements of the extent of prolate or oblate asphericity of nominally spherical MNPs in solution where the current implementation affords an asphericity detection limit of $\sim 2.5\%$ assuming a 10% relative error. SP-DLS should serve as a powerful, nondestructive technique for characterizing the shapes of individual MNPs and other nanostructures.

Status: published work at Nano Lett. 2019, **19**, 5530-5536

Charge Density Waves and Magnetism in Topological Semimetal Candidates $\text{GdSb}_x\text{Te}_{2-x-\delta}$

Shiming Lei,¹ Viola Duppel,² Judith M. Lippmann,² Jurgen Nuss,² Bettina V. Lotsch,^{2,3} and Leslie M. Schoop¹

¹Department of Chemistry, Princeton University, Princeton, NJ 08544, USA; ²Max Planck Institute for Solid State Research Heisenbergstraße 1, 70569 Stuttgart, Germany; ³Department of Chemistry, University of Munich (LMU), Butenandstraße 5-13 (Haus D), 81377 München, Germany



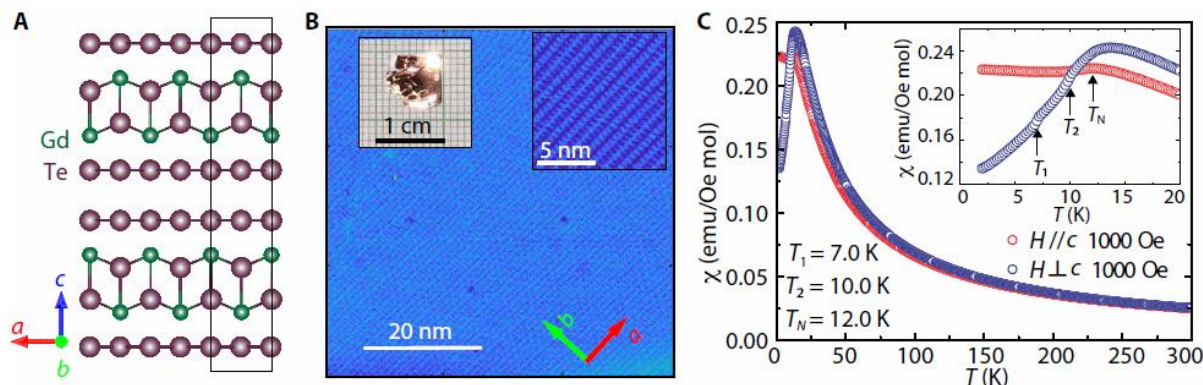
Many topological semimetals are known to exhibit exceptional electronic properties, which are the fundamental basis for design of novel devices and further applications. Materials containing the structural motif of a square net are known to frequently be topological semimetals. In this work, the synthesis and structural characterization of the square-net-based magnetic topological semimetal candidates $\text{GdSb}_x\text{Te}_{2-x-\delta}$ ($0 \leq x \leq 1$, δ indicating the vacancy level) are reported. The structural evolution of the series with Sb substitution is studied, finding a transition between a simple tetragonal square-net structure to complex superstructure formations due to the presence of charge density waves. The structural modulations coincide with a significant modification of the magnetic order. This work thus establishes $\text{GdSb}_x\text{Te}_{2-x-\delta}$ as a platform to study the interplay between crystal symmetry, band filling, charge density wave, and magnetism in a topological semimetal candidate.

Status: published work at Advanced Quantum Technology 2019, **2**, 1900045

High mobility in a van der Waals layered antiferromagnetic metal

Shiming Lei,¹ Jingjing Lin,² Yanyu Jia,² Mason Gray,³ Andreas Topp,⁴ Gelareh Farahi,² Sebastian Klemenz,¹ Tong Gao,² Fanny Rodolakis,⁵ Jessica L. McChesney,⁵ Christian R. Ast,⁴ Ali Yazdani,² Kenneth S. Burch,³ Sanfeng Wu,² Nai Phuan Ong,² Leslie M. Schoop¹

¹Department of Chemistry, Princeton University, Princeton, NJ 08544, USA. ²Department of Physics, Princeton University, Princeton, NJ 08544, USA. ³Department of Physics, Boston College, Boston, MA 02467, USA. ⁴Max-Planck-Institut für Festkörperforschung, Heisenbergstraße 1, D-70569 Stuttgart, Germany. ⁵Argonne National Laboratory, 9700 South Cass Avenue, Argonne, IL 60439, USA.

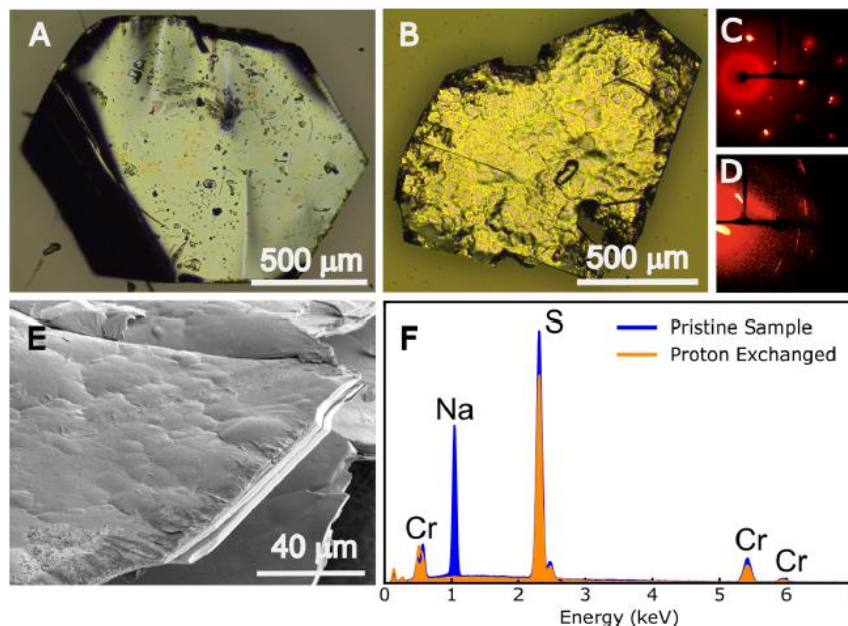


Van der Waals (vdW) materials with magnetic order have been heavily pursued for fundamental physics as well as for device design. Despite the rapid advances, so far, they are mainly insulating or semiconducting, and none of them has a high electronic mobility—a property that is rare in layered vdW materials in general. The realization of a high-mobility vdW material that also exhibits magnetic order would open the possibility for novel magnetic twistronic or spintronic devices. Here, we report very high carrier mobility in the layered vdW antiferromagnet GdTe₃. The electron mobility is beyond 60,000 cm² V⁻¹ s⁻¹, which is the highest among all known layered magnetic materials, to the best of our knowledge. Among all known vdW materials, the mobility of bulk GdTe₃ is comparable to that of black phosphorus. By mechanical exfoliation, we further demonstrate that GdTe₃ can be exfoliated to ultrathin flakes of three monolayers.

Status: published work at Science Advances 2020, **6**, eaay6407

Soft Chemical Synthesis of H_xCrS_2 : An Antiferromagnetic Material with Alternating Amorphous and Crystalline Layers

Xiaoyu Song,¹ Guangming Cheng,² Daniel Weber,³ Florian Pielhofer,⁴ Shiming Lei,¹ Sebastian Klemenz,¹ Yao-Wen Yeh,² Kai A. Filsinger,⁵ Craig B. Arnold,⁵ Nan Yao,² and Leslie M. Schoop¹
¹Department of Chemistry, Princeton University, Princeton, NJ 08544, USA; ²Princeton Institute for Science and Technology of Materials, Princeton, NJ 08544, USA; ³Department of Chemistry, Ohio State University, Columbus, OH 43201, USA; ⁴Institute of Inorganic Chemistry, University of Regensburg, D-93040 Regensburg, Germany; ⁵Department of Mechanical and Aerospace Engineering, Princeton University, Princeton, NJ 08544, USA



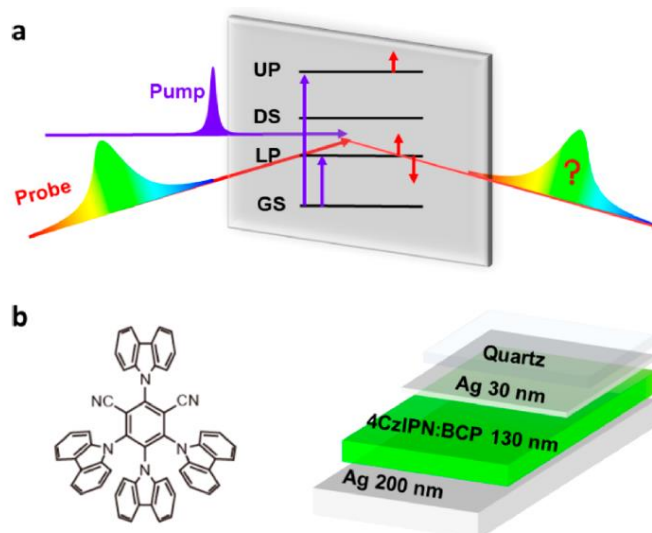
We report a new H_xCrS_2 -based crystalline/amorphous layered material synthesized by soft chemical methods. We study the structural nature and composition of this material with atomic resolution scanning transmission electron microscopy (STEM), revealing a complex structure consisting of alternating layers of amorphous and crystalline lamellae. Furthermore, the magnetic properties show evidence for increased magnetic frustration compared to the parent compound $NaCrS_2$. Finally, we show that this material can be exfoliated, thus providing a facile synthesis method for chromium-sulfide-based ultrathin layers. The material reported herein can not only be a source of new thin TMD-related sheets for potential application in catalysis but also be of interest for realizing new 2D magnetic materials.

Status: published work at Journal of the American Chemical Society 2019, **141**, 15634-15640

Polariton Transitions in Femtosecond Transient Absorption Studies of Ultrastrong Light–Molecule Coupling

Courtney A. DelPo,¹ Bryan Kudisch,¹ Kyu Hyung Park,¹ Saeed-Uz-Zaman Khan,² Francesca Fassioli,^{1,3} Daniele Fausti,^{1,4,5} Barry P. Rand,^{2,6} and Gregory D. Scholes¹

¹Department of Chemistry, Princeton University, Princeton, New Jersey 08544, United States; ²Department of Electrical Engineering, Princeton University, Princeton, New Jersey 08544, United States; ³SISSA– Scuola Internazionale Superiore di Studi Avanzati, Trieste 34136, Italy; ⁴Department of Physics, University of Trieste, 34127 Trieste, Italy; ⁵Elettra-Sincrotrone Trieste S.C.p.A., 34149 Basovizza, Trieste, Italy; ⁶Andlinger Center for Energy and the Environment, Princeton University, Princeton, New Jersey 08544, United States



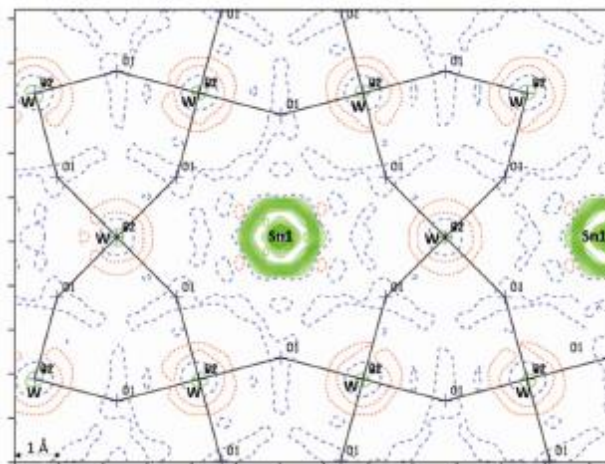
Strong light–matter coupling is emerging as a fascinating way to tune optical properties and modify the photophysics of molecular systems. In this work, we studied a molecular chromophore under strong coupling with the optical mode of a Fabry–Perot cavity resonant to the first electronic absorption band. Using femtosecond pump–probe spectroscopy, we investigated the transient response of the cavity-coupled molecules upon photoexcitation resonant to the upper and lower polaritons. We identified an excited state absorption from upper and lower polaritons to a state at the energy of the second cavity mode. Quantum mechanical calculations of the many molecule energy structure of cavity polaritons suggest assignment of this state as a two-particle polaritonic state with optically allowed transitions from the upper and lower polaritons. We provide new physical insight into the role of two-particle polaritonic states in explaining transient signatures in hybrid light–matter coupling systems consistent with analogous many-body systems.

Status: published work in *J. Phys. Chem. Lett.* 2020, **11**, 2667-1674

Sn_{0.24}WO₃ hexagonal tungsten bronze prepared via the metal chloride route

Lun Jin, Shu Guo, Robert J. Cava

Department of Chemistry, Princeton University, Princeton, NJ, 08544, USA



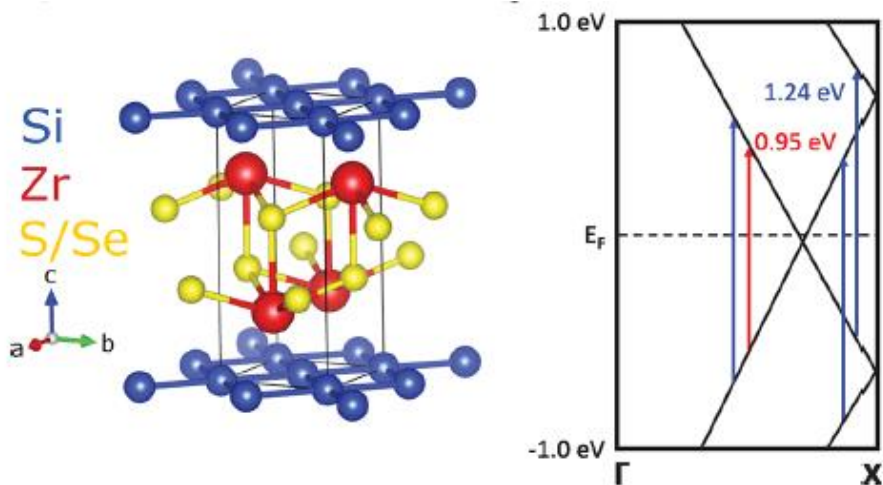
We report the synthesis of Sn_{0.24}WO₃ single crystals via an alternative, less well-known, solid-state synthetic approach that involves the use of tin chloride as a starting material. The compound adopts an unusual variant of the hexagonal tungsten bronze structure in space group P6/mmm ($a = 7.4264(7)$ Å and $c = 3.7843(4)$ Å) with a previously unreported distribution of Sn cations, disordered over two distinct sites in the tunnels. Sn_{0.24}WO₃ shows no signs of superconductivity down to 170 mK and exhibits weakly-metallic conducting behavior.

Status: published work in *J. Solid State Chem.* 2020, **291**, 121553

Transient Drude Response Dominates Near-Infrared Pump–Probe Reflectivity in Nodal-Line Semimetals ZrSiS and ZrSiSe

Robert J. Kirby,¹ Austin Ferrenti,¹ Caroline Weinberg,¹ Sebastian Klemenz,¹ Mohamed Oudah,^{1,2} Shiming Lei,¹ Chris P. Weber,³ Daniele Fausti,^{1,4} Gregory D. Scholes,¹ and Leslie M. Schoop¹

¹Department of Chemistry, Princeton University, Princeton, NJ 08544, USA; ²Quantum Matter Institute, University of British Columbia, Vancouver, BC V6T 1Z4, Canada; ³Department of Physics, Santa Clara University, Santa Clara, CA 95053-0315, USA; ⁴Department of Physics, Università degli Studi di Trieste, Trieste I-34127, Italy; Sincrotrone Trieste S.C.p.A., Trieste I-34012, Italy



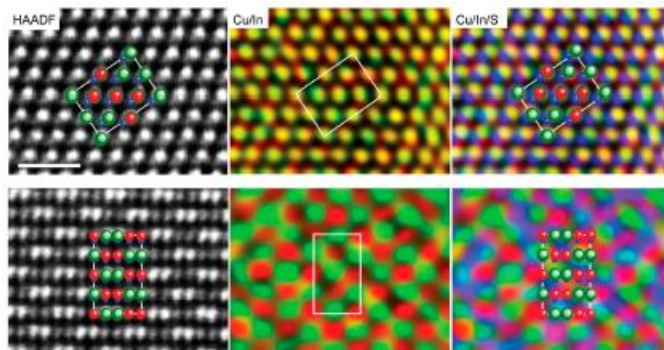
The ultrafast optical response of nodal-line semimetals ZrSiS and ZrSiSe was studied in the near-infrared using transient reflectivity. The materials exhibit similar responses, characterized by two features, well-resolved in time and energy; the first decays after hundreds of femtoseconds, and the second lasts for nanoseconds. Using Drude–Lorentz fits of the materials’ equilibrium reflectance, we show that these are well-represented by a sudden change of the electronic properties (increase of screening or reduction of the plasma frequency) followed by an increase of the Drude scattering rate. This directly connects the transient data to a physical picture in which carriers, after excitation into the conduction band, return to the valence band by sharing excess energy with the phonon bath, resulting in a hot lattice that relaxes through slow diffusive processes. The emerging picture reveals that the sudden electronic reorganization instantaneously modifies the materials’ electronic properties on a time scale not compatible with electron–phonon thermalization.

Status: published work at J. Phys. Chem. Lett. 2020, **11**, 6105-6111

Observation of $[V_{Cu}^{1-} In_i^{2+} V_{Cu}^{1-}]$ Defect Triplets in Cu-Deficient $CuInS_2$

Jessica J. Frick,¹ Guangming Cheng,² Satya Kushwaha,¹ Nan Yao,² Sigurd Wagner,³ Andrew B. Bocarsly,¹ and Robert J. Cava¹

¹Department of Chemistry, Princeton University, Princeton, NJ 08544, USA; ²PRISM, Princeton University, Princeton, NJ 08544, USA; ³Department of Electrical Engineering, Princeton University, Princeton, NJ 08544, USA



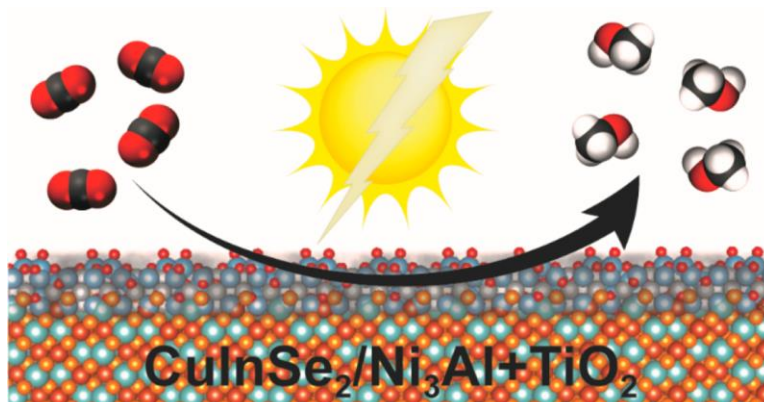
Copper indium disulfide ($CuInS_2$) is a semiconductor with a direct energy band gap of 1.53 eV – an optimal value for highly efficient thin-film solar cells. But it has reached only $\sim 11\%$ power conversion efficiency, far less than the theoretically achievable value of $\sim 30\%$. The cause of this low performance is not understood. A single crystal grown from 1 mol % Cu-deficient melt was studied by using high-angle annular dark-field (HAADF) scanning transmission electron microscopy (STEM) and electron dispersive spectroscopy (EDS). While the bulk crystal is exactly stoichiometric $CuInS_2$, it contains nanometer thick, Cu-deficient interphases that form along rotational twin boundaries in the $\{112\}$ plane. Transition zones from the bulk crystal to the interphase are observed, where In is seen to move from its normal site In_{In} in the chalcopyrite structure to a tetrahedral interstitial site In_i , while Cu remains in its normal Cu_{Cu} position. The concentrations of Cu_{Cu} and In_i reflect a ratio of Cu vacancies, V_{Cu} , to an excess In_i of ~ 2 . Their relative lattice positions, and the high electrical resistivity of the crystal, suggest that V_{Cu} and excess In_i “precipitate” as self-compensating, electrically neutral, $[V_{Cu}^{1-} In_i^{2+} V_{Cu}^{1-}]$ defect triplets. This is the first atomic-level observation of the ordered defect that has been invoked as the basic structural modifier in chalcopyrite compound homologues. The interphases introduce an optical gap of 1.47 eV. The overall result is that making $CuInS_2$ slightly copper-poor inserts nanometer thick layers of the interphase into the bulk crystal. This study shows that apparently conflicting results of the effect of Cu deficiency on $CuInS_2$ thin-film solar cells may be resolved by analyzing structure and composition at nanometer spatial resolution.

Status: published work at J. Phys. Chem. C 2020, **124**, 26415-26427

Catalytic Mismatching of CuInSe_2 and Ni_3Al Demonstrates Selective Photoelectrochemical CO_2 Reduction to Methanol

Brian M. Foster, Aubrey R. Paris, Jessica J. Frick, Daniel A. Blasini-Pérez, Robert J. Cava, and Andrew B. Bocarsly

Department of Chemistry, Princeton University, Princeton, NJ 08544, USA



Photoelectrochemical catalysts are often plagued by ineffective interfacial charge transfer or nonideal optical conversion properties. To overcome this challenge, strategically pairing a catalytically inactive, optically proficient semiconductor with a selective electrocatalyst, coined “catalytic mismatching”, is suggested. Here, chalcopyrite semiconductor CuInSe_2 is paired with the electrocatalyst Ni_3Al to selectively reduce CO_2 . This catalytically mismatched system produces methanol at a Faradaic efficiency 25 times greater than that achieved using the purely electrochemical Ni_3Al system while reducing the operating potential requirement by 600 mV. These results suggest that catalytic mismatching is a promising tactic to achieve reaction selectivity in synergistic photoelectrochemical CO_2 reduction systems.

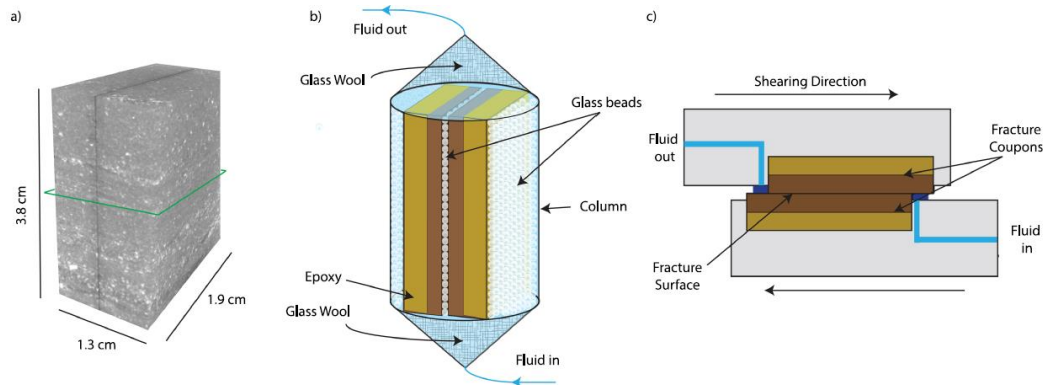
Status: published work at ACS Appl. Energy Mater. 2020, **3**, 109-113

Department of Civil and Environmental Engineering

Collapse of Reacted Fracture Surface Decreases Permeability and Frictional Strength

K. Spokas,¹ Y. Fang,^{2,3} J. P. Fitts,¹ C. A. Peters,¹ and D. Elsworth²

¹Civil and Environmental Engineering Department, Princeton University, Princeton, NJ, USA; ²Energy and Mineral Engineering, Pennsylvania State University, University Park, PA, USA; ³Jackson School of Geosciences, Now at University of Texas at Austin, Austin, TX, USA



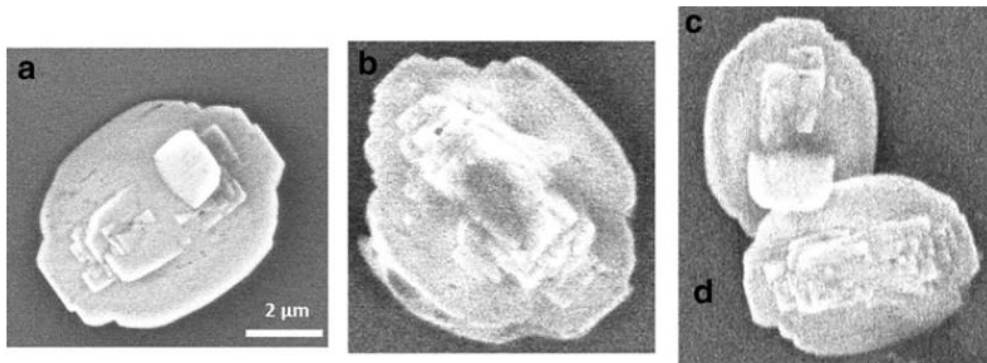
Geochemical and geomechanical perturbations of the subsurface caused by the injection of fluids present risks of leakage and seismicity. This study investigated how acidic fluid flow affects hydraulic and frictional properties of fractures using experiments with 3.8-cm-long specimens of Eagle Ford shale, a laminated shale with carbonate-rich strata. In low-pressure flow cells, one set of samples was exposed to acidic brine and another set was exposed to neutral brine. X-ray computed tomography (μ CT) and energy-dispersive X-ray spectroscopy (EDS-SEM) revealed that samples exposed to acidic brine were calcite-depleted and had developed a porous altered layer, while the other set showed no evidence of alteration. After reaction, samples were compressed and sheared in a triaxial cell that supplied normal stress and differential pore pressure at prescribed sliding velocities, independently measuring friction and permeability. During the initial compression, the porous altered layer collapsed into fine particles that filled the fracture. This effectively impeded flow and sealed the fracture, resulting in fracture permeability to decrease 1 to 2 orders of magnitude relative to the unaltered fractures. Coupled geochemical and geomechanical processes that could favorably seal fractures could also increase the likelihood of induced seismicity. These findings have important implications for geological carbon sequestration, pressurized fluid energy storage, geothermal energy, and other subsurface technologies.

Status: published work at J. Geophys. Research: Solid Earth 2019, **124**, 12799

Metals Coprecipitation with Barite: Nano-XRF Observation of Enhanced Strontium Incorporation

Heather A. Hunter, Florence T. Ling, and Catherine A. Peters

Department of Civil & Environmental Engineering, Princeton University, Princeton, NJ 08544, USA



Coprecipitation can be an effective treatment method for the removal of environmentally relevant metals from industrial wastewaters such as produced waters from the oil and gas industry. The precipitation of barite, BaSO_4 , through the addition of sulfate removes barium while coprecipitating strontium and other alkaline earth metals even when these are present at concentrations below their solubility limit. Among other analytical methods, X-ray fluorescence (XRF) nanospectroscopy at the Hard X-ray Nanoprobe (HXN) beamline at the National Synchrotron Light Source II (NSLS-II) was used to quantify Sr incorporation into barite. Thermodynamic modeling of $(\text{Ba,Sr})\text{SO}_4$ solid solutions was done using solid solution—aqueous solution (SS-AS) theory. The quantitative, high-resolution nano-XRF data show clearly that the Sr content in $(\text{Ba,Sr})\text{SO}_4$ solid solutions varies widely among particles and even within a single particle. We observed substantial Sr incorporation that is far larger than thermodynamic models predict, likely indicating the formation of metastable solid solutions. We also observed that increasing barite supersaturation of the aqueous phase led to increased Sr incorporation, as predicted by available kinetic models. These results suggest that coprecipitation offers significant potential for designing treatment systems for aqueous metals' removal in desired metastable compositions. Solution conditions may be optimized to enhance the incorporation of Sr by increasing sulfate addition such that the barite saturation index remains above ~ 3 or by increasing the aqueous Sr to Ba ratio.

Status: published work at *Environmental Engineering Science* 2020, **37**, 235-245

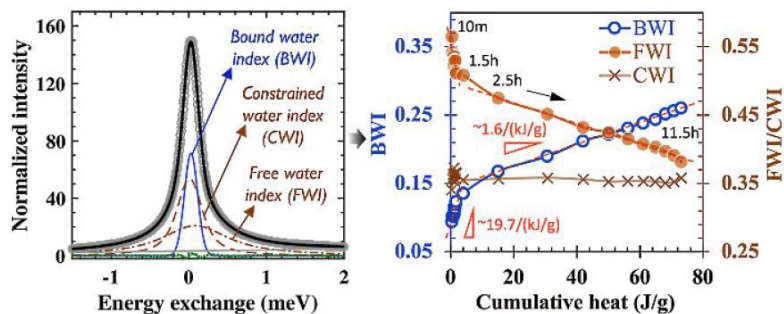
In situ quasi-elastic neutron scattering study on the water dynamics and reaction mechanisms in alkali-activated slags

Kai Gong,^{1,2} Yongqiang Cheng,³ Luke L. Daemen,³ Claire E. White,^{1,2}

¹Department of Civil and Environmental Engineering, Princeton University, Princeton NJ

08544, USA; ²Andlinger Center for Energy and the Environment, Princeton University, Princeton NJ 08544, USA;

³Chemical and Engineering Materials Division, Oak Ridge National Laboratory, Oak Ridge TN 37830, USA.



In this study, in situ quasi-elastic neutron scattering (QENS) has been employed to probe the water dynamics and reaction mechanisms occurring during the formation of NaOH- and Na₂SiO₃-activated slags, an important class of low-CO₂ cements, in conjunction with isothermal conduction calorimetry (ICC), Fourier transform infrared spectroscopy (FTIR) analysis and N₂ sorption measurements. We show that the single ICC reaction peak in the NaOH-activated slag is accompanied with a transformation of free water to bound water (from QENS analysis), which directly signals formation of a sodium-containing aluminum-substituted calcium-silicate-hydrate (C-(N)-A-S-H) gel, as confirmed by FTIR. In contrast, the Na₂SiO₃-activated slag sample exhibits two distinct reaction peaks in the ICC data, where the first reaction peak is associated with conversion of constrained water to bound and free water, and the second peak is accompanied with conversion of free water to bound and constrained water. The second conversion is attributed to formation of the main reaction product (i.e., C-(N)-A-S-H gel) as confirmed by FTIR and N₂ sorption data. Analysis of the QENS, FTIR and N₂ sorption data together with information from the literature explicitly shows that the first reaction peak is associated with the formation of an initial gel (similar to C-(N)-A-S-H gel) that is governed by the Na⁺ ions and silicate species in Na₂SiO₃ solution and the dissolved Ca/Al species from slag. Hence, this study exemplifies the power of in situ QENS, and has provided important mechanistic insight on the early-age reactions occurring during formation of two alkali-activated slags.

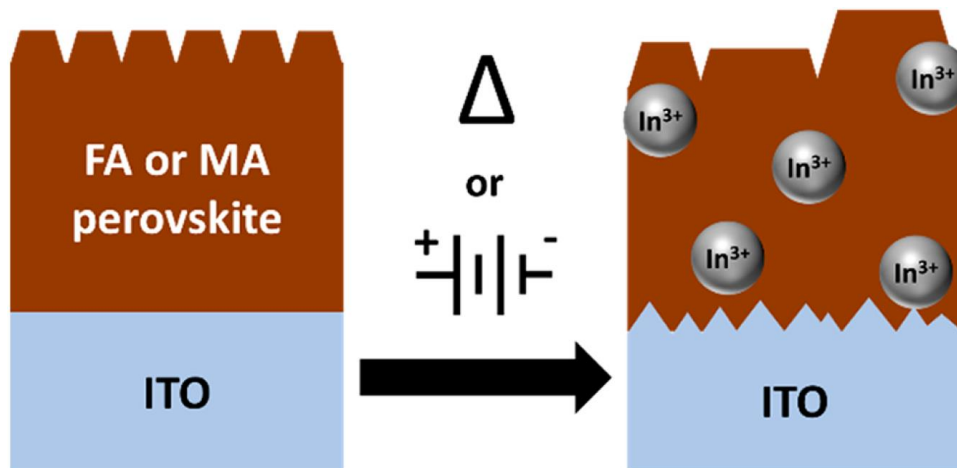
Status: published work at Phys. Chem. Chem. Phys. 2019, **21**, 10277-10292

Department of Electrical Engineering

Electrochemical and Thermal Etching of Indium Tin Oxide by Solid-State Hybrid Organic-Inorganic Perovskites

Ross A. Kerner¹ and Barry P. Rand^{1,2}

¹Department of Electrical Engineering and ²Andlinger Center for Energy and the Environment, Princeton University, Princeton, New Jersey 08544, United States



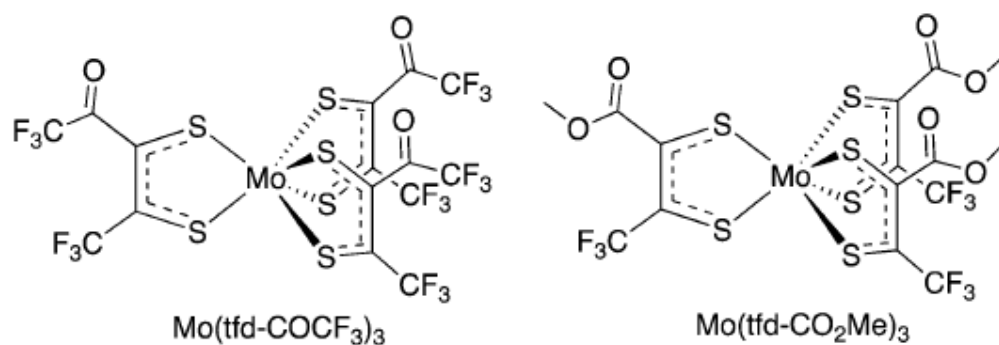
We show that tin-doped indium oxide (ITO) can be thermally etched by the Brønsted acid salts methyl-ammonium iodide (MAI), methylammonium lead triiodide (MAPbI₃), and formamidinium lead triiodide (FAPbI₃) in solid-state films and devices at common processing temperatures. More importantly, a series of reactions within an ITO/hybrid perovskite/Au device can be electrochemically induced near room temperature by applied cathodic voltages as low as -1.2 V. Cyclic voltammetry in this range leads to eventual In^{3+} leaching into the perovskite layer in the form of InI_3 , unambiguously identified by a binding energy signature of 445.9–446.3 eV measured by X-ray photoelectron spectroscopy. Furthermore, the etching is exacerbated by defects generated by O₂-plasma treatment of the ITO compared to UV-ozone cleaning, lowering the reaction potential and the electrochemical stability window of an ITO/MAPbI₃/Au device. Low-temperature, electrochemical reactivity at this interface has implications on operational stability, fundamental studies of hybrid perovskite materials, electron (or hole) transport layer free perovskite devices, reverse bias degradation, and other applications where ITO/hybrid perovskite contact is possible.

Status: published work at ACS Appl. Energy Mater. 2019, **2**, 6097-6101

Interfacial charge-transfer doping of metal halide perovskites for high performance photovoltaics

Nakita K. Noel,^{1,2} Severin N. Habisreutinger,³ Alba Pellaroque,⁴ Federico Pulvirenti,⁵ Bernard Wenger,⁴ Fengyu Zhang,¹ Yen-Hung Lin,⁴ Obadiah G. Reid,^{3,6} Johannes Leisen,⁵ Yadong Zhang,⁵ Stephen Barlow,⁵ Seth R. Marder,⁵ Antoine Kahn,¹ Henry J. Snaith,⁴ Craig B. Arnold,² and Barry P. Rand^{1,7}

¹Department of Electrical Engineering, Princeton University, Princeton, NJ, 08544, USA. ²Princeton Institute for the Science and Technology of Materials, Princeton University, Princeton, NJ, 08544, USA. ³National Renewable Energy Laboratory, 15013 Denver West Parkway, Golden, Colorado, 80401, USA. ⁴Clarendon Laboratory, Department of Physics, University of Oxford, Parks Road, Oxford, OX1 3PU, UK. ⁵School of Chemistry and Biochemistry and Center for Organic Photonics and Electronics, Georgia Institute of Technology, Atlanta, Georgia 30332-0400, USA. ⁶Renewable and Sustainable Energy Institute, University of Colorado at Boulder, Boulder, CO 80309, USA. ⁷Andlinger Center for Energy and the Environment, Princeton University, Princeton, NJ, 08544, USA



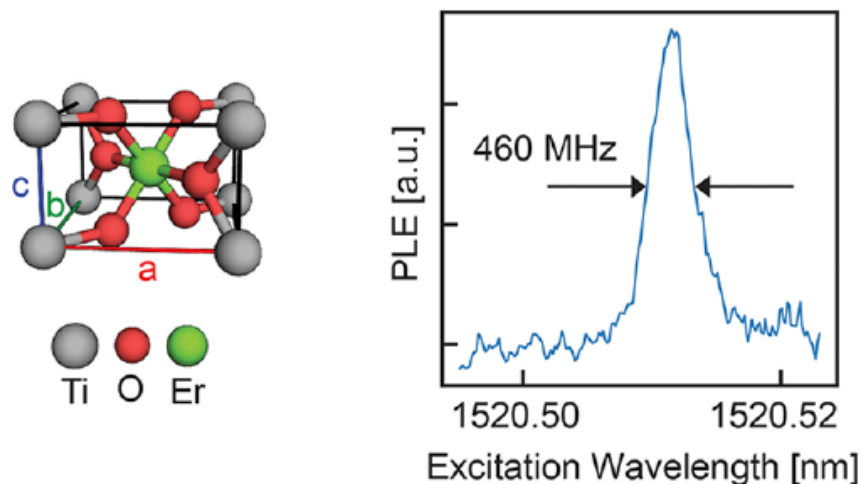
In this study, we use surface doping of the mixed-cation, mixed-halide perovskite FA_{0.85}MA_{0.15}Pb(I_{0.85}Br_{0.15})₃ to improve the hole extraction from the perovskite solar cell. By treating the surface of the perovskite film with a strongly oxidizing molybdenum tris(dithiolene) complex, we achieve a shift in the work function that is indicative of p-doping. The resulting p-doped interface constitutes a homojunction with increased hole-selectivity. With charge-selective layers, the surface doping enhances the device performance of perovskite solar cells resulting in steady-state efficiencies approaching 21%. Finally, we demonstrate that a surface treatment with this dopant produces the same effect as the commonly employed additive 4-*tert* butylpyridine (*t*BP), allowing us to achieve “*t*BP-free” devices with steady-state efficiencies of over 20%, and enhanced thermal stability as compared to devices processed using *t*BP. Our findings demonstrate that molecular doping is a feasible route to tune and control the surface properties of metal halide perovskites.

Status: published work at Energy Environ. Sci. 2019, **12**, 3063-3073

Narrow Optical Line Widths in Erbium Implanted in TiO₂

Christopher M. Phenicie,[†] Paul Stevenson,[†] Sacha Welinski,[†] Brendon C. Rose,[†] Abraham T. Asfaw,[†] Robert J. Cava,[‡] Stephen A. Lyon,[†] Nathalie P. de Leon,[†] and Jeff D. Thompson[†]

[†]Department of Electrical Engineering and [‡]Department of Chemistry, Princeton University, Princeton, New Jersey 08544, United States



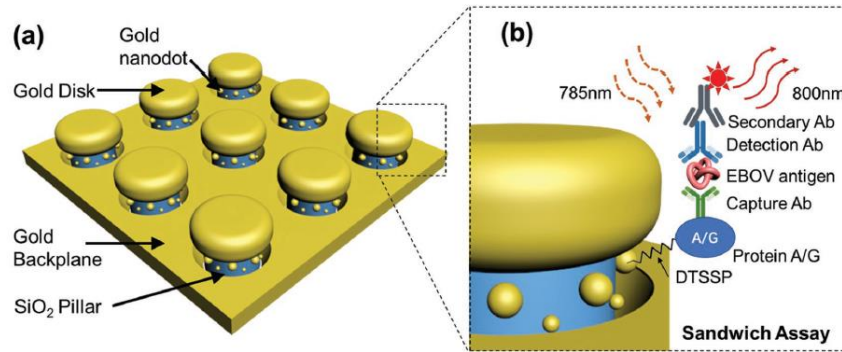
Atomic and atomlike defects in the solid state are widely explored for quantum computers, networks, and sensors. Rare earth ions are an attractive class of atomic defects that feature narrow spin and optical transitions that are isolated from the host crystal, allowing incorporation into a wide range of materials. However, the realization of long electronic spin coherence times is hampered by magnetic noise from abundant nuclear spins in the most widely studied host crystals. Here, we demonstrate that Er³⁺ ions can be introduced via ion implantation into TiO₂, a host crystal that has not been studied extensively for rare earth ions and has a low natural abundance of nuclear spins. We observe efficient incorporation of the implanted Er³⁺ into the Ti⁴⁺ site (>50% yield) and measure narrow inhomogeneous spin and optical line widths (20 and 460 MHz, respectively) that are comparable to bulk-doped crystalline hosts for Er³⁺. This work demonstrates that ion implantation is a viable path to studying rare earth ions in new hosts and is a significant step toward realizing individually addressed rare earth ions with long spin coherence times for quantum technologies.

Status: published work at Nano Letters 2019, **19**, 8928-8933

Ultrasensitive Ebola Virus Antigen Sensing via 3D Nanoantenna Arrays

Faheng Zang,¹ Zhijuan Su,¹ Liangcheng Zhou,¹ Krishnamurthy Konduru,² Gerardo Kaplan,² and Stephen Y. Chou¹

¹Department of Electrical Engineering, Princeton University, Princeton, NJ 08544, USA; ²Laboratory of Emerging Pathogens Center for Biologics Evaluation and Research Food and Drug Administration, Silver Spring, MD 20993, USA



Sensitive detection of pathogens is crucial for early disease diagnosis and quarantine, which is of tremendous need in controlling severe and fatal illness epidemics such as of Ebola virus (EBOV) disease. Serology assays can detect EBOV-specific antigens and antibodies cost-effectively without sophisticated equipment; however, they are less sensitive than reverse transcriptase polymerase chain reaction (RT-PCR) tests. Herein, a 3D plasmonic nanoantenna assay sensor is developed as an on-chip immunoassay platform for ultrasensitive detection of Ebola virus (EBOV) antigens. The EBOV sensor exhibits substantial fluorescence intensity enhancement in immunoassays compared to flat gold substrate. The nanoantenna-based biosensor successfully detects EBOV soluble glycoprotein (sGP) in human plasma down to 220 fg mL^{-1} , a significant 240 000-fold sensitivity improvement compared to the 53 ng mL^{-1} EBOV antigen detection limit of the existing rapid EBOV immunoassay. In a mock clinical trial, the sensor detects sGP-spiked human plasma samples at two times the limit of detection with 95.8% sensitivity. The results combined highlight the nanosensor's extraordinary capability of detecting EBOV antigen at ultralow concentration compared to existing immunoassay methods. It is a promising next-generation bioassay platform for early-stage disease diagnosis and pathogen detection for both public health and national security applications.

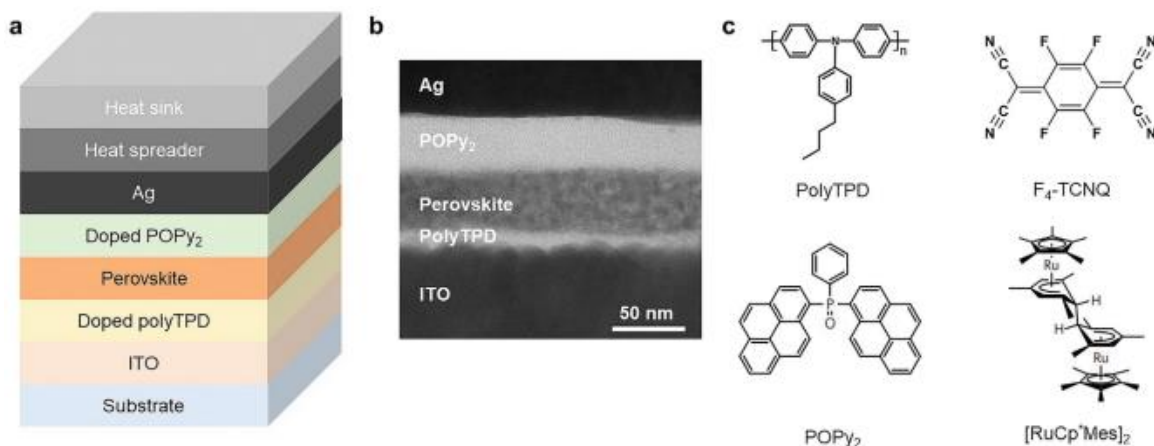
Status: published work at Adv. Mater. 2019, **31**, 1902331

Thermal Management Enables Bright and Stable Perovskite Light-Emitting Diodes

Lianfeng Zhao¹, Kwangdong Roh¹, Sara Kacmoli¹, Khaled Al Kurdi², Samik Jhulki², Stephen Barlow², Seth R. Marder², Claire Gmachl¹, and Barry P. Rand^{1,3}

¹Department of Electrical Engineering, Princeton University, Princeton, NJ 08544, USA; ²School of Chemistry and Biochemistry Center for Organic Electronics, Georgia Institute of Technology, Atlanta, GA 30332-0400, USA;

³Andlinger Center for Energy and the Environment, Princeton University, Princeton, NJ 08544, USA

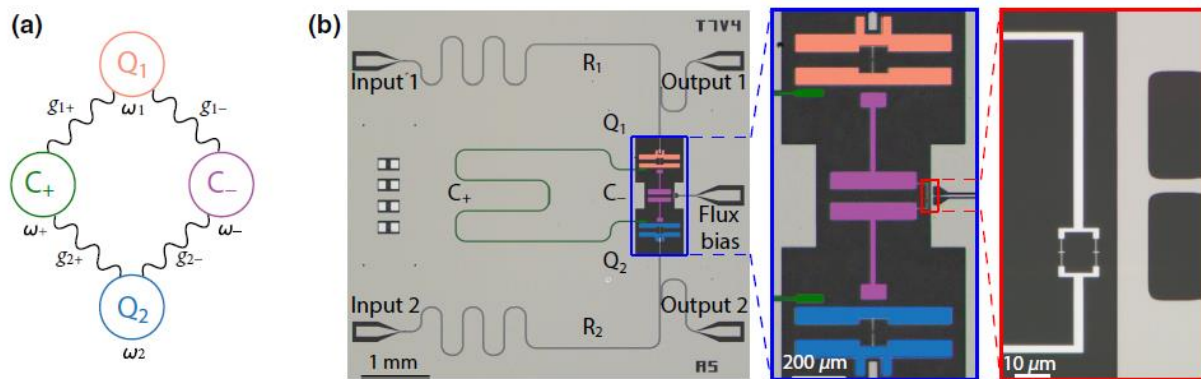


The performance of lead-halide perovskite light-emitting diodes (LEDs) has increased rapidly in recent years. However, most reports feature devices operated at relatively small current densities ($<500 \text{ mA cm}^{-2}$) with moderate radiance ($<400 \text{ W sr}^{-1}\text{m}^{-2}$). Here, Joule heating and inefficient thermal dissipation are shown to be major obstacles toward high radiance and long lifetime. Several thermal management strategies are proposed in this work, such as doping charge-transport layers, optimizing device geometry, and attaching heat spreaders and sinks. Combining these strategies, high-performance perovskite LEDs are demonstrated with maximum radiance of $2555 \text{ W sr}^{-1}\text{m}^{-2}$, peak external quantum efficiency (EQE) of 17%, considerably reduced EQE roll-off (EQE $> 10\%$ to current densities as high as 2000 mA cm^{-2}), and tenfold increase in operational lifetime (when driven at 100 mA cm^{-2}). Furthermore, with proper thermal management, a maximum current density of 2.5 kA cm^{-2} and an EQE of $\approx 1\%$ at 1 kA cm^{-2} are shown using electrical pulses, which represents an important milestone toward electrically driven perovskite lasers.

Status: published work at Adv. Mater. 2020, **32**, 2000752

Suppression of Qubit Crosstalk in a Tunable Coupling Superconducting Circuit

Pranav Mundada, Gengyan Zhang, Thomas Hazard, and Andrew Houck
Department of Electrical Engineering, Princeton University, Princeton, NJ 08540, USA



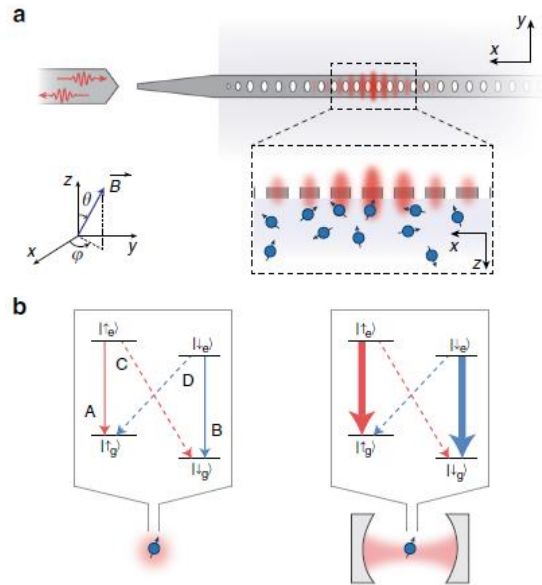
Parasitic crosstalk in superconducting quantum devices is a leading limitation for quantum gates. We demonstrate the suppression of static ZZ crosstalk in a two-qubit, two-coupler superconducting circuit, where the frequency of a tunable coupler can be adjusted such that the ZZ interactions from each coupler destructively interfere. We verify the crosstalk elimination with simultaneous randomized benchmarking, and use a parametrically activated i SWAP interaction to achieve a Bell-state preparation fidelity of 98.5% and a \sqrt{i} SWAP-gate fidelity of 94.8% obtained via quantum-process tomography.

Status: published work at Physical Review Applied 2019, **12**, 054023

Optical quantum nondemolition measurement of a single rare earth ion qubit

Mouktik Raha,¹ Songtao Chen,¹ Christopher M. Phenicie,¹ Salim Ourari,¹ Alan M. Dibos,^{1,2} and Jeff D. Thompson¹

¹Department of Electrical Engineering, Princeton University, Princeton, NJ 08544, USA. ²Present address: Nanoscience and Technology Division, Argonne National Laboratory, Argonne, IL 60439, USA



Optically-interfaced spins in the solid state are a promising platform for quantum technologies. A crucial component of these systems is high-fidelity, projective measurement of the spin state. Here, we demonstrate single-shot spin readout of a single rare earth ion qubit, Er^{3+} , which is attractive for its telecom-wavelength optical transition and compatibility with silicon nanophotonic circuits. In previous work with laser-cooled atoms and ions, and solid-state defects, spin readout is accomplished using fluorescence on an optical cycling transition; however, Er^{3+} and other rare earth ions generally lack strong cycling transitions. We demonstrate that modifying the electromagnetic environment around the ion can increase the strength and cyclicity of the optical transition by several orders of magnitude, enabling single-shot quantum nondemolition readout of the ion's spin with 94.6% fidelity. We use this readout to probe coherent dynamics and relaxation of the spin.

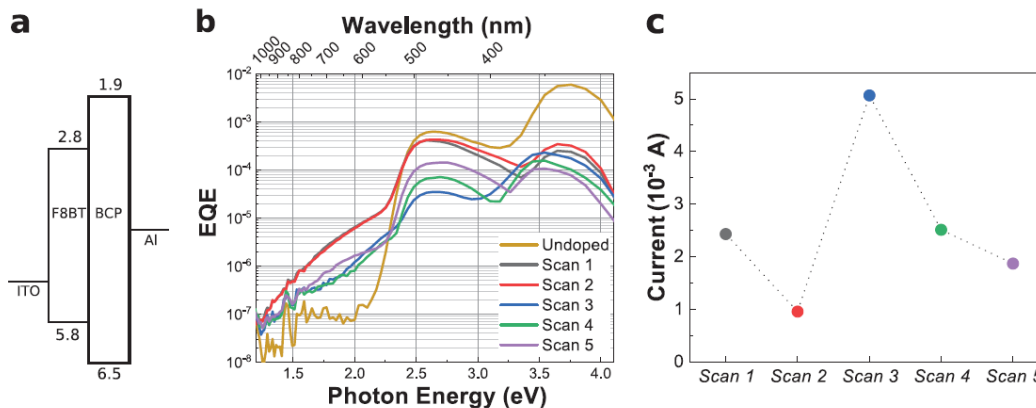
Status: published work at Nature Communications 2020, **11**, 1605

n-Doping of a Low-Electron-Affinity Polymer Used as an Electron-Transport Layer in Organic Light-Emitting Diodes

Hannah L. Smith,¹ Jordan T. Dull,¹ Elena Longhi,² Stephen Barlow,² Barry P. Rand,^{1,3} Seth R. Marder,² and Antoine Kahn¹

¹Department of Electrical Engineering, Princeton University, Princeton, NJ 08544, USA; ²School of Chemistry and Biochemistry and Center for Organic Photonics, Georgia Institute of Technology, Atlanta, GA 30332, USA;

³Andlinger Center for Energy and the Environment, Princeton University, Princeton, NJ 08544, USA



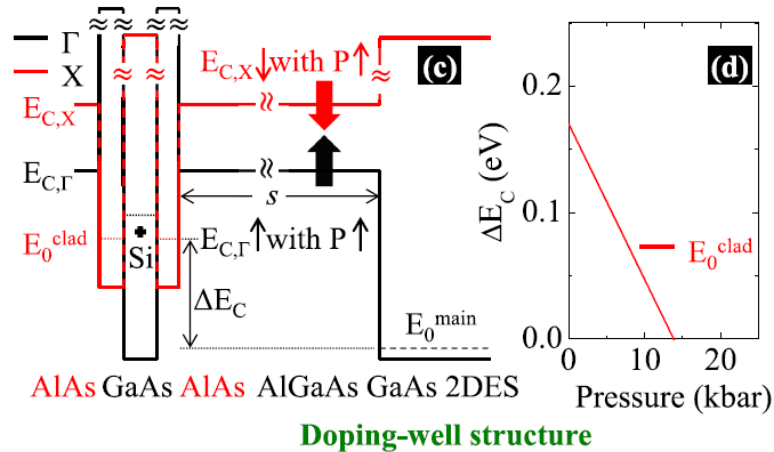
n-Doping electron-transport layers (ETLs) increases their conductivity and improves electron injection into organic light-emitting diodes (OLEDs). Because of the low electron affinity and large bandgaps of ETLs used in green and blue OLEDs, n-doping has been notoriously more difficult for these materials. In this work, n-doping of the polymer poly[(9,9-dioctylfluorene-2,7-diyl)-alt-(benzo[2,1,3]thiadiazol-4,7-diyl)] (F8BT) is demonstrated via solution processing, using the air-stable n-dopant (pentamethylcyclopentadienyl) (1,3,5-trimethylbenzene)ruthenium dimer [RuCp**Mes*]₂. Undoped and doped F8BT films are characterized using ultraviolet and inverse photoelectron spectroscopy. The ionization energy and electron affinity of the undoped F8BT are found to be 5.8 and 2.8 eV, respectively. Upon doping F8BT with [RuCp**Mes*]₂, the Fermi level shifts to within 0.25 eV of the F8BT lowest unoccupied molecular orbital, which is indicative of n-doping. Conductivity measurements reveal a four orders of magnitude increase in the conductivity upon doping and irradiation with ultraviolet light. The [RuCp**Mes*]₂-doped F8BT films are incorporated as an ETL into phosphorescent green OLEDs, and the luminance is improved by three orders of magnitude when compared to identical devices with an undoped F8BT ETL.

Status: published work at *Advanced Functional Materials* 2020, **30**, 2000328

Heterostructure design to achieve high quality, high density GaAs 2D electron system with g-factor tending to zero

Y.J. Chung,¹ S. Yuan,² Y. Liu,² K.W. Baldwin,¹ K.W. West,¹ M. Shayegan,¹ and L.N. Pfeiffer¹

¹Department of Electrical Engineering, Princeton University, Princeton, New Jersey 08544, USA; ²International Center for Quantum Materials, Peking University, Beijing 100871, China



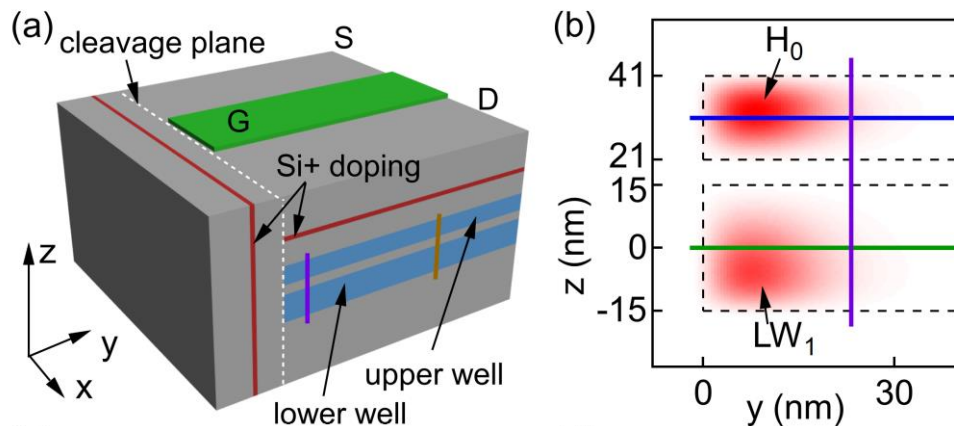
Hydrostatic pressure is a useful tool that can tune several key parameters in solid state materials. For example, the Lande g-factor in GaAs two-dimensional electron systems (2DESs) is expected to change from its bulk value $g \approx 0.44$ to zero and even to positive values under sufficiently large hydrostatic pressure. Although this presents an intriguing platform to investigate electron-electron interaction in a system with $g = 0$, studies are quite limited because the GaAs 2DES density decreases significantly with increasing hydrostatic pressure. Here, we show that a simple model, based on pressure-dependent changes in the conduction band alignment, quantitatively explains this commonly observed trend. Furthermore, we demonstrate that the decrease in the 2DES density can be suppressed by more than a factor of 3 through an innovative heterostructure design.

Status: published work at Applied Physical Letters 2020, **117**, 022102

Edge State Wave Functions from Momentum-Conserving Tunneling Spectroscopy

T. Patlatiuk,¹ C. P. Scheller,¹ D. Hill,² Y. Tserkovnyak,² J. C. Egues,³ G. Barak,⁴ A. Yacoby,⁴ L. N. Pfeiffer,⁵ K. W. West,⁵ and D. M. Zumbuhl¹

¹Departement Physik, University of Basel, Klingelbergstrasse 82, CH-4056 Basel, Switzerland; ²Department of Physics and Astronomy, University of California, Los Angeles, California 90095, USA; ³Instituto de Física de Sao Carlos, Universidade de Sao Paulo, 13560-970 Sao Carlos, Sao Paulo, Brazil; ⁴Department of Physics, Harvard University, Cambridge, Massachusetts 02138, USA; ⁵Department of Electrical Engineering, Princeton University, Princeton, New Jersey 08544, USA



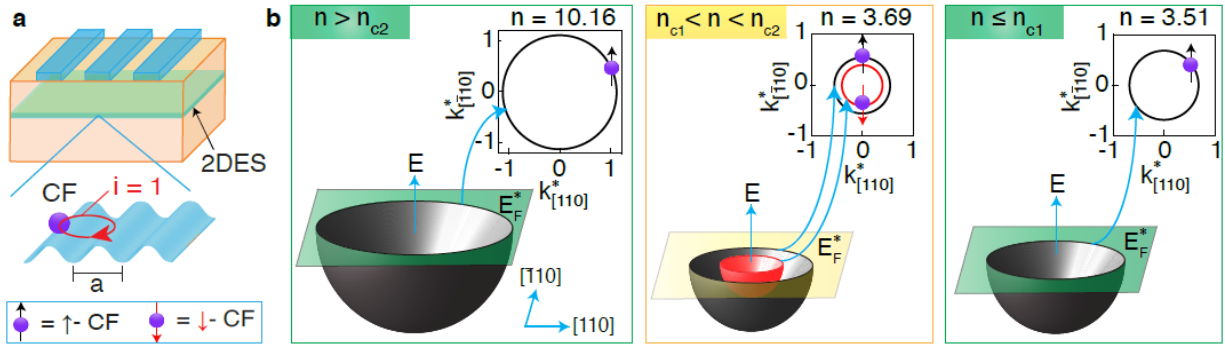
We perform momentum-conserving tunneling spectroscopy using a GaAs cleaved-edge overgrowth quantum wire to investigate adjacent quantum Hall edge states. We use the lowest five wire modes with their distinct wave functions to probe each edge state and apply magnetic fields to modify the wave functions and their overlap. This reveals an intricate and rich tunneling conductance fan structure which is succinctly different for each of the wire modes. We self-consistently solve the Poisson-Schrodinger equations to simulate the spectroscopy, reproducing the striking fans in great detail, thus confirming the calculations. Further, the model predicts hybridization between wire states and Landau levels, which is also confirmed experimentally. This establishes momentum conserving tunneling spectroscopy as a powerful technique to probe edge state wave functions.

Status: published work in Physical Review Letters 2020, **125**, 087701

Bloch Ferromagnetism of Composite Fermions

M.S. Hossain,¹ T. Zhao,² S.Y. Pu,² M.A. Mueed,¹ M.K. Ma,¹ K.A.V. Rosales,¹ Y.J. Chung,¹ L.N. Pfeiffer,¹ K.W. West,¹ K.W. Baldwin,¹ J.K. Jain,² M. Shayegan¹

¹Department of Electrical Engineering, Princeton University, Princeton, New Jersey 08544, USA; ²Department of Physics, 104 Davey Lab, Pennsylvania State University, University Park, Pennsylvania 16802, USA



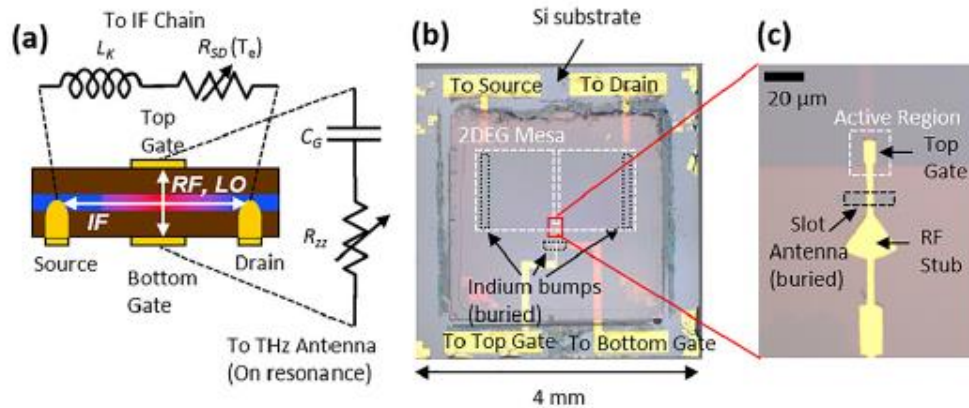
In 1929 Felix Bloch suggested that the paramagnetic Fermi sea of electrons should make a spontaneous transition to a fully-magnetized state at very low densities, because the exchange energy gained by aligning the spins exceeds the enhancement in the kinetic energy. We report here the observation of an abrupt, interaction-driven transition to full magnetization, highly reminiscent of Bloch ferromagnetism that has eluded experiments for the last ninety years. Our platform is the exotic two-dimensional Fermi sea of composite fermions at half-filling of the lowest Landau level. Via quantitative measurements of the Fermi wavevector, which provides a direct measure of the spin polarization, we observe a sudden transition from a partially-spin-polarized to a fully spin-polarized ground state as we lower the composite fermions' density. Our detailed theoretical calculations provide a semi-quantitative account of this phenomenon.

Status: published work in Nature Physics 2020

Demonstration of a tunable antenna-coupled intersubband terahertz (TACIT) mixer

C. Yoo,¹ M. Huang,¹ J. H. Kawamura,² K. W. West,³ L. N. Pfeiffer,³ B. S. Karasik,² and M. S. Sherwin¹

¹Physics Department and Institute for Terahertz Science and Technology, University of California, Santa Barbara, California 93106, USA; ²Jet Propulsion Laboratory, California Institute of Technology, Pasadena, California 91109, USA; ³Department of Electrical Engineering, Princeton University, Princeton, New Jersey 08544, USA.



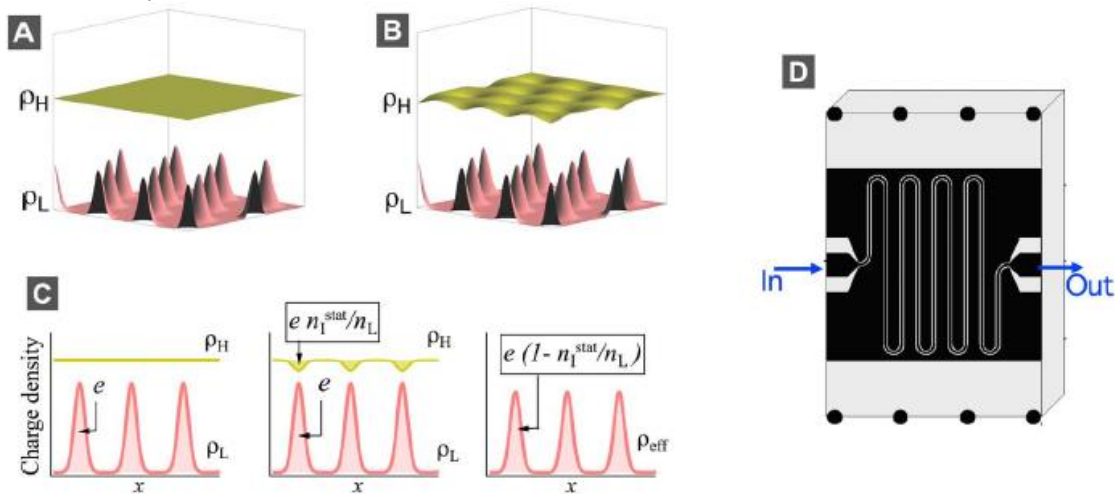
A fast, voltage-tunable terahertz mixer based on the intersubband transition of a high-mobility 2-dimensional electron gas has been fabricated from a single 40 nm GaAs-AlGaAs square quantum well heterostructure. The device is called a Tunable Antenna-Coupled Intersubband Terahertz mixer and shows tunability of the detection frequency from 2.52 to 3.11 THz with small (<1 V) top gate and bottom gate voltage biases. Mixing at 2.52 THz has been observed at 60 K with a -3dB intermediate frequency bandwidth exceeding 6 GHz.

Status: published work in Applied Physics Letters 2020, **116**, 013504

Wigner solid pinning modes tuned by fractional quantum Hall states of a nearby layer

A. T. Hatke,¹ H. Deng,² Yang Liu,² L. W. Engel,¹ L. N. Pfeiffer,² K. W. West,² K. W. Baldwin,² M. Shayegan²

¹National High Magnetic Field Laboratory, Tallahassee, FL 32310, USA. ²Department of Electrical Engineering, Princeton University, Princeton, NJ 08544, USA.



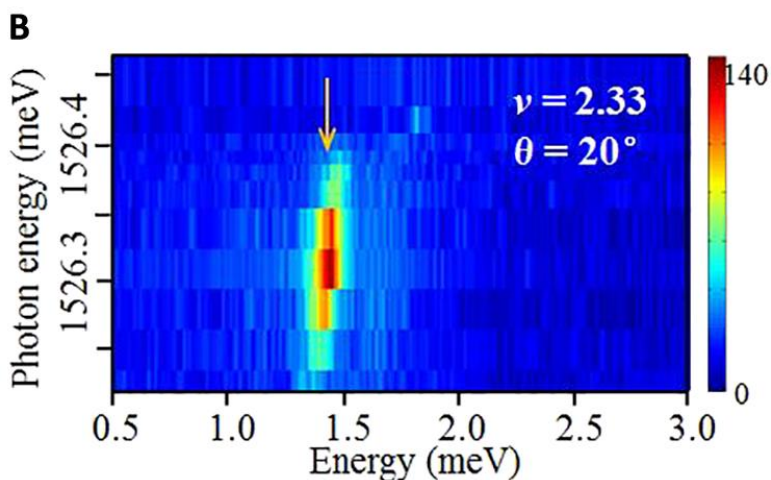
We studied a bilayer system hosting two-dimensional electron systems (2DESs) in close proximity but isolated from one another by a thin barrier. One 2DES has low electron density and forms a Wigner solid (WS) at high magnetic fields. The other has much higher density and, in the same field, exhibits fractional quantum Hall states (FQHSs). The WS spectrum has resonances which are understood as pinning modes, oscillations of the WS within the residual disorder. We found the pinning mode frequencies of the WS are strongly affected by the FQHSs in the nearby layer. Analysis of the spectra indicates that the majority layer screens like a dielectric medium even when its Landau filling is $\sim 1/2$, at which the layer is essentially a composite fermion (CF) metal. Although the majority layer is only \sim one WS lattice constant away, a WS site only induces an image charge of $\sim 0.1e$ in the CF metal.

Status: published work in Science Advances 2019, **5**, eaao2848

Observation of new plasmons in the fractional quantum Hall effect: Interplay of topological and nematic orders

L. Du,¹ U. Wurstbauer,^{2,3} K. W. West,⁴ L. N. Pfeiffer,⁴ S. Fallahi,^{5,6} G. C. Gardner,^{6,7} M. J. Manfra,^{5,6,7,8} A. Pinczuk^{1,9}

¹Department of Applied Physics and Applied Mathematics, Columbia University, New York, NY 10027, USA. ²Walter Schottky Institut and Physik-Department, Technische Universität München, Am Coulombwall 4a, 85748 Garching, Germany. ³Institute of Physics, University of Münster, Wilhelm-Klemm-Str.10, 48149 Münster, Germany. ⁴Department of Electrical Engineering, Princeton University, Princeton, NJ 08544, USA. ⁵Department of Physics and Astronomy, Purdue University, IN 47907, USA. ⁶Birck Nanotechnology Center, Purdue University, IN 47907, USA. ⁷Microsoft Station Q Purdue, Purdue University, IN 47907, USA. ⁸School of Materials Engineering and School of Electrical and Computer Engineering, IN 47907, USA. ⁹Department of Physics, Columbia University, New York, NY 10027, USA.



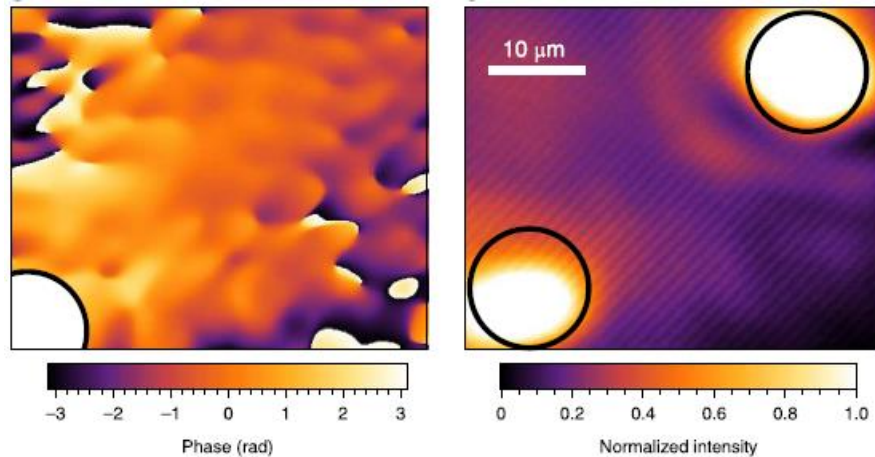
Collective modes of exotic quantum fluids reveal underlying physical mechanisms responsible for emergent quantum states. We observe unexpected new collective modes in the fractional quantum Hall (FQH) regime: intra-Landau-level plasmons measured by resonant inelastic light scattering. The plasmons herald rotational-symmetry-breaking (nematic) phases in the second Landau level and uncover the nature of long-range translational invariance in these phases. The intricate dependence of plasmon features on filling factor provides insights on interplays between topological quantum Hall order and nematic electronic liquid crystal phases. A marked intensity minimum in the plasmon spectrum at Landau level filling factor $\nu = 5/2$ strongly suggests that this paired state, which may support non-Abelian excitations, overwhelms competing nematic phases, unveiling the robustness of the $5/2$ superfluid state for small tilt angles. At $\nu=7/3$, a sharp and strong plasmon peak that links to emerging macroscopic coherence supports the proposed model of a FQH nematic state.

Status: published work in Science Advances 2019, **5**, eaav3407

Josephson vortices induced by phase twisting a polariton superfluid

D. Caputo,^{1,2} N. Bobrovska,³ D. Ballarini,¹ M. Matuszewski,³ M. De Giorgi,¹ L. Dominici,¹ K. West,⁴ L. N. Pfeiffer,⁴ G. Gigli,^{1,2} and D. Sanvitto^{1,5}

¹CNR Nanotec—Institute of Nanotechnology, Lecce, Italy; ²University of Salento, Lecce, Italy; ³Institute of Physics, Polish Academy of Sciences, Warsaw, Poland; ⁴Department of Electrical Engineering, Princeton University, Princeton, NJ, USA; ⁵INFN, Sezione Lecce, Lecce, Italy.



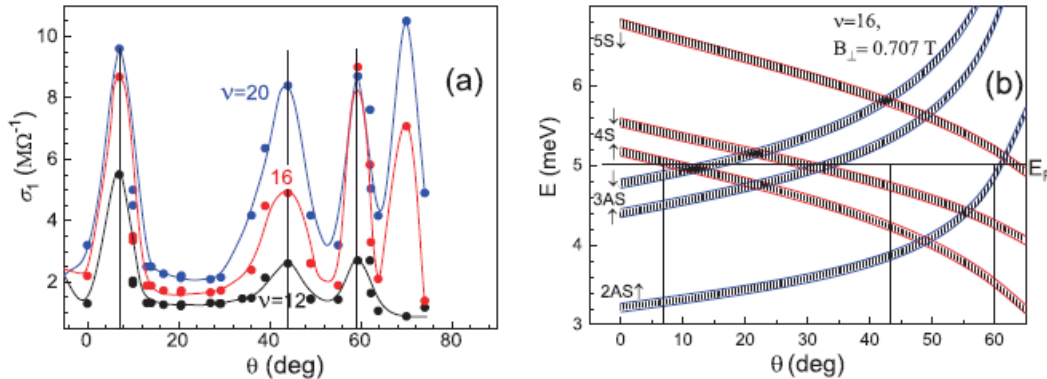
Quantum fluids of light are an emerging platform for energy-efficient signal processing, ultrasensitive interferometry and quantum simulators at elevated temperatures. Here we demonstrate all-optical control of the topological excitations in a large polariton condensate realizing the bosonic analogue of a long Josephson junction and inducing the nucleation of Josephson vortices. When a phase difference is imposed at the boundaries of the condensate, two extended regions become separated by a sharp phase jump of π radians and a solitonic depletion of the density, forming an insulating barrier with a suppressed order parameter. The superfluid behaviour—characterized by a smooth phase gradient across the system instead of the sharp phase jump—is recovered at higher polariton densities and is mediated by the nucleation of Josephson vortices within the barrier. Our results contribute to the understanding of dissipation and stability of elementary excitations in macroscale quantum systems.

Status: published work in Nature Photonics 2019, **13**, 488-493

Electronic band structure in n-type GaAs/AlGaAs wide quantum wells in tilted magnetic field

I. L. Drichko,¹ I. Yu. Smirnov,¹ A. V. Suslov,² M. O. Nestoklon,¹ D. Kamburov,³ K. W. Baldwin,³ L. N. Pfeiffer,³ K. W. West,³ and L. E. Golub¹

¹Ioffe Institute, 194021 St. Petersburg, Russia; ²National High Magnetic Field Laboratory, Tallahassee, FL 32310, United States of America; ³Department of Electrical Engineering, Princeton University, Princeton, NJ 08544, United States of America.



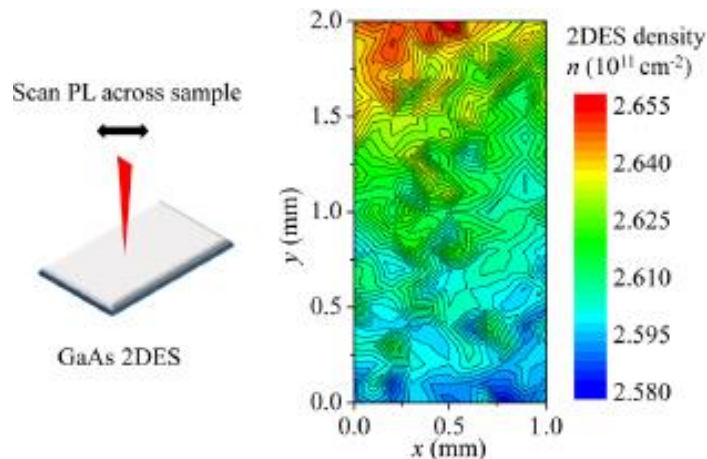
Oscillations of the real component of AC conductivity σ_1 in a magnetic field were measured in the n-AlGaAs/GaAs structure with a wide (75 nm) quantum well by contactless acoustic methods at $T = (20\text{--}500)$ mK. In a wide quantum well, the electronic band structure is associated with the two-subband electron spectrum, namely the symmetric (S) and antisymmetric (AS) subbands formed due to electrostatic repulsion of electrons. A change of the oscillations amplitude in tilted magnetic field observed in the experiments occurs due to crossings of Landau levels of different subbands (S and AS) at the Fermi level. The theory developed in this work shows that these crossings are caused by the difference in the cyclotron energies in the S and AS subbands induced by the in-plane magnetic field.

Status: published work in Journal of Physics: Condensed Matter 2020, **32**, 035303

Spatial Mapping of Local Density Variations in Two-dimensional Electron Systems Using Scanning Photoluminescence

Y. J. Chung, K. W. Baldwin, K. W. West, N. Haug, J. van de Wetering, M. Shayegan, and L. N. Pfeiffer

Department of Electrical Engineering, Princeton University, Princeton, New Jersey 08544, USA



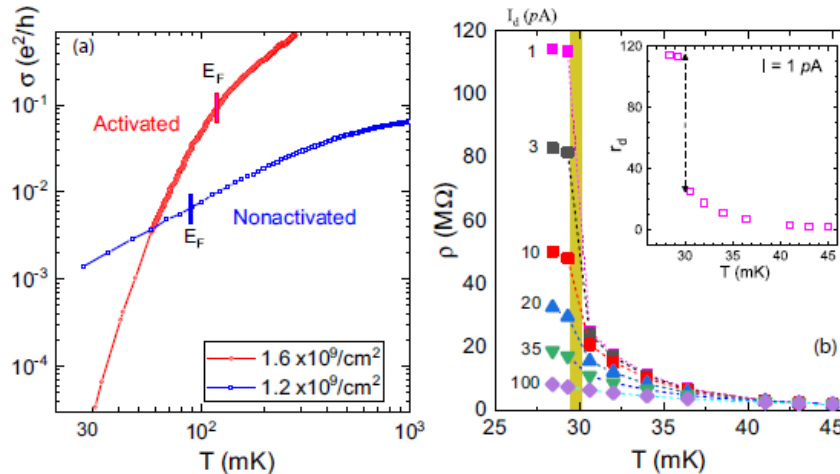
We have developed a scanning photoluminescence technique that can directly map out the local two-dimensional electron density with a relative accuracy of $\sim 2.2 \times 10^8 \text{ cm}^{-2}$. The validity of this approach is confirmed by the observation of the expected density gradient in a high-quality GaAs quantum well sample that was not rotated during the molecular beam epitaxy of its spacer layer. In addition to this global variation in electron density, we observe local density fluctuations across the sample. These random density fluctuations are also seen in samples that were continuously rotated during growth, and we attribute them to residual space charges at the substrate–epitaxy interface. This is corroborated by the fact that the average magnitude of density fluctuations is increased to $\sim 9 \times 10^9 \text{ cm}^{-2}$ from $\sim 1.2 \times 10^9 \text{ cm}^{-2}$ when the buffer layer between the substrate and the quantum well is decreased by a factor of 7. Our data provide direct evidence for local density inhomogeneities even in very high-quality two-dimensional carrier systems.

Status: published work in Nano Letters 2019, **19**, 1908-1913

Discontinuity in the transport of strongly correlated two-dimensional hole systems in zero magnetic field

J. Huang,¹ L. N. Pfeiffer,² and K. W. West²

¹Wayne State University, Department of Physics and Astronomy, Detroit, MI 48201 USA; ²Princeton University, Department of Electrical Engineering, Princeton, NJ 08544 USA



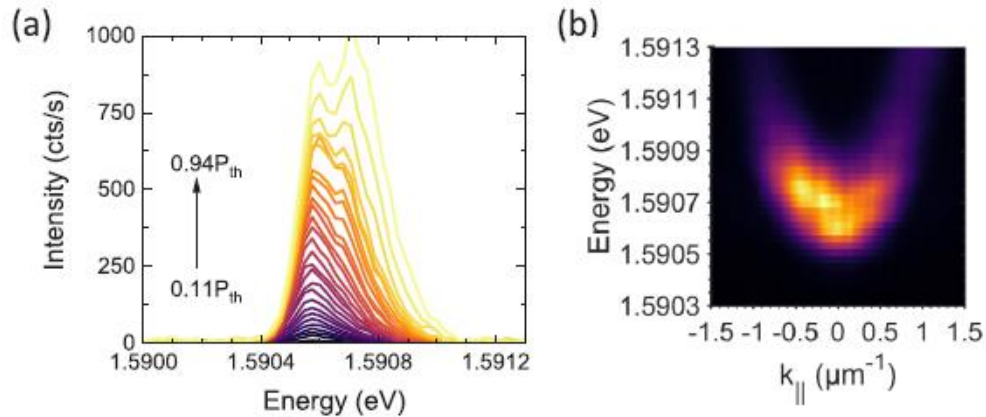
Adopting undoped ultraclean two-dimensional hole systems, we approach a strongly correlated limit by reducing the carrier density down to $1 \times 10^9 \text{ cm}^{-2}$. The temperature dependence of the resistivity as a function of the carrier density reveals a characteristic energy scale displaying a benchmark critical behavior near a critical density of $p_c \approx 4 \times 10^9 \text{ cm}^{-2}$. The insulating state below p_c exhibits a sharp resistance discontinuity in response to heating across a critical temperature $T_{c1} \approx 30$ mK, consistent with a first-order transition. The dc response also identifies a second critical temperature T_{c2} where linear IV behavior is recovered. Similar effects are also demonstrated by varying an external electric field. The results support a complex quantum phase transition with intermediate phases.

Status: published work in Physical Review B 2020, **101**, 161110

Effect of optically-induced potential on the energy of trapped exciton-polaritons below the condensation threshold

M. Pieczarka,^{1,2,3} M. Boozarjmehr,^{1,2} E. Estrecho,^{1,2} Y. Yoon,⁴ M. Steger,⁵ K. West,⁶ L. N. Pfeiffer,⁶ K. A. Nelson,⁴ D. W. Snoke,⁷ A. G. Truscott,⁸ and E. A. Ostrovskaya^{1,2}

¹Nonlinear Physics Centre, Research School of Physics and Engineering, The Australian National University, Canberra ACT 2601, Australia; ²ARC Centre of Excellence in Future Low-Energy Electronics Technologies ³Department of Experimental Physics, Faculty of Fundamental Problems of Technology, Wroclaw University of Science and Technology, Wyb. Wyspianskiego 27, 50-370 Wroclaw, Poland; ⁴Department of Chemistry, Massachusetts Institute of Technology, Cambridge, MA 02139, USA; ⁵National Renewable Energy Lab, Golden, CO 80401, USA; ⁶Department of Electrical Engineering, Princeton University, Princeton, NJ 08544, USA; ⁷Department of Physics and Astronomy, University of Pittsburgh, Pittsburgh, PA 15260, USA; ⁸Laser Physics Centre, Research School of Physics and Engineering, The Australian National University, Canberra ACT 2601, Australia



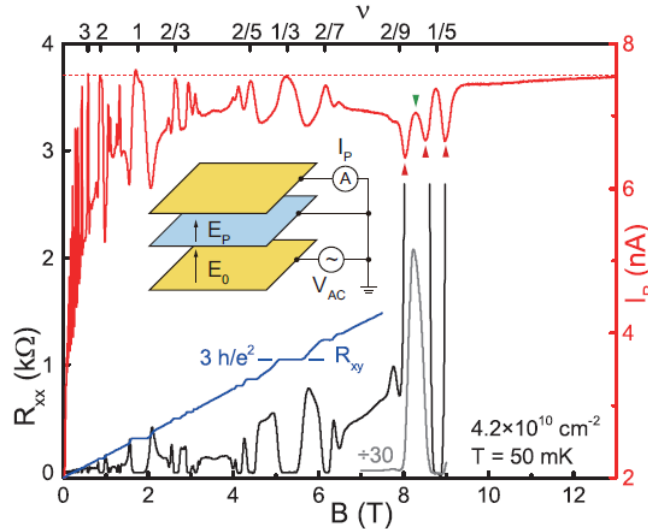
Exciton-polaritons (polaritons herein) offer a unique nonlinear platform for studies of collective macroscopic quantum phenomena in a solid state system. Shaping of polariton flow and polariton confinement via potential landscapes created by nonresonant optical pumping has gained considerable attention due to the flexibility and control enabled by optically-induced potentials. Recently, large density-dependent energy shifts (blueshifts) exhibited by optically trapped polaritons at low densities, below the bosonic condensation threshold, were interpreted as an evidence of strong polariton-polariton interactions. In this work, we further investigate the origins of these blueshifts in optically-induced circular traps and present evidence of significant blueshifts of the polariton energy due to reshaping of the optically-induced potential with laser pump power. Our work demonstrates the strong influence of the effective potential formed by an optically-injected excitonic reservoir on the energy blueshifts observed below and up to the polariton condensation threshold and suggests that the observed blueshifts arise due to interaction of polaritons with the excitonic reservoir, rather than due to polariton-polariton interaction.

Status: published work in Physical Review B 2019, **100**, 085301

Probing the Melting of a Two-Dimensional Quantum Wigner Crystal via its Screening Efficiency

H. Deng,¹ L. N. Pfeiffer,¹ K. W. West,¹ K. W. Baldwin,¹ L. W. Engel,² and M. Shayegan¹

¹Department of Electrical Engineering, Princeton University, Princeton, NJ 08544, USA; ²National High Magnetic Field Laboratory, Tallahassee, FL 32310, USA.



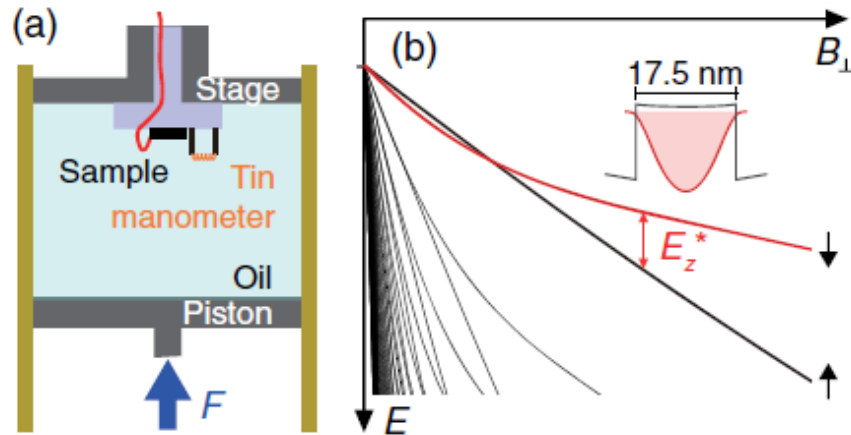
One of the most fundamental and yet elusive collective phases of an interacting electron system is the quantum Wigner crystal (WC), an ordered array of electrons expected to form when the electrons' Coulomb repulsion energy eclipses their kinetic (Fermi) energy. In low-disorder, two-dimensional (2D) electron systems, the quantum WC is known to be favored at very low temperatures (T) and small Landau level filling factors (ν), near the termination of the fractional quantum Hall states. This WC phase exhibits an insulating behavior, reflecting its pinning by the small but finite disorder potential. An experimental determination of a T vs ν phase diagram for the melting of the WC, however, has proved to be challenging. Here we use capacitance measurements to probe the 2D WC through its effective screening as a function of T and ν . We find that, as expected, the screening efficiency of the pinned WC is very poor at very low T and improves at higher T once the WC melts. Surprisingly, however, rather than monotonically changing with increasing T , the screening efficiency shows a well-defined maximum at a T which is close to the previously-reported melting temperature of the WC. Our experimental results suggest a new method to map out a T vs ν phase diagram of the magnetic-field-induced WC precisely.

Status: published work in Physical Review Letters 2019, **122**, 116601

Resymmetrizing Broken Symmetry with Hydraulic Pressure

K. Huang,¹ P. Wang,¹ L. N. Pfeiffer,² K.W. West,² K.W. Baldwin,² Y. Liu,¹ and X. Lin^{1,3}

¹International Center for Quantum Materials, Peking University, Beijing 100871, China; ²Department of Electrical Engineering, Princeton University, Princeton, New Jersey 08544, USA; ³CAS Center for Excellence in Topological Quantum Computation, University of Chinese Academy of Sciences, Beijing 100190, China



Recent progress in condensed matter physics, such as for graphene, topological insulators, and Weyl semimetals, often originate from the specific topological symmetries of their lattice structures. Quantum states with different degrees of freedom, e.g., spin, valley, layer, etc., arise from these symmetries, and the coherent superposition of these states form multiple energy subbands. The pseudospin, a concept analogous to the Dirac spinor matrices, is a successful description of such multisubband systems. When the electron-electron interaction dominates, many-body quantum phases arise. They usually have discrete pseudospin polarizations and exhibit sharp phase transitions at certain universal critical pseudospin energy splittings. In this Letter, we present our discovery of hydrostatic-pressure-induced degeneracy between the two lowest Landau levels. This degeneracy is evidenced by the pseudospin polarization transitions of the fragile correlated quantum liquid phases near the Landau level filling factor $\nu = 3/2$. Benefitting from the constant hole concentration and the sensitive nature of these transitions, we study the fine-tuning effect of the hydrostatic pressure at the order of $10 \mu\text{eV}$, well beyond the meV-level state-of-the-art resolution of other techniques.

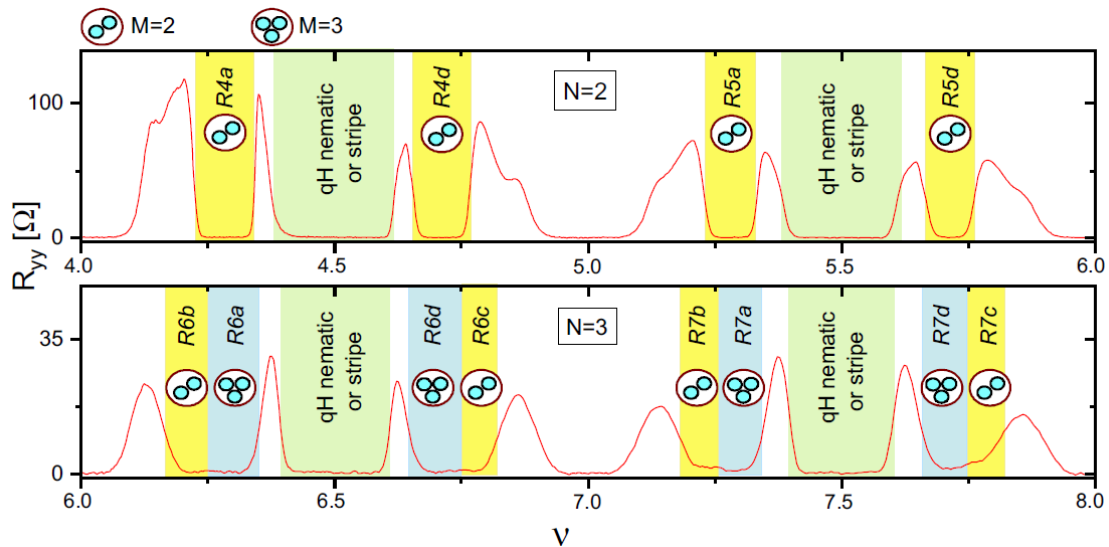
Status: published work in Physical Review Letters 2019, **123**, 206602

Stability of multielectron bubbles in high Landau levels

Dohyung Ro,¹ S. A. Myers,¹ N. Deng,¹ J. D. Watson,¹ M. J. Manfra,^{1,2,3} L. N. Pfeiffer,⁴ K. W. West,⁴ and G. A. Csáthy^{1,3}

¹Department of Physics and Astronomy, Purdue University, West Lafayette, Indiana 47907, USA; ²School of Materials Engineering and School of Electrical and Computer Engineering, Purdue University, West Lafayette, Indiana 47907, USA; ³Birck Nanotechnology Center Purdue University, West Lafayette, Indiana 47907, USA;

⁴Department of Electrical Engineering, Princeton University, Princeton, New Jersey 08544, USA

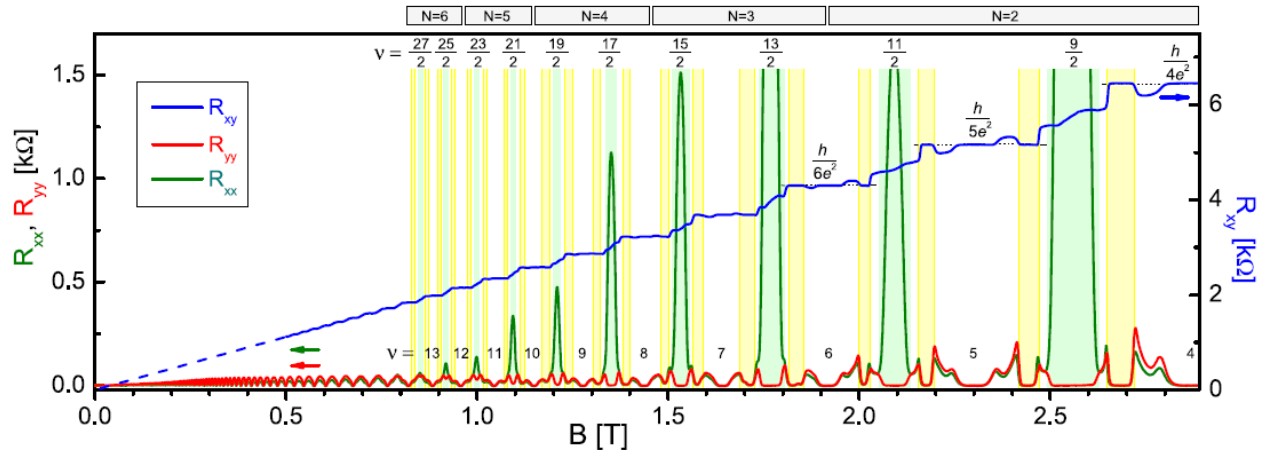


We study multielectron bubble phases in the $N = 2$ and $N = 3$ Landau levels in a high mobility GaAs/AlGaAs sample. We found that the longitudinal magnetoresistance versus temperature curves in the multielectron bubble region exhibit sharp peaks, irrespective of the Landau-level index. We associate these peaks with an enhanced scattering caused by thermally fluctuating domains of a bubble phase and a uniform uncorrelated electron liquid at the onset of the bubble phases. Within the $N = 3$ Landau level, onset temperatures of three-electron and two electron bubbles exhibit linear trends with respect to the filling factor; the onset temperatures of three-electron bubbles are systematically higher than those of two-electron bubbles. Furthermore, onset temperatures of the two-electron bubble phases across $N = 2$ and $N = 3$ Landau levels are similar, but exhibit an offset. This offset and the dominant nature of the three-electron bubbles in the $N = 3$ Landau level reveals the role of the shortrange part of the electron-electron interaction in the formation of the bubbles.

Status: published work in Physical Review B 2020, **102**, 115303

Electron bubbles and the structure of the orbital wave function

D. Ro,¹ N. Deng,¹ J. D. Watson,¹ M. J. Manfra,^{1,2,3} L. N. Pfeiffer,⁴ K. W. West,⁴ and G. A. Csáthy^{1,3}
¹Department of Physics and Astronomy, Purdue University, West Lafayette, Indiana 47907, USA; ²School of Materials Engineering and School of Electrical and Computer Engineering, Purdue University, West Lafayette, Indiana 47907, USA; ³Birck Nanotechnology Center, Purdue University, West Lafayette, Indiana 47907, USA; ⁴Department of Electrical Engineering, Princeton University, Princeton, New Jersey 08544, USA



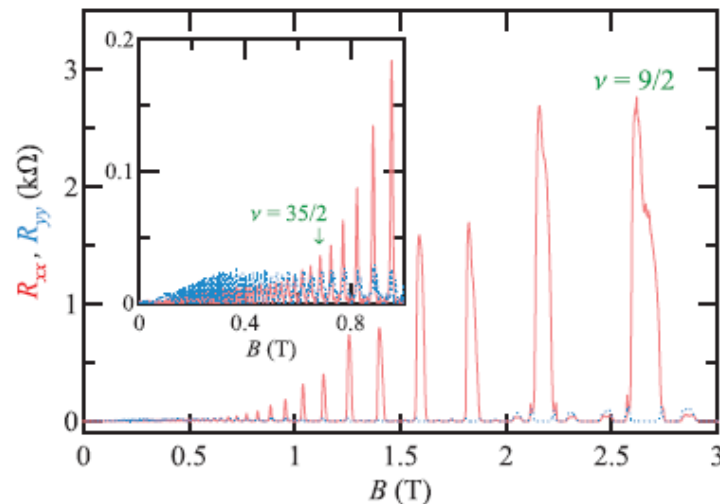
Stripelike and bubblelike patterns spontaneously form in numerous physical, chemical, and biological systems when competing long-range and short-range interactions banish uniformity. Stripelike and the related nematic morphology are also under intense scrutiny in various strongly correlated electron systems. In contrast, the electronic bubble morphology is rare. Some of the most intriguing electron bubbles develop in the two-dimensional electron gas subjected to a perpendicular magnetic field. However, in contrast to bubbles forming in classical systems such as the Turing activator-inhibitor reaction or Langmuir films, bubbles in electron gases owe their existence to elementary quantum mechanics: They are stabilized as wave functions of individual electrons overlap. Here, we report a rich pattern of multielectron bubble phases in a high Landau level and we conclude that this richness is due to the nodal structure of the orbital component of the electronic wave function.

Status: published work in Physical Review B 2019, **99**, 201111

Resistivity anisotropy of quantum Hall stripe phases

M. Sammon,¹ X. Fu,¹ Yi Huang,¹ M. A. Zudov,¹ B. I. Shklovskii,¹ G. C. Gardner,^{2,3} J. D. Watson,^{3,4} M. J. Manfra,^{2,3,4,5} K. W. Baldwin,⁶ L. N. Pfeiffer,⁶ and K. W. West⁶

¹*School of Physics and Astronomy, University of Minnesota, Minneapolis, Minnesota 55455, USA;* ²*Microsoft Quantum Lab Purdue, Purdue University, West Lafayette, Indiana 47907, USA;* ³*Birck Nanotechnology Center, Purdue University, West Lafayette, Indiana 47907, USA;* ⁴*Department of Physics and Astronomy, Purdue University, West Lafayette, Indiana 47907, USA;* ⁵*School of Electrical and Computer Engineering and School of Materials Engineering, Purdue University, West Lafayette, Indiana 47907, USA;* ⁶*Department of Electrical Engineering, Princeton University, Princeton, New Jersey 08544, USA*



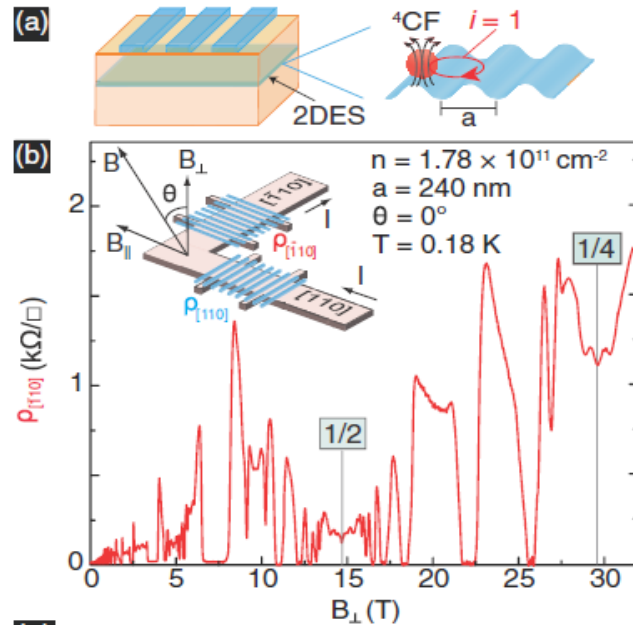
Quantum Hall stripe phases near half-integer filling factors $\nu \geq 9/2$ were predicted by Hartree-Fock (HF) theory and confirmed by discoveries of giant resistance anisotropies in high-mobility two-dimensional electron gases. A theory of such anisotropy was proposed by MacDonald and Fisher, although they used parameters whose dependencies on the filling factor, electron density, and mobility remained unspecified. Here, we fill this void by calculating the hard-to-easy resistivity ratio as a function of these three variables. Quantitative comparison with experiment yields very good agreement, which we view as evidence for the “plain vanilla” smectic stripe HF phases.

Status: published work in Physical Review B 2019, **100**, 241303

Geometric resonance of four-flux composite fermions

M. S. Hossain,¹ M. K. Ma,¹ M. A. Mueed,¹ D. Kamburov,¹ L. N. Pfeiffer,¹ K. W. West,¹ K. W. Baldwin,¹ R. Winkler,² and M. Shayegan¹

¹Department of Electrical Engineering, Princeton University, Princeton, New Jersey 08544, USA; ²Department of Physics, Northern Illinois University, DeKalb, Illinois 60115, USA



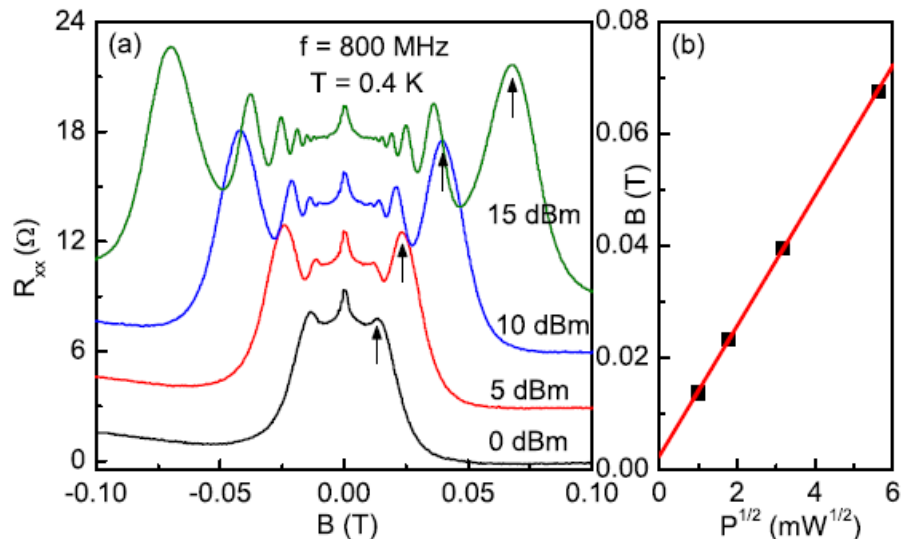
Two-dimensional interacting electrons exposed to strong perpendicular magnetic fields generate emergent, exotic quasiparticles phenomenologically distinct from electrons. Specifically, electrons bind with an even number of flux quanta, and transform into composite fermions (CFs). Besides providing an intuitive explanation for the fractional quantum Hall states, CFs also possess Fermi-liquid-like properties, including a well-defined Fermi sea, at and near even-denominator Landau-level filling factors such as $\nu = 1/2$ or $1/4$. Here, we directly probe the Fermi sea of the rarely studied four-flux CFs near $\nu = 1/4$ via geometric resonance experiments. The data reveal some unique characteristics. Unlike in the case of two-flux CFs, the magnetic field positions of the geometric resonance resistance minima for $\nu < 1/4$ and $\nu > 1/4$ are symmetric with respect to the position of $\nu = 1/4$. However, when an in-plane magnetic field is applied, the minima positions become asymmetric, implying a mysterious asymmetry in the CF Fermi sea anisotropy for $\nu < 1/4$ and $\nu > 1/4$. This asymmetry, which is in stark contrast to the two-flux CFs, suggests that the four-flux CFs on the two sides of $\nu = 1/4$ have very different effective masses, possibly because of the proximity of the Wigner crystal formation at small ν .

Status: published work in Physical Review B 2019, **100**, 041112

Quantum oscillations in a two-dimensional electron system under low-frequency microwave irradiation

J. Mi,^{1,2} H. Liu,² J. Shi,^{2,3} L. N. Pfeiffer,⁴ K. W. West,⁴ K. W. Baldwin,⁴ and Chi Zhang^{5,2,3}

¹Nanjing Research Institute of Electronic Technology, Nanjing 210039, China; ²International Center for Quantum Materials, Peking University, Beijing 100871, China; ³Collaborative Innovation Center of Quantum Matter, Beijing 100871, China; ⁴Department of Electrical Engineering, Princeton University, Princeton, New Jersey 08544, USA; ⁵SKLSM, Institute of Semiconductors, Chinese Academy of Science, P.O. Box 912, Beijing 100083, China



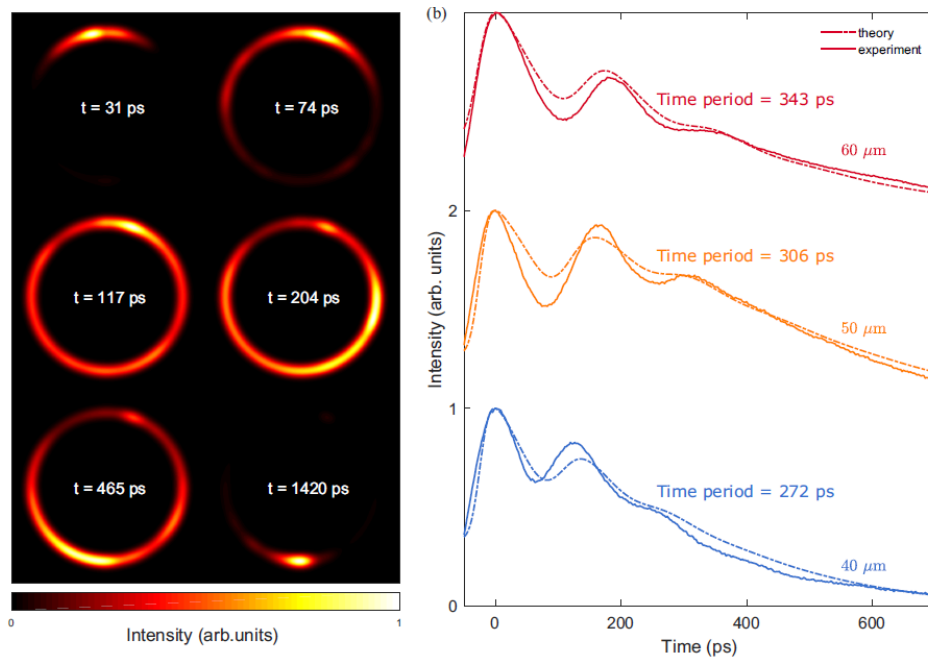
We study the magnetoresistance of an ultrahigh mobility GaAs/AlGaAs two-dimensional electron system (2DES) in a weak magnetic field under low-frequency ($f < 20$ GHz) microwave (MW) irradiation. We observe that, with decreasing MW frequency, microwave induced resistance oscillations (MIRO) are damped and multiphoton processes become dominant. At very low MW frequency ($f < 4$ GHz), MIRO disappear gradually and an SdH-like oscillation develops. Our analysis indicates that the oscillation may originate from alternating Hall-field induced resistance oscillations (ac-HIRO), due to the transition from the elastic scattering in real space. On the other hand, from the view of photon energy, the oscillations can be understood as a multiphoton process of MIRO in the low MW frequency limit. We show that the two different nonequilibrium mechanisms of MIRO and HIRO can be unified under low-frequency MW irradiation.

Status: published work in Physical Review B 2019, **100**, 235437

Observation of nonequilibrium motion and equilibration in polariton rings

S. Mukherjee,¹ D. M. Myers,¹ R. G. Lena,² B. Ozden,^{1,3} J. Beaumariage,¹ Z. Sun,¹ M. Steger,¹ L. N. Pfeiffer,⁴ K. West,⁴ A. J. Daley,² and D. W. Snoke¹

¹Department of Physics and Astronomy, University of Pittsburgh, Pittsburgh, Pennsylvania 15260, USA; ²Department of Physics and SUPA, University of Strathclyde, Glasgow G4 0NG, United Kingdom; ³Department of Physics and Engineering, Penn State Abington, Abington, Pennsylvania 19001, USA; ⁴Department of Electrical Engineering, Princeton University, Princeton, New Jersey 08544, USA;



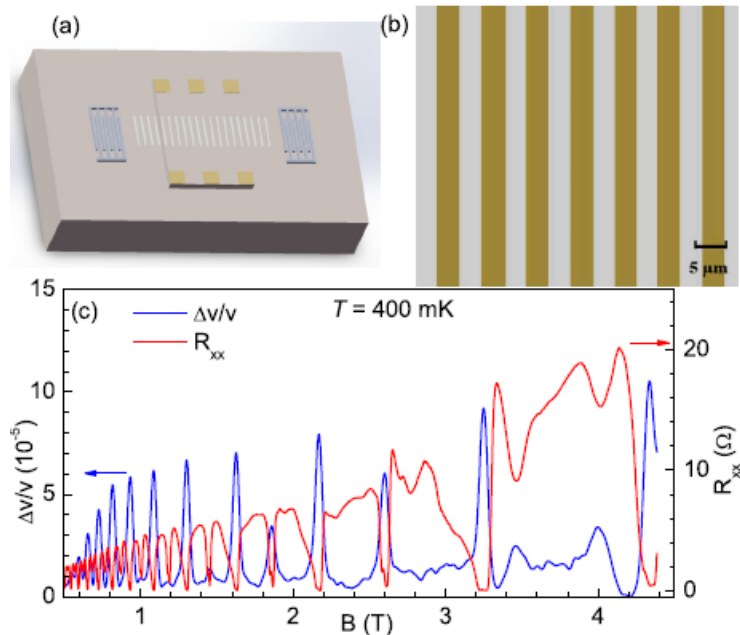
We present a study of the macroscopic dynamics of a polariton condensate formed by nonresonant optical excitation in a quasi-one-dimensional ring-shaped microcavity. The presence of a gradient in the cavity photon energy creates a macroscopic trap for the polaritons in which a coherent condensate is formed which evolves into a single-mode condensate at late times. With time- and energy-resolved imaging we show the role of interactions in the motion of the condensate as it undergoes equilibration in the ring. These experiments also give a direct measurement of the polariton-polariton interaction strength above the condensation threshold. Our observations are compared to the open-dissipative one-dimensional Gross-Pitaevskii equation, which shows excellent qualitative agreement.

Status: published work in Physical Review B 2019, **100**, 245304

Surface acoustic wave detection of robust zero-resistance states under microwaves

J. Wang,¹ L. N. Pfeiffer,² K. W. West,² K. W. Baldwin,² and Chi Zhang^{3,4,1,5}

¹International Center for Quantum Materials, Peking University, Beijing 100871, China; ²Department of Electrical Engineering, Princeton University, Princeton, New Jersey 08544, USA; ³SKLSM, Institute of Semiconductors, Chinese Academy of Science, P.O. Box 912, Beijing 100083, China; ⁴CAS Center for Excellence in Topological Quantum Computation, University of Chinese Academy of Sciences, Beijing 100190, China; ⁵Collaborative Innovation Center of Quantum Matter, Beijing 100871, China



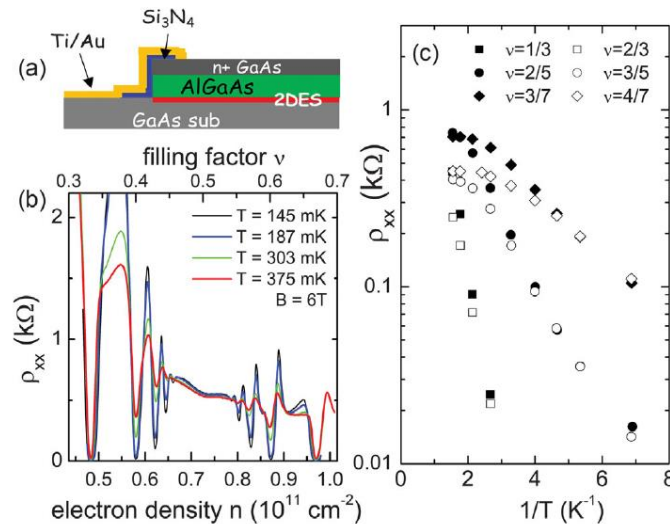
Microwave-induced resistance oscillations (MIROs) and zero-resistance states (ZRSs) occur in high-mobility two-dimensional electron gas exposed to microwave (MW). We observe that the velocity shift ($\Delta v/v$) oscillates in anticorrelation with MIRO, and $\Delta v/v$ shows peaks at the minimal resistance of MIRO or at ZRS. The SAW velocity features of ZRS remain robust even in the absence of external driving current, which suggests the involvement of intrinsic mechanism in the nonequilibrium phase. In addition, under high-power MW, the phase (ϕ_{ac}) of ZRS stays constant at about $1/4$, whereas the phase of the transitions in MIRO is reduced to below 0.10 . We argue that the peaks of SAW velocity at ZRS may result from the inhomogeneity of superposed current domain structures. Moreover, a multiphoton process around $\epsilon = 1/2$ is observed in the SAW measurements.

Status: published work in Physical Review B 2020, **101**, 165413

Particle-Hole Symmetry and the Fractional Quantum Hall Effect in the Lowest Landau Level

W. Pan,^{1,2,3} W. Kang,⁴ M. P. Lilly,³ J. L. Reno,³ K.W. Baldwin,⁵ K.W. West,⁵ L. N. Pfeiffer,⁵ and D. C. Tsui⁵

¹Materials Physics Department, Sandia National Laboratories, Livermore, California 94551, USA; ²Quantum Phenomena Department, Sandia National Laboratories, Albuquerque, New Mexico 87185, USA; ³Center for Integrated Nanotechnologies, Sandia National Laboratories, Albuquerque, New Mexico 87185, USA; ⁴Department of Physics, University of Chicago, Chicago, Illinois 60637, USA; ⁵Department of Electrical Engineering, Princeton University, Princeton, New Jersey 08544, USA



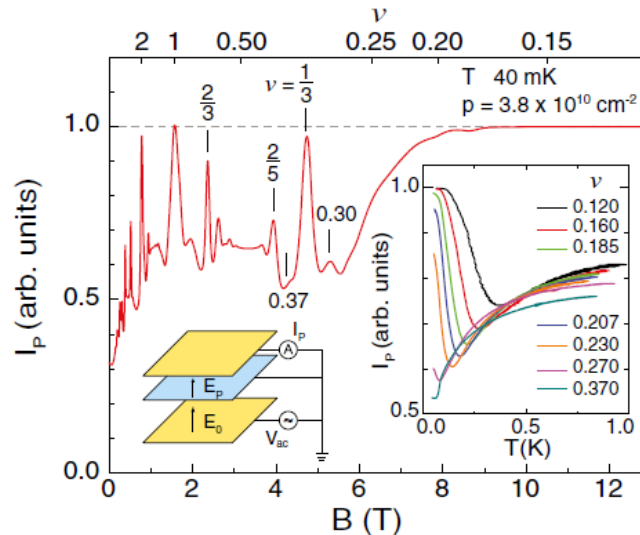
We report on detailed experimental studies of a high-quality heterojunction insulated-gate field-effect transistor (HIGFET) to probe the particle-hole symmetry of the fractional quantum Hall effect (FQHE) states about half-filling in the lowest Landau level. The HIGFET is specially designed to vary the density of a two-dimensional electronic system under constant magnetic fields. We find in our constant magnetic field, variable density measurements that the sequence of FQHE states at filling factors $\nu = 1/3; 2/5; 3/7\dots$ and its particle-hole conjugate states at filling factors $1 - \nu = 2/3; 3/5; 4/7\dots$ have a very similar energy gap. Moreover, a reflection symmetry can be established in the magnetoconductivities between the ν and $1 - \nu$ states about half-filling. Our results demonstrate that the FQHE states in the lowest Landau level are manifestly particle-hole symmetric.

Status: published work in Physical Review Letters 2020, **124**, 156801

Thermal and Quantum Melting Phase Diagrams for a Magnetic-Field-Induced Wigner Solid

M. K. Ma,¹ K. A. V. Rosales,¹ H. Deng,¹ Y. J. Chung,¹ L. N. Pfeiffer,¹ K.W. West,¹ K.W. Baldwin,¹ R. Winkler,² and M. Shayegan¹

¹Department of Electrical Engineering, Princeton University, Princeton, New Jersey 08544, USA; ²Department of Physics, Northern Illinois University, DeKalb, Illinois 60115, USA



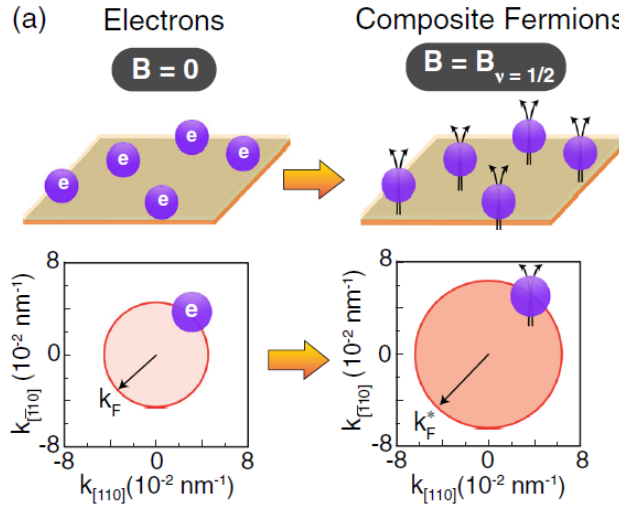
A sufficiently large perpendicular magnetic field quenches the kinetic (Fermi) energy of an interacting two-dimensional (2D) system of fermions, making them susceptible to the formation of a Wigner solid (WS) phase in which the charged carriers organize themselves in a periodic array in order to minimize their Coulomb repulsion energy. In low-disorder 2D electron systems confined to modulation-doped GaAs heterostructures, signatures of a magnetic-field-induced WS appear at low temperatures and very small Landau level filling factors ($\nu \approx 1/5$). In dilute GaAs 2D hole systems, on the other hand, thanks to the larger hole effective mass and the ensuing Landau level mixing, the WS forms at relatively higher fillings ($\nu \approx 1/3$). Here we report our measurements of the fundamental temperature vs filling phase diagram for the 2D holes' WS-liquid thermal melting. Moreover, via changing the 2D hole density, we also probe their Landau level mixing vs filling WS-liquid quantum melting phase diagram. We find our data to be in good agreement with the results of very recent calculations, although intriguing subtleties remain.

Status: published work in Physical Review Letters 2020, **125**, 036601

Precise Experimental Test of the Luttinger Theorem and Particle-Hole Symmetry for a Strongly Correlated Fermionic System

M. S. Hossain, M. A. Mueed, M. K. Ma, K. A. V. Rosales, Y. J. Chung, L. N. Pfeiffer, K.W. West, K.W. Baldwin, and M. Shayegan

Department of Electrical Engineering, Princeton University, Princeton, New Jersey 08544, USA



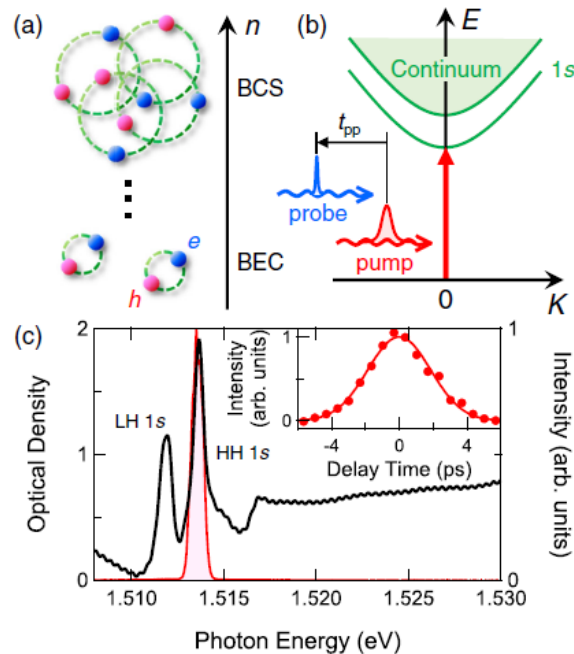
A fundamental concept in physics is the Fermi surface, the constant-energy surface in momentum space encompassing all the occupied quantum states at absolute zero temperature. In 1960, Luttinger postulated that the area enclosed by the Fermi surface should remain unaffected even when electron-electron interaction is turned on, so long as the interaction does not cause a phase transition. Understanding what determines the Fermi surface size is a crucial and yet unsolved problem in strongly interacting systems such as high- T_c superconductors. Here we present a precise test of the Luttinger theorem for a two-dimensional Fermi liquid system where the exotic quasiparticles themselves emerge from the strong interaction, namely, for the Fermi sea of composite fermions (CFs). Via direct, geometric resonance measurements of the CFs' Fermi wave vector down to very low electron densities, we show that the Luttinger theorem is obeyed over a significant range of interaction strengths, in the sense that the Fermi sea area is determined by the density of the minority carriers in the lowest Landau level. Our data also address the ongoing debates on whether or not CFs obey particle-hole symmetry, and if they are Dirac particles. We find that particle-hole symmetry is obeyed, but the measured Fermi sea area differs quantitatively from that predicted by the Dirac model for CFs.

Status: published work in Physical Review Letters 2020, **125**, 046601

Light-Driven Electron-Hole Bardeen-Cooper-Schrieffer-Like State in Bulk GaAs

Y. Murotani,¹ C. Kim,² H. Akiyama,² L. N. Pfeiffer,³ K. W. West,³ and R. Shimano^{1,4}

¹Department of Physics, The University of Tokyo, Tokyo 113-0033, Japan; ²The Institute for Solid State Physics, The University of Tokyo, and OPERANDO-OIL, Kashiwa 277-8581, Japan; ³Department of Electrical Engineering, Princeton University, Princeton, New Jersey 08544, USA; ⁴Cryogenic Research Center, The University of Tokyo, Tokyo 113-0032, Japan



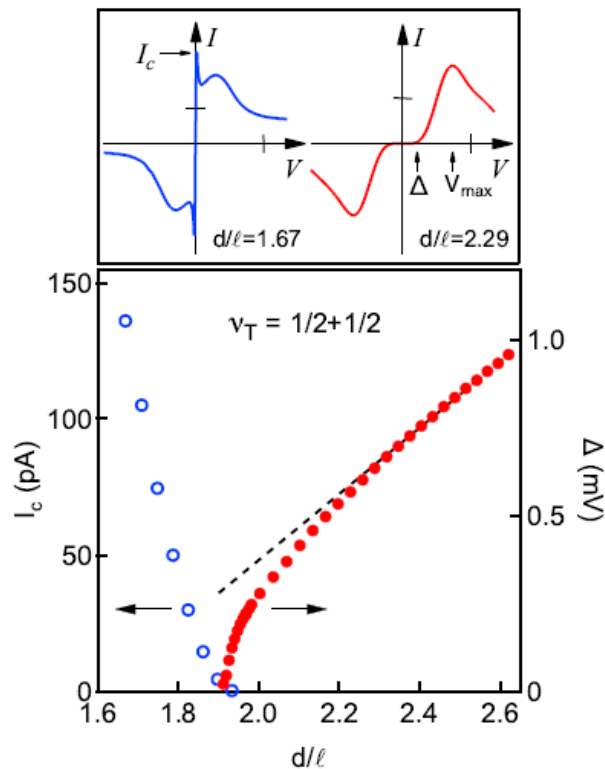
We investigate the photon-dressed state of excitons in bulk GaAs by optical pump-probe spectroscopy. We reveal that the high-energy branch of the dressed states continuously evolves into a singular enhancement at the absorption edge in the high-density region where the exciton picture is no longer valid. Comparing the experimental result with a simulation based on semiconductor Bloch equations, we show that the dressed state in such a high-density region is better viewed as a Bardeen-Cooper-Schrieffer-like state, which has been theoretically anticipated to exist over decades. Having seen that the dressed state can be regarded as a macroscopic coherent state driven by an external light field, we also discuss the decoherence from the dressed state to an incoherent state after the photoexcitation in view of the Coulomb enhancement in the transient absorption.

Status: published work in Physical Review Letters 2019, **123**, 197401

Precursors to Exciton Condensation in Quantum Hall Bilayers

J. P. Eisenstein,¹ L. N. Pfeiffer,² and K. W. West²

¹*Institute for Quantum Information and Matter, Department of Physics, California Institute of Technology, Pasadena, CA 91125, USA;* ²*Department of Electrical Engineering, Princeton University, Princeton, NJ 08544, USA*



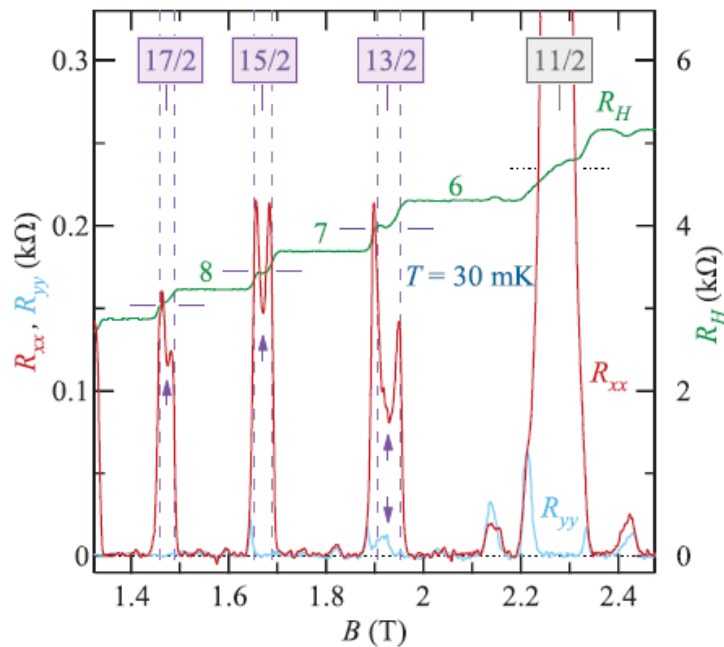
Tunneling spectroscopy reveals evidence for interlayer electron-hole correlations in quantum Hall bilayer two-dimensional electron systems at layer separations near, but above, the transition to the incompressible exciton condensate at total Landau level filling $\nu_T = 1$. These correlations are manifested by a non-linear suppression of the Coulomb pseudogap which inhibits low energy interlayer tunneling in weakly-coupled bilayers. The pseudogap suppression is strongest at $\nu_T = 1$ and grows rapidly as the critical layer separation for exciton condensation is approached from above.

Status: published work in Physical Review Letters 2019, **123**, 066802

Anomalous Nematic States in High Half-Filled Landau Levels

X. Fu,¹ Q. Shi,¹ M. A. Zudov,¹ G. C. Gardner,^{2,3} J. D. Watson,^{3,4} M. J. Manfra,^{2,3,4,5} K.W. Baldwin,⁶ L. N. Pfeiffer,⁶ and K.W. West⁶

¹School of Physics and Astronomy, University of Minnesota, Minneapolis, Minnesota 55455, USA; ²Microsoft Quantum Lab Purdue, Purdue University, West Lafayette, Indiana 47907, USA; ³Birck Nanotechnology Center, Purdue University, West Lafayette, Indiana 47907, USA; ⁴Department of Physics and Astronomy, Purdue University, West Lafayette, Indiana 47907, USA; ⁵School of Electrical and Computer Engineering and School of Materials Engineering, Purdue University, West Lafayette, Indiana 47907, USA; ⁶Department of Electrical Engineering, Princeton University, Princeton, New Jersey 08544, USA



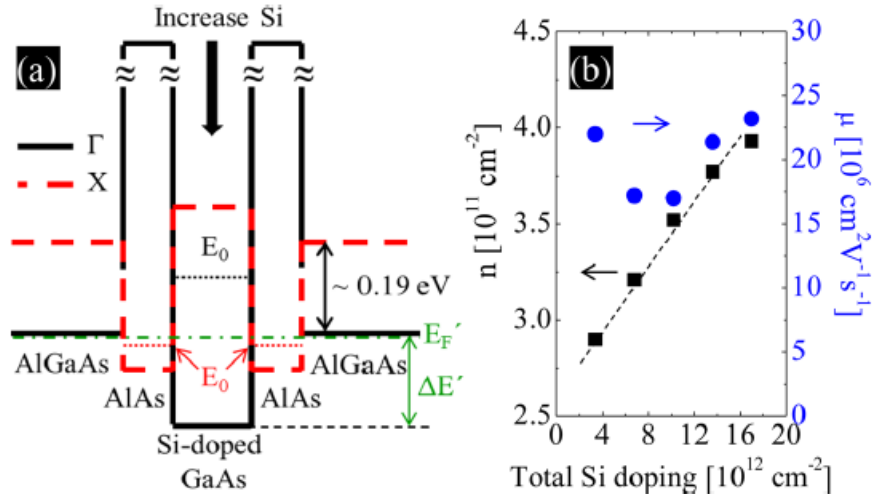
It is well established that the ground states of a two-dimensional electron gas with half-filled high ($N \geq 2$) Landau levels are compressible charge-ordered states, known as quantum Hall stripe (QHS) phases. The generic features of QHSs are a maximum (minimum) in a longitudinal resistance R_{xx} (R_{yy}) and a nonquantized Hall resistance R_H . Here, we report on emergent minima (maxima) in R_{xx} (R_{yy}) and plateaulike features in R_H in half-filled $N \geq 3$ Landau levels. Remarkably, these unexpected features develop at temperatures considerably lower than the onset temperature of QHSs, suggestive of a new ground state.

Status: published work in Physical Review Letters 2020, **124**, 067601

Working principles of doping-well structures for high-mobility two-dimensional electron systems

Yoon Jang Chung, K. A. Villegas Rosales, K. W. Baldwin, K. W. West, M. Shayegan, and L. N. Pfeiffer

Department of Electrical Engineering, Princeton University, Princeton, New Jersey 08544, USA



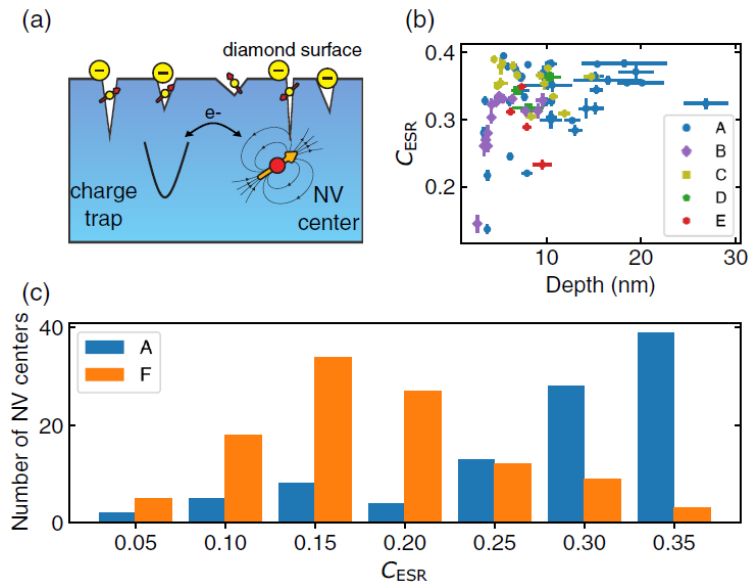
Suppressing electron scattering is essential to achieve high-mobility two-dimensional electron systems (2DESs) that are clean enough to probe exotic interaction-driven phenomena. In heterostructures it is common practice to utilize modulation doping, where the ionized dopants are physically separated from the 2DES channel. The doping-well structure augments modulation doping by providing additional screening for all types of charged impurities in the vicinity of the 2DES, which is necessary to achieve record-breaking samples. Despite its prevalence in the design of ultrahigh-mobility 2DESs, the working principles of the doping-well structure have not been reported. Here we elaborate on the mechanics of electron transfer from doping wells to the 2DES, focusing on GaAs/AlGaAs samples grown by molecular beam epitaxy. Based on this understanding we demonstrate how structural parameters in the doping well can be varied to tune the properties of the 2DES.

Status: published work in Physical Review Materials 2020, **4**, 044003

Charge state dynamics and optically detected electron spin resonance contrast of shallow nitrogen-vacancy centers in diamond

Zhiyang Yuan, Mattias Fitzpatrick, Lila V. H. Rodgers, Sorawis Sangtawesin, Srikanth Srinivasan, and Nathalie P. de Leon

Department of Electrical Engineering, Princeton University, Princeton, New Jersey 08544, USA



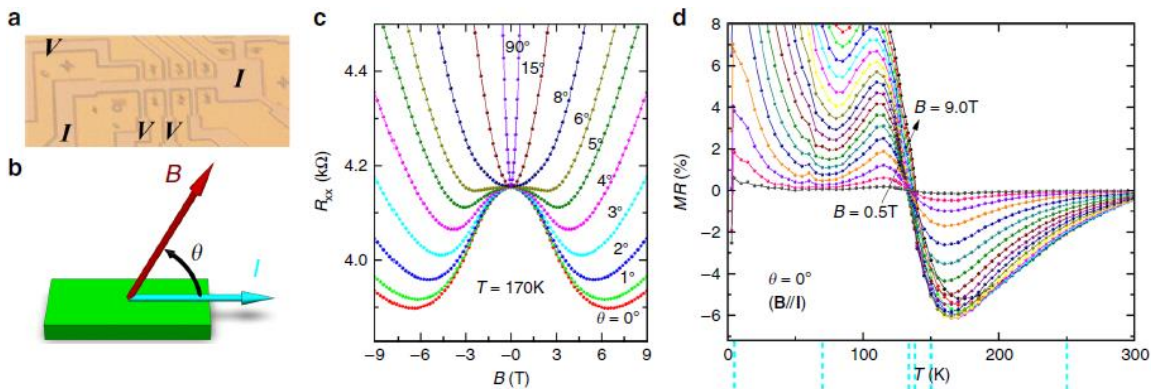
Nitrogen-vacancy (NV) centers in diamond can be used for nanoscale sensing with atomic resolution and sensitivity; however, it has been observed that their properties degrade as they approach the diamond surface. Here we report that in addition to degraded spin coherence, NV centers within nanometers of the surface can also exhibit decreased fluorescence contrast for optically detected electron spin resonance (OD-ESR). We demonstrate that this decreased OD-ESR contrast arises from charge state dynamics of the NV center, and that it is strongly surface-dependent, indicating that surface engineering will be critical for nanoscale sensing applications based on color centers in diamond.

Status: published work in Physical Review Research 2020, 2, 033263

Negative longitudinal magnetoresistance in gallium arsenide quantum wells

Jing Xu,^{1,2} Meng K. Ma,³ Maksim Sultanov,² Zhi-Li Xiao,^{1,2} Yong-Lei Wang,^{1,4} Dafei Jin,⁵ Yang-Yang Lyu,^{1,4} Wei Zhang,^{1,6} Loren N. Pfeiffer,³ Ken W. West,³ Kirk W. Baldwin,³ Mansour Shayegan,³ and Wai-Kwong Kwok¹

¹Argonne National Laboratory, Materials Science Division, Argonne, IL 60439, USA. ²Department of Physics, Northern Illinois University, DeKalb, IL 60115, USA. ³Department of Electrical Engineering, Princeton University, Princeton, NJ 08544, USA. ⁴Research Institute of Superconductor Electronics, School of Electronic Science and Engineering, Nanjing University, 210093 Nanjing, China. ⁵Argonne National Laboratory, Center for Nanoscale Materials, Argonne, IL 60439, USA. ⁶Department of Physics, Oakland University, Rochester, MI 48309, USA.



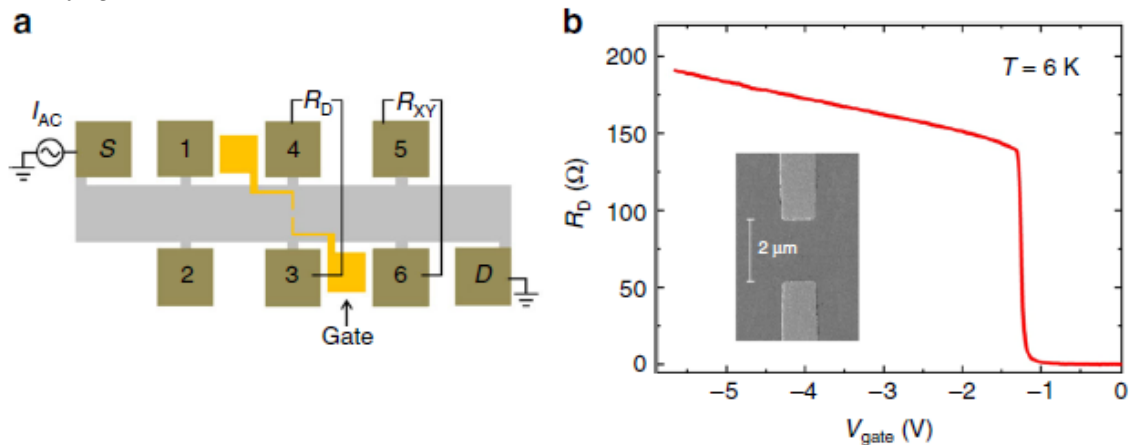
Negative longitudinal magnetoresistances (NLMRs) have been recently observed in a variety of topological materials and often considered to be associated with Weyl fermions that have a defined chirality. Here we report NLMRs in non-Weyl GaAs quantum wells. In the absence of a magnetic field the quantum wells show a transition from semiconducting-like to metallic behaviour with decreasing temperature. We observe pronounced NLMRs up to 9 Tesla at temperatures above the transition and weak NLMRs in low magnetic fields at temperatures close to the transition and below 5 K. The observed NLMRs show various types of magnetic field behaviour resembling those reported in topological materials. We attribute them to microscopic disorder and use a phenomenological three-resistor model to account for their various features. Our results showcase a contribution of microscopic disorder in the occurrence of unusual phenomena. They may stimulate further work on tuning electronic properties via disorder/defect nano-engineering.

Status: published work in Nature Communications 2019, **10**, 287

3/2 fractional quantum Hall plateau in confined two-dimensional electron gas

Hailong Fu,^{1,2,7} Yijia Wu,^{1,7} Ruoxi Zhang,¹ Jian Sun,¹ Pujia Shan,¹ Pengjie Wang,¹ Zheyi Zhu,¹ L.N. Pfeiffer,³ K.W. West,³ Haiwen Liu,⁴ X.C. Xie,^{1,5,6} and Xi Lin,^{1,5,6}

¹International Center for Quantum Materials, Peking University, 100871 Beijing, China. ²Department of Physics, The Pennsylvania State University, University Park, PA 16802, USA. ³Department of Electrical Engineering, Princeton University, Princeton, NJ 08544, USA. ⁴Center for Advanced Quantum Studies, Department of Physics, Beijing Normal University, 100875 Beijing, China. ⁵Beijing Academy of Quantum Information Sciences, 100193 Beijing, China. ⁶CAS Center for Excellence in Topological Quantum Computation, University of Chinese Academy of Sciences, 100190 Beijing, China



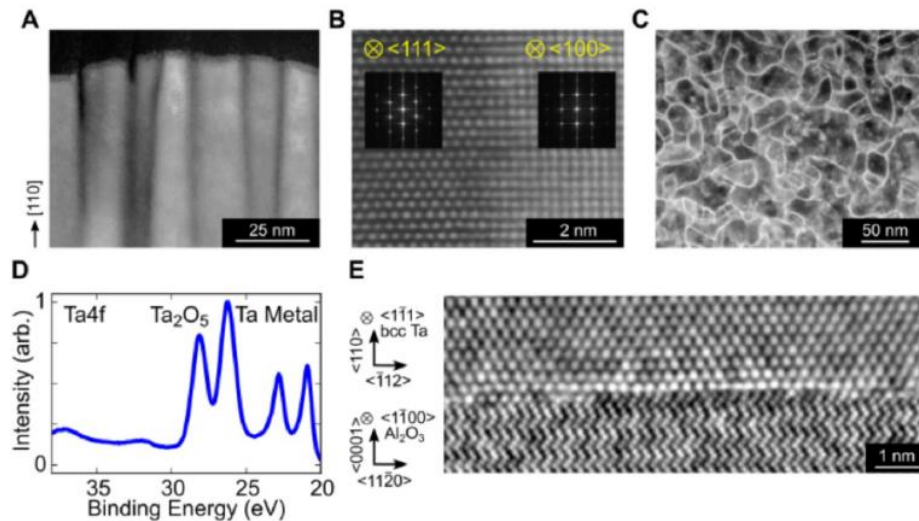
Even-denominator fractional quantum Hall (FQH) states, such as $5/2$ and $7/2$, have been well known in a two-dimensional electron gas (2DEG) for decades and are still investigated as candidates of non-Abelian statistics. In this paper, we present the observation of a $3/2$ FQH plateau in a single-layer 2DEG with lateral confinement at a bulk filling factor of $5/3$. The $3/2$ FQH plateau is quantized at $(h/e^2)/(3/2)$ within 0.02%, and can survive up to 300 mK. This even-denominator FQH plateau may imply intriguing edge structure and excitation in FQH system with lateral confinement. The observations in this work demonstrate that understanding the effect of the lateral confinement on the many-body system is critical in the pursuit of important theoretical proposals involving edge physics, such as the demonstration of non-Abelian statistics and the realization of braiding for fault-tolerant quantum computation.

Status: published work in Nature Communications 2019, **10**, 4351

New material platform for superconducting transmon qubits with coherence times exceeding 0.3 milliseconds

A.P.M Place,¹ L.V.H. Rodgers,¹ P. Mundada,¹ B.M. Smitham,¹ M. Fitzpatrick,¹ Z. Leng,² A. Premkumar,¹ J. Bryon,¹ S. Sussman,² G.M. Cheng,³ T. Madhavan,¹ H.K. Babla,¹ B. Jack,² A. Gyenis,¹ N. Yao,³ R.J. Cava,⁴ N.P. de Leon,¹ and A.A. Houck¹

¹Department of Electrical Engineering, Princeton University, Princeton, NJ 08544, USA; ²Department of Physics, Princeton University, Princeton, NJ 08544, USA; ³Princeton Institute for Science and Technology of Materials, Princeton University, Princeton, NJ 08544, USA; ⁴Department of Chemistry, Princeton University, Princeton, NJ 08544, USA.



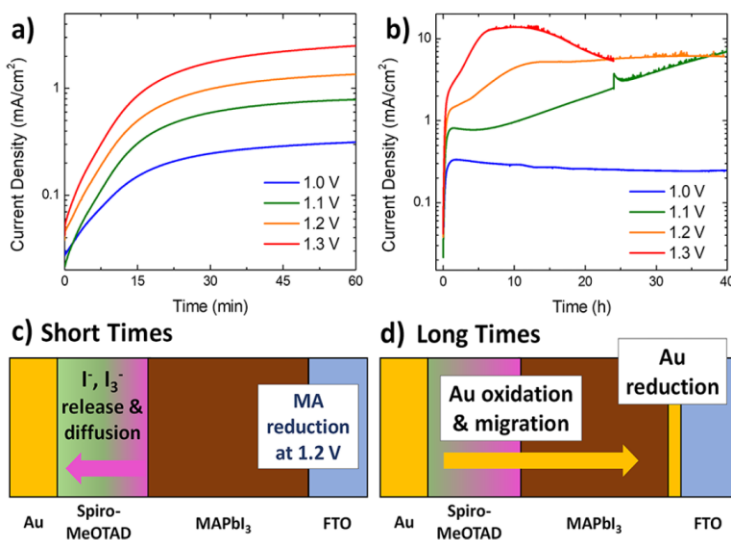
The superconducting transmon qubit is a leading platform for quantum computing and quantum science. Building large, useful quantum systems based on transmon qubits will require significant improvements in qubit relaxation and coherence times, which are orders of magnitude shorter than limits imposed by bulk properties of the constituent materials. This indicates that relaxation likely originates from uncontrolled surfaces, interfaces, and contaminants. Previous efforts to improve qubit lifetimes have focused primarily on designs that minimize contributions from surfaces. However, significant improvements in the lifetime of two-dimensional transmon qubits have remained elusive for several years. Here, we fabricate two-dimensional transmon qubits that have both lifetimes and coherence times with dynamical decoupling exceeding 0.3 milliseconds by replacing niobium with tantalum in the device. We have observed increased lifetimes for seventeen devices, indicating that these material improvements are robust, paving the way for higher gate fidelities in multi-qubit processors.

Status: published work in arXiv:2003.00024 [quant-ph]

Low Threshold Voltages Electrochemically Drive Gold Migration in Halide Perovskite Devices

Ross A. Kerner,^{1,2} Lianfeng Zhao,¹ Steven P. Harvey,² Joseph J. Berry,² Jeffrey Schwartz,³ and Barry P. Rand^{1,4}

¹Department of Electrical Engineering, Princeton University, Princeton, NJ 08544, USA; ²National Renewable Energy Laboratory, Golden, CO 80401, USA ³Department of Chemistry, Princeton University, Princeton, NJ 08544, USA; ⁴Andlinger Center for Energy and the Environment, Princeton University, Princeton, NJ 08544, USA;



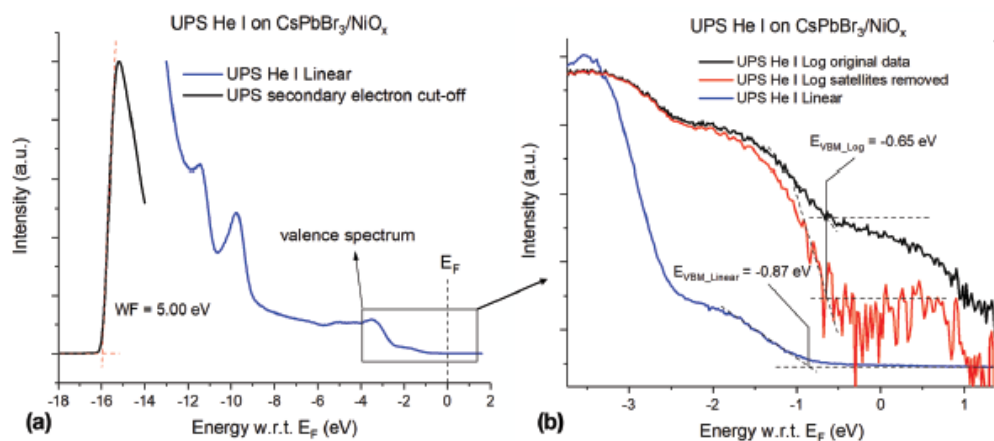
The constituent ions of halide perovskite materials are mobile in the solid state and known to participate in reduction/oxidation reactions. Yet few parameters related to electrochemical processes occurring within devices have been carefully determined. Here, we characterize such reactions in model MAPbI₃ perovskite devices, and we quantify threshold voltages for key reactions. Gold is oxidized and mobilized under nitrogen, in the dark, at the MAPbI₃/Au interface at 0.8 V. When this interface is buffered with the organic hole transport material (HTM), 2,2',7,7'-tetrakis(N,N-di-p-methoxyphenylamino)-9,9'-spirobifluorene, MAPbI₃ begins to degrade at 1.2 V; degradation liberates ions that subsequently enable Au migration. Thresholds are insensitive to MAPbI₃ thickness or choice of organic HTM or oxide cathode, which suggests that these reactions are driven electrochemically; the electric field across the device is less important. These results have profound implications for understanding in operando degradation pathways of optoelectronic perovskite devices that are varied in terms of interface structures, active material compositions, and ranges of external stressors.

Status: published work at ACS Energy Letters 2020, **5**, 3352–3356

Ultraviolet Photoemission Spectroscopy and Kelvin Probe Measurements on Metal Halide Perovskites: Advantages and Pitfalls

Fengyu Zhang,¹ Scott H. Silver,¹ Nakita K. Noel,^{1,2} Florian Ullrich,³ Barry P. Rand,^{1,4} and Antoine Kahn¹

¹Department of Electrical Engineering, Princeton University, Princeton, NJ 08544, USA; ²Princeton Institute for the Science and Technology of Materials, Princeton University, Princeton, NJ 08544, USA; ³Materials Science Department, Technische Universität Darmstadt, 64287 Darmstadt, Germany; ⁴Andlinger Center for Energy and the Environment, Princeton University, Princeton, NJ 08544, USA



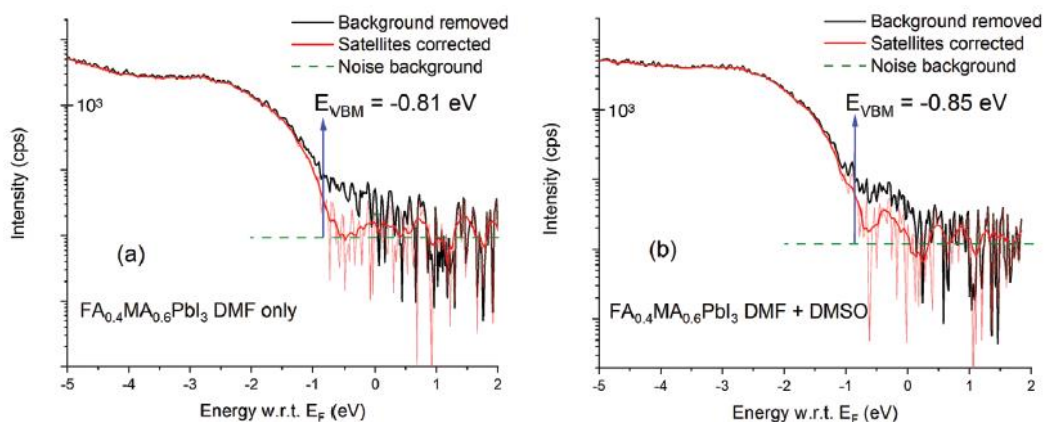
In this essay, a case study is presented on the electronic structure of several metal halide perovskites (MHP) using Kelvin probe (KP)-based surface photovoltage (SPV) measurements and ultraviolet photoemission spectroscopy (UPS) to demonstrate the advantages, but also the pitfalls, of using these techniques to characterize the surfaces of these materials. The first part addresses the loss of halide species from perovskite surfaces upon supragap illumination in vacuum. This has the potential to cause both a long-term alteration of the sample work function and a modification of the KP tip during SPV measurements. If undetected, this leads to a misinterpretation of the MHP surface potential. The second part illustrates the difficulties in determining the valence band maximum (VBM) of MHP surfaces with UPS and stresses the importance of taking into account the low density of states at the VBM edge. Given this circumstance, specific care must be taken to eliminate measurement artifacts in order to ascertain the presence or absence of low densities of electronic gap states above the VBM. This essay also highlights issues such as film degradation, nonequilibrium situations (e.g., SPV), and satellite emissions, which occur during photoemission spectroscopy

Status: published work at *Advanced Energy Materials* 2020, **10**, 1903252

Gap States in Methylammonium Lead Halides: The Link to Dimethylsulfoxide?

Fengyu Zhang,¹ J. Clay Hamill,² Jr., Yueh-Lin Loo,² and Antoine Kahn¹

¹Department of Electrical Engineering, Princeton University, Princeton, NJ 08544, USA; ²Department of Chemical and Biological Engineering, Princeton University, Princeton, NJ 08544, USA; ³Andlinger Center for Energy and the Environment, Princeton University, Princeton, NJ 08544, USA



Understanding the origin and distribution of electronic gap states in metal halide perovskite (MHP) thin films is crucial to the further improvement of the efficiency and long-term stability of MHP-based optoelectronic devices. In this work, the impact of Lewis-basic additives introduced in the precursor solution on the density of states in the perovskite bandgap is investigated. Ultraviolet photoemission spectroscopy and contact potential difference measurements are conducted on MHP thin films processed from dimethylformamide (DMF)-based solutions to which either no additive, dimethylsulfoxide (DMSO), or N-methylpyrrolidine-2-thione (NMPT) is added. The results show the presence of a density of states in the gap of methylammonium lead halide films processed from DMSO-containing solution. The density of gap states is either suppressed when the methylammonium concentration in mixed cation films is reduced or when NMPT is used as an additive, and eliminated when methylammonium (MA) is replaced with cesium or formamidinium (FA). These results are consistent with the notion that reaction products that result from DMSO reacting with MA⁺ in the precursor solution are responsible for the formation of gap states.

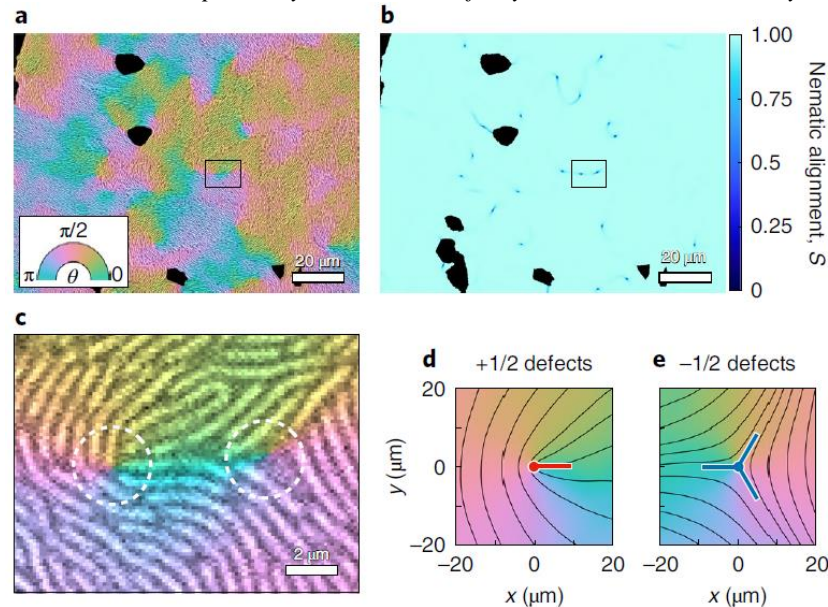
Status: published work at *Advanced Materials* 2020, **32**, 2003482

Lewis-Sigler Institute for Integrative Genomics

Topological defects promote layer formation in *Myxococcus xanthus* colonies

Katherine Copenhagen,¹ Ricard Alert,^{1,2} Ned S. Wingreen,^{1,3} and Joshua W. Shaevitz.^{1,4}

¹Lewis-Sigler Institute for Integrative Genomics, Princeton University, Princeton, NJ, USA. ²Princeton Center for Theoretical Science, Princeton University, Princeton, NJ, USA. ³Department of Molecular Biology, Princeton University, Princeton, NJ, USA. ⁴Joseph Henry Laboratories of Physics, Princeton University, Princeton, NJ, USA.



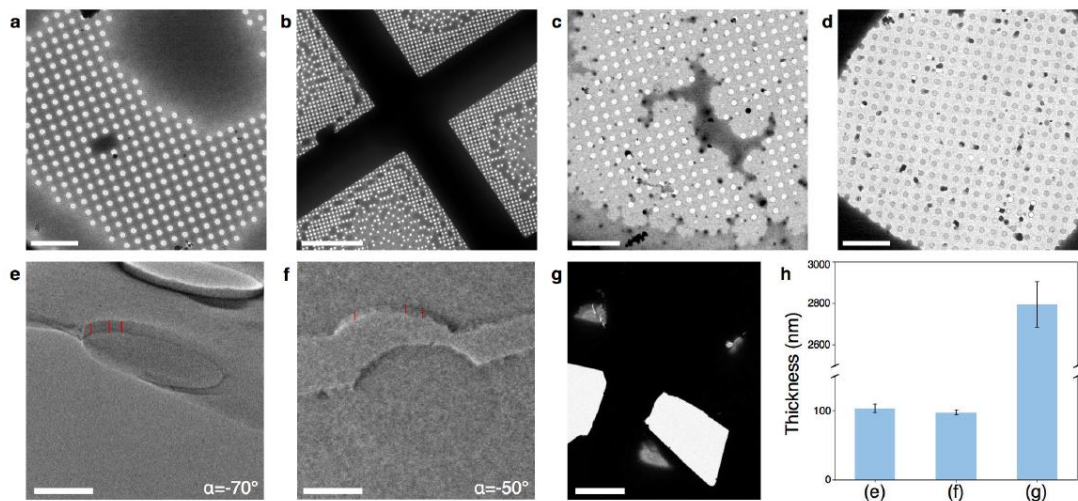
The soil bacterium *Myxococcus xanthus* lives in densely packed groups that form dynamic three-dimensional patterns in response to environmental changes, such as droplet-like fruiting bodies during starvation. The development of these multicellular structures begins with the sequential formation of cell layers in a process that is poorly understood. Here, using confocal three-dimensional imaging, we find that motile, rod-shaped *M. xanthus* cells are densely packed and aligned in each layer, forming an active nematic liquid crystal. Cell alignment is nearly perfect throughout the population except at point defects that carry half-integer topological charge. We observe that new cell layers preferentially form at the position of $+1/2$ defects, whereas holes preferentially open at $-1/2$ defects. To explain these findings, we model the bacterial colony as an extensile active nematic fluid with anisotropic friction. In agreement with our experimental measurements, this model predicts an influx of cells towards the $+1/2$ defects and an outflux of cells from the $-1/2$ defects. Our results suggest that cell motility and mechanical cell–cell interactions are sufficient to promote the formation of cell layers at topological defects, thereby seeding fruiting bodies in colonies of *M. xanthus*.

Status: published work at Nature Physics 2020

**Princeton Institute for the Science and Technology of
Materials (PRISM)**

Understanding solution processing of inorganic materials using cryo-EM

Nikita S. Dutta,^{1,2} Paul Shao,¹ Kai Gong,^{3,4} Claire E. White,^{3,4} Nan Yao,¹ and Craig B. Arnold^{1,2}
¹Princeton Institute for the Science and Technology of Materials, Princeton University, Princeton, New Jersey 08544, USA; ²Department of Mechanical and Aerospace Engineering, Princeton University, Princeton, New Jersey 08544, USA; ³Department of Civil and Environmental Engineering, Princeton University, Princeton, New Jersey 08544, USA; ⁴Andlinger Center for Energy and the Environment, Princeton University, Princeton, New Jersey 08544, USA



Cryo-electron microscopy (cryo-EM) single particle analysis (SPA) has revolutionized biology, revealing the hydrated structure of numerous macromolecules. Yet, the potential of SPA to study inorganic materials remains largely unexplored. An area that could see great impact is solution-processed device materials, where solution changes affect everything from crystal morphology for perovskite photovoltaics to stability of photoluminescent quantum dots. While with traditional microscopy, structures underlying these effects can only be analyzed after drying, cryo-EM allows characterization of in-solution structures, revealing how features arise during processing. A top candidate for such characterization is found in chalcogenide glasses (ChGs), which researchers in the 1980s proposed take on solvent-dependent solution nanostructures whose morphologies have yet to be confirmed. Here we show that cryo-EM can directly image ChGs in solution and combine with other techniques to connect solution structure to film characteristics. Our results bring closure to a long open question in optoelectronics and establish SPA as a tool for solution-processed materials.

Status: published work at *Optical Materials Express* 2020, **10**, 119

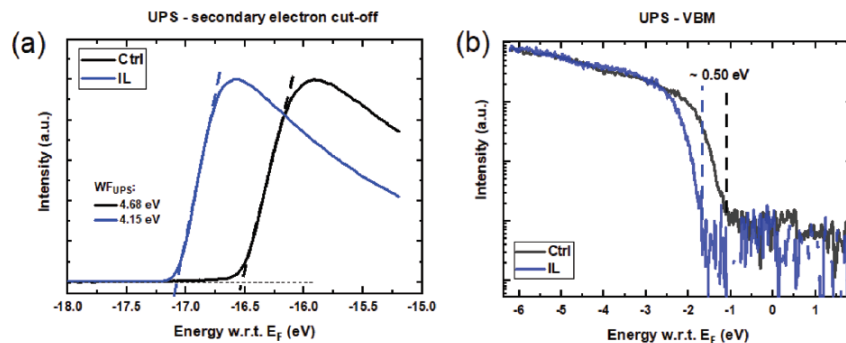
Elucidating the Role of a Tetrafluoroborate-Based Ionic Liquid at the n-Type Oxide/Perovskite Interface

Nakita K. Noel^{1,2}, Severin N. Habisreutinger³, Bernard Wenger⁴, Yen-Hung Lin⁴, Fengyu Zhang², Jay B. Patel⁴, Antoine Kahn², Michael B. Johnston⁴, and Henry J. Snaith⁴

¹Princeton Institute for the Science and Technology of Materials, Princeton University, Princeton, NJ 08544, USA;

²Department of Electrical Engineering, Princeton University, Princeton, NJ 08544, USA; ³National Renewable

Energy Laboratory, Golden, CO 80401, USA; ⁴Clarendon Laboratory, Department of Physics, University of Oxford, Parks Road, Oxford OX1 3PU, UK



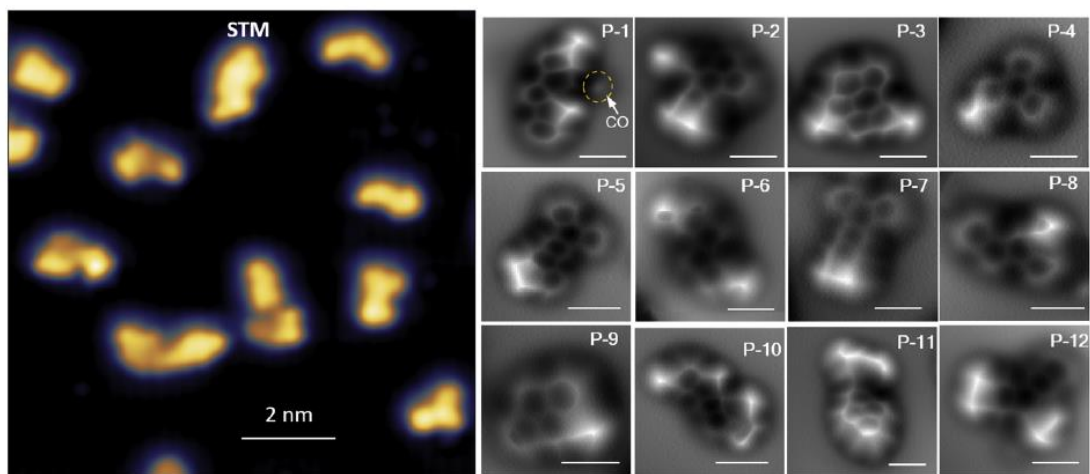
Halide perovskites are currently one of the most heavily researched emerging photovoltaic materials. Despite achieving remarkable power conversion efficiencies, perovskite solar cells have not yet achieved their full potential, with the interfaces between the perovskite and the charge-selective layers being where most recombination losses occur. In this study, a fluorinated ionic liquid (IL) is employed to modify the perovskite/SnO₂ interface. Using Kelvin probe and photoelectron spectroscopy measurements, it is shown that depositing the perovskite onto an IL-treated substrate results in the crystallization of a perovskite film which has a more n-type character, evidenced by a decrease of the work function and a shift of the Fermi level toward the conduction band. Photoluminescence spectroscopy and time-resolved microwave conductivity are used to investigate the optoelectronic properties of the perovskite grown on neat and IL-modified surfaces and it is found that the modified substrate yields a perovskite film which exhibits an order of magnitude lower trap density than the control. When incorporated into solar cells, this interface modification results in a reduction in the current–voltage hysteresis and an improvement in device performance, with the best performing devices achieving steady-state PCEs exceeding 20%.

Status: published work at Adv. Energy Mater. 2020, **10**, 1903231

Petroleum pitch: Exploring a 50-year structure puzzle with real-space molecular imaging

Pengcheng Chen,¹ Jordan N. Metz,² Anthony S. Mennito,² Shamel Merchant,² Stuart E. Smith,² Michael Siskin,² Steven P. Rucker,² David C. Dankworth,² J. Douglas Kushnerick,² Nan Yao,¹ and Yunlong Zhang,²

¹PRISM Imaging and Analysis Center, Princeton University, Princeton, NJ, 08544, USA; ²ExxonMobil Research and Engineering Company, 1545 Route 22 E., Annandale, NJ, 08801, USA



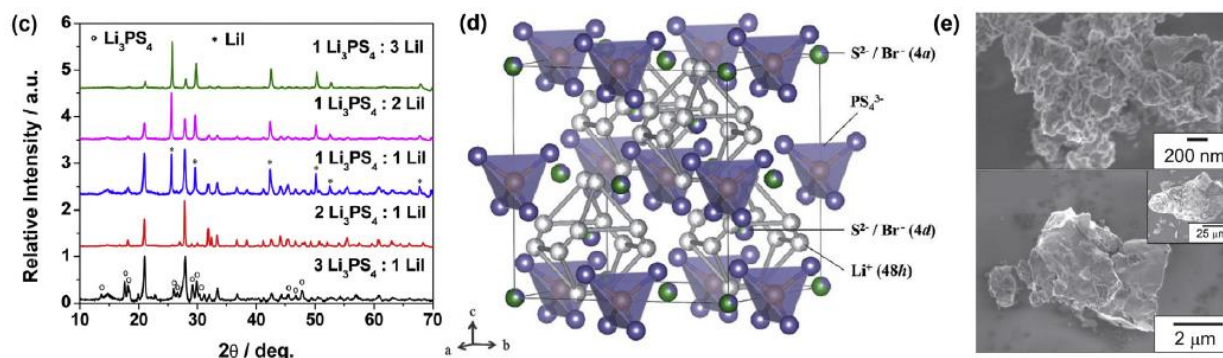
Petroleum pitch has played a significant role in carbon science as a key abundant resource for polycyclic aromatic hydrocarbons in making various higher value carbon materials. Despite many detailed studies using advanced characterization techniques over 50 years, the exact nature of the molecular structures of petroleum M-50 pitch and their mesophase products remains unclear, due to the molecular diversity and the low solubility of this material. In this study, we applied real-space single molecule imaging noncontact atomic force microscopy to obtain exact structures of individual molecules, and compared the results from other characterization techniques to validate some of the previously hypothesized average structures. We identified a diverse slate of largely catacondensed polycyclic aromatic hydrocarbons with short alkyl chains, such as methyl and methylene groups. Furthermore, both single core and multi-core structures have been observed, in contrast to previous assertions that only one type would be present. The presence of these structures enables a mechanistic rationalization for their formation and allows potential mechanisms for the thermal conversion of pitch into larger bonding networks to be postulated.

Status: published work at Carbon 2020, **161**, 456-465

Liquid-involved synthesis and processing of sulfide-based solid electrolytes, electrodes, and all-solid-state batteries

J. Xu,^{1,2} L. Liu,³ N. Yao,⁴ F. Wu,^{1,2,3,5} H. Li,^{1,2,3,5} L. Chen,^{1,2,3,5}

¹Key Laboratory for Renewable Energy, Beijing Key Laboratory for New Energy Materials and Devices, Beijing National Laboratory for Condensed Matter Physics, Institute of Physics, Chinese Academy of Sciences, Beijing, 100190, China; ²Center of Materials Science and Optoelectronics Engineering, University of Chinese Academy of Sciences, Beijing, 100049, China; ³Tianmu Lake Institute of Advanced Energy Storage Technologies, Liyang, 213300, China; ⁴Princeton Institute for the Science and Technology of Materials (PRISM), Princeton University, Princeton, NJ, 08540, USA; ⁵Yangtze River Delta Physics Research Center, Liyang, 213300, China



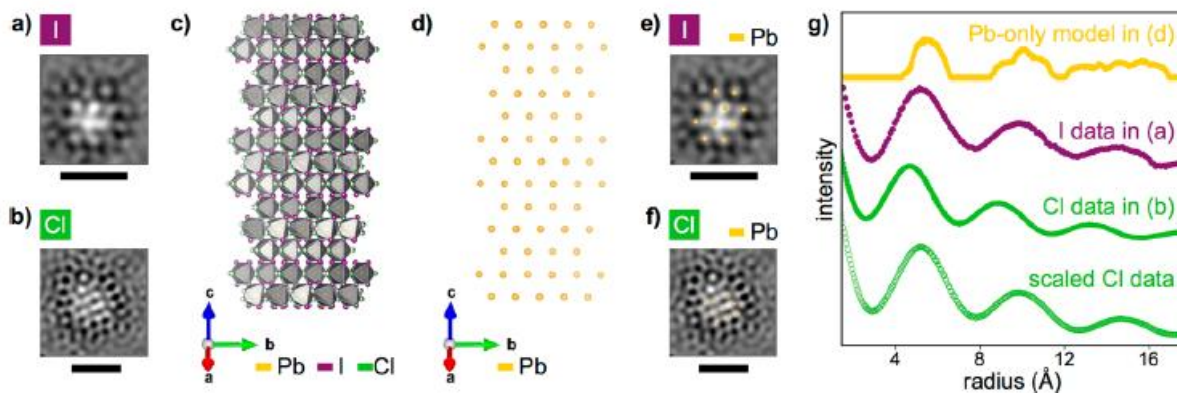
Solid-state battery has been widely accepted as the next-generation energy-storage technology because of its better safety and potentially higher energy density. Solid electrolyte plays the most critical role in its performance, among which sulfides show the highest lithium-ion conductivities. To realize the mass production and practical application of sulfide-based electrolytes and all-solid-state batteries, one of the most promising methods is by in-situ solidification of sulfide-electrolyte solution/slurries with liquid-involved processing that can be performed in controlled atmosphere with low temperature. This enables wet coating process for electrolyte/electrode layer formation and thus opens up the possibility of mass production of sulfide solid-state batteries. In this review, liquid-involved process is carefully classified into liquid-phase synthesis, solution, and slurry process with clear definition to avoid any confusion among these different processes. The liquid-involved processes of sulfide solid electrolytes themselves on material level, sulfide-based composite electrolytes/electrodes on component level, and sulfide-based all-solid-state batteries on device level are summarized and discussed in details. Strategies to design and prepare solid sulfide-based electrolytes/electrode layers and batteries with liquid-involved process are also suggested.

Status: published work at Materials Today Nano 2019, **8**, 100048

Crystalline Nature of Colloids in Methylammonium Lead Halide Perovskite Precursor Inks Revealed by Cryo-Electron Microscopy

Nikita S. Dutta,^{1,2} Nakita K. Noel,^{1,3} and Craig B. Arnold^{1,2}

¹Princeton Institute for the Science and Technology of Materials, Princeton University, Princeton, New Jersey 08544, USA; ²Department of Mechanical and Aerospace Engineering, Princeton University, Princeton, New Jersey 08544, USA; ³Department of Electrical Engineering, Princeton University, Princeton, New Jersey 08544, USA.



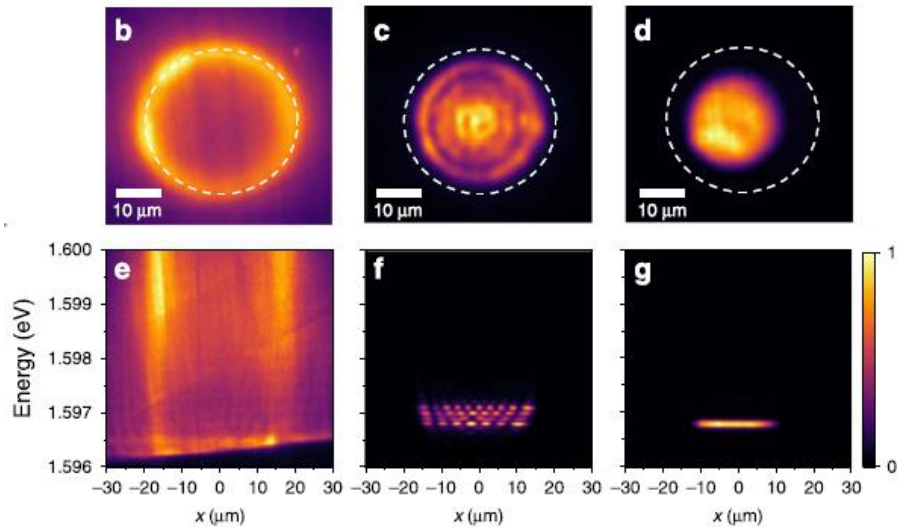
Metal halide perovskites have generated interest across many fields for the impressive optoelectronic properties achievable in films produced using facile solution processing techniques. Previous research has revealed the colloidal nature of perovskite precursor inks and established a relationship between the colloid distribution and the film optoelectronic quality. Yet, the identity of colloids remains unknown, hindering our understanding of their role in perovskite crystallization. Here, we investigate precursor inks of the prototypical methylammonium lead triiodide perovskite using cryo-electron microscopy (cryo-EM) and show, for the first time, that the colloids are neither amorphous nor undissolved lead iodide, as previously speculated, but are a crystalline, non-perovskite material. We identify this as a perovskite precursor phase and discuss this as a potential means to understanding the role of chloride in processing. This work establishes cryo-EM as a viable technique to elucidate the nature of colloids in perovskite inks, a vital step toward a fundamental understanding of thin-film crystallization.

Status: published work in J. Phys. Chem. Lett. 2020, **11**, 5980-5986

Observation of quantum depletion in a non-equilibrium exciton-polariton condensate

M. Pieczarka,¹ E. Estrecho,¹ M. Boozarjmehr,¹ O. Bleu,² M. Steger,^{3,6} K. West,⁴ L. N. Pfeiffer,⁴ D. W. Snoke,³ J. Levinsen,² M. M. Parish,² A. G. Truscott,⁵ and E. A. Ostrovskaya¹

¹ARC Centre of Excellence in Future Low-Energy Electronics Technologies and Nonlinear Physics Centre, Research School of Physics, The Australian National University, Canberra, ACT 2601, Australia; ²ARC Centre of Excellence in Future Low-Energy Electronics Technologies and School of Physics and Astronomy, Monash University, Melbourne, VIC 3800, Australia; ³Department of Physics and Astronomy, University of Pittsburgh, Pittsburgh, PA 15260, USA; ⁴Princeton Institute for the Science and Technology of Materials (PRISM), Princeton University, Princeton, NJ 08544, USA; ⁵Laser Physics Centre, Research School of Physics, The Australian National University, Canberra, ACT 2601, Australia; ⁶Present address: National Renewable Energy Lab, Golden, CO 80401, USA



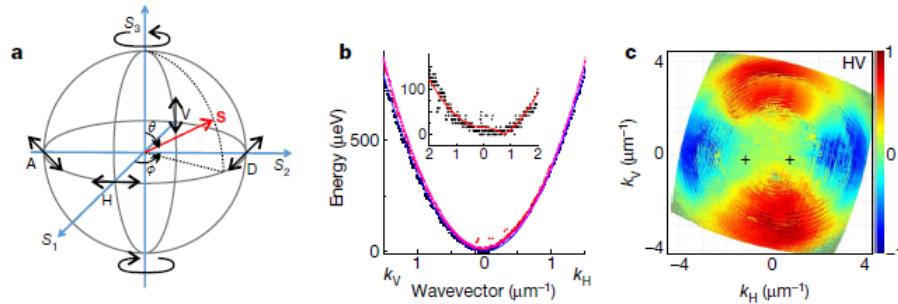
Superfluidity, first discovered in liquid ^4He , is closely related to Bose–Einstein condensation (BEC) phenomenon. However, even at zero temperature, a fraction of the quantum liquid is excited out of the condensate into higher momentum states via interaction-induced fluctuations—the phenomenon of quantum depletion. Quantum depletion of atomic BECs in thermal equilibrium is well understood theoretically but is difficult to measure. This measurement is even more challenging in driven-dissipative exciton–polariton condensates, since their non-equilibrium nature is predicted to suppress quantum depletion. Here, we observe quantum depletion of a high-density exciton–polariton condensate by detecting the spectral branch of elementary excitations. Analysis of this excitation branch shows that quantum depletion of exciton–polariton condensates can closely follow or strongly deviate from the equilibrium Bogoliubov theory. Our results reveal beyond mean-field effects of exciton–polariton interactions and call for a deeper understanding of the relationship between equilibrium and non-equilibrium BECs.

Status: published work in Nature Communication 2020, **11**, 429

Measurement of the quantum geometric tensor and of the anomalous Hall drift

A. Gianfrate,^{1,4} O. Bleu,^{2,4} L. Dominici,¹ V. Ardizzone,¹ M. De Giorgi,¹ D. Ballarini,¹ G. Lerario,¹ K. W. West,³ L. N. Pfeiffer,³ D. D. Solnyshkov,² D. Sanvitto,¹ and G. Malpuech²

¹CNR NANOTEC, Istituto di Nanotecnologia, Lecce, Italy; ²Institut Pascal, PHOTON-N2, Université Clermont Auvergne, CNRS, SIGMA Clermont, Clermont-Ferrand, France; ³Princeton Institute for the Science and Technology of Materials, Princeton University, Princeton, NJ, USA



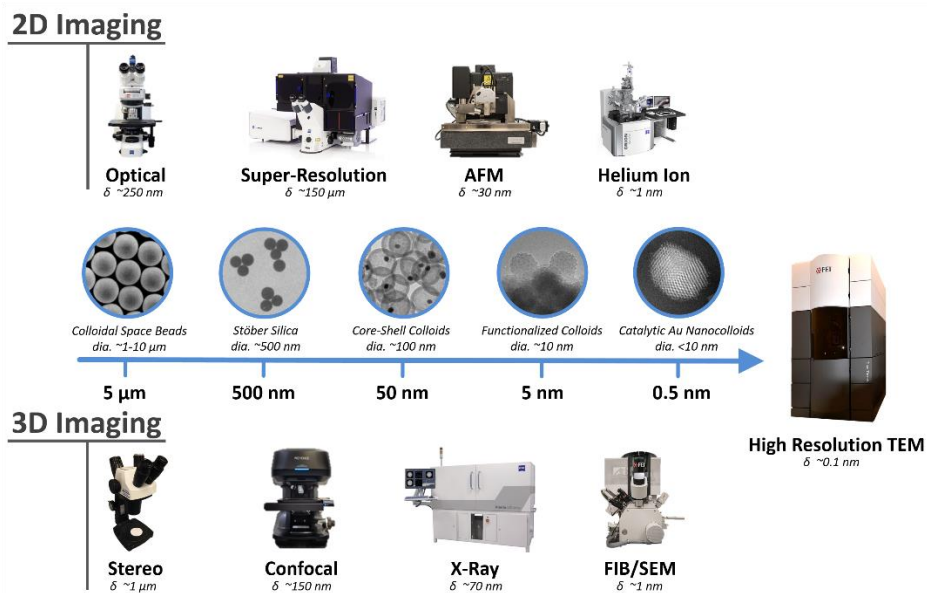
Topological physics relies on the structure of the eigenstates of the Hamiltonians. The geometry of the eigenstates is encoded in the quantum geometric tensor - comprising the Berry curvature and the quantum metric, which defines the distance between the eigenstates. Knowledge of the quantum metric is essential for understanding many phenomena, such as superfluidity in flat bands, orbital magnetic susceptibility, the exciton Lamb shift and the non-adiabatic anomalous Hall effect. However, the quantum geometry of energy bands has not been measured. Here we report the direct measurement of both the Berry curvature and the quantum metric in a two-dimensional continuous medium—a high-finesse planar microcavity—together with the related anomalous Hall drift. The microcavity hosts strongly coupled exciton–photon modes (exciton polaritons) that are subject to photonic spin–orbit coupling from which Dirac cones emerge, and to exciton Zeeman splitting, breaking time-reversal symmetry. The monopolar and half-skyrmion pseudospin textures are measured using polarization resolved photoluminescence. The associated quantum geometry of the bands is extracted, enabling prediction of the anomalous Hall drift, which we measure independently using high-resolution spatially resolved epifluorescence. Our results unveil the intrinsic chirality of photonic modes, the cornerstone of topological photonics. These results also experimentally validate the semiclassical description of wavepacket motion in geometrically non-trivial bands. The use of exciton polaritons (interacting photons) opens up possibilities for future studies of quantum fluid physics in topological systems.

Status: published work in Nature 2020, **578**, 381-385

The Advanced Microscopy of Colloids

Daniel G. Gregory and Nan Yao

Princeton Institute for the Science and Technology of Materials, Princeton University, Princeton, NJ, USA



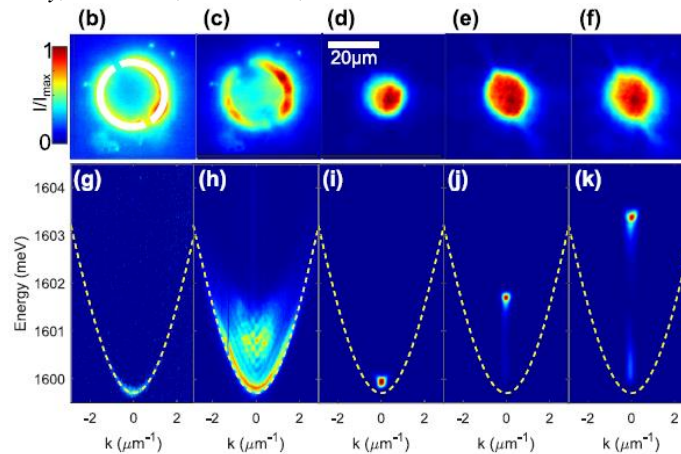
Modern colloidal researchers are equipped with a suite of microscopes which facilitate the accurate characterization of colloids, microscopic features, and even individual atoms. Colloids, which range in diameter from one nanometer to one micron, present a challenging material to accurately characterize due to the broad range in size over which they span. By harnessing a variety of analytical probes including light, X-rays, ions, and electrons, today's spectrum of microscope instrumentation can resolve ever smaller microscopic features. Microscope resolution has consistently improved over the years due to innovative technological advances including the improvement of lenses, mitigation of aberrations, and the employment of analytical probes with ever smaller wavelengths – which reduce the diffraction barrier of the microscope. These technological developments have positioned microscopy as an essential technique for colloid characterization, as it allows the researcher to visibly image newly synthesized colloidal specimens. This chapter will review the spectrum of microscopes available to the modern researcher for the characterization of colloidal materials.

Status: book chapter in *Polymer Colloids: Formation, Characterization and Applications*, CRI Group (UK) Ltd., Croydon, UK, 2019, pp. 191-239.

Direct measurement of polariton-polariton interaction strength in the Thomas-Fermi regime of exciton-polariton condensation

E. Estrecho,¹ T. Gao,² N. Bobrovska,³ D. Comber-Todd,¹ M. D. Fraser,^{4,5} M. Steger,⁶ K. West,⁷ L. N. Pfeiffer,⁸ J. Levinsen,⁹ M. M. Parish,⁹ T. C. H. Liew,¹⁰ M. Matuszewski,¹¹ D. W. Snoke,¹² A. G. Truscott,¹³ and E. A. Ostrovskaya¹

¹ARC Centre of Excellence and Nonlinear Physics Centre, Research School of Physics and Engineering, The Australian National University, Canberra, ACT 2601, Australia; ²Institute of Molecular Plus, Tianjin University, 300072 Tianjin, China; ³Institute of Physics, Polish Academy of Sciences, A. Lotników 32/46, PL-02-668 Warsaw, Poland; ⁴JST, PRESTO, 4-1-8 Honcho, Kawaguchi, Saitama 332-0012, Japan; ⁵RIKEN Center for Emergent Matter Science, 2-1 Hirosawa, Wako-shi, Saitama 351-0198, Japan; ⁶National Renewable Energy Lab, Golden, Colorado 80401, USA; ⁷PRISM, Princeton University, Princeton, New Jersey 08544, USA; ⁸Department of Electrical Engineering, Princeton University, Princeton, New Jersey 08544, USA; ⁹ARC Centre of Excellence and School of Physics and Astronomy, Monash University, Melbourne, VIC 3800, Australia; ¹⁰Division of Physics and Applied Physics, Nanyang Technological University, Singapore; ¹¹Institute of Physics, Polish Academy of Sciences, A. Lotników 32/46, PL-02-668 Warsaw, Poland; ¹²Department of Physics and Astronomy, University of Pittsburgh, Pittsburgh, Pennsylvania 15260, USA; ¹³Laser Physics Centre, Research School of Physics and Engineering, The Australian National University, Canberra, ACT 2601, Australia



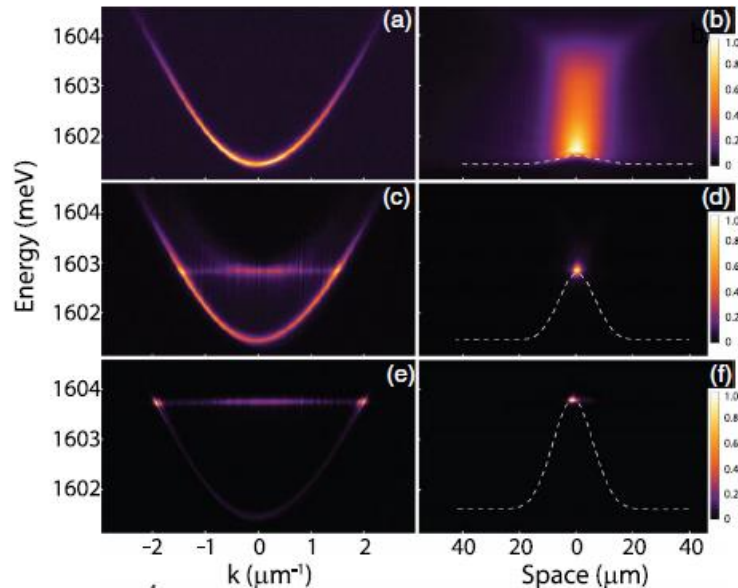
Bosonic condensates of exciton polaritons provide a solid-state platform for studies of nonequilibrium quantum systems with a spontaneous macroscopic coherence. These driven, dissipative condensates typically coexist and interact with an incoherent reservoir, which undermines measurements of key parameters of the condensate. Here, we overcome this limitation by creating a high-density exciton-polariton condensate in an optically induced box trap. In this so-called Thomas-Fermi regime, the condensate is fully separated from the reservoir and its behavior is dominated by interparticle interactions. We use this regime to directly measure the polariton-polariton interaction strength, and reduce the existing uncertainty in its value from four orders of magnitude to within three times the theoretical prediction. In a nonequilibrium exciton-polariton system, this regime offers a novel opportunity to study interaction-driven effects unmasked by an incoherent reservoir.

Status: published work in Physical Review B 2019, **100**, 035306

Self-Trapping of Exciton-Polariton Condensates in GaAs Microcavities

D. Ballarini,¹ I. Chestnov,^{2,3,4} D. Caputo,^{1,5} M. De Giorgi,¹ L. Dominici,¹ K. West,⁶ L. N. Pfeiffer,⁶ G. Gigli,^{1,5} A. Kavokin,^{2,3,7,8} and D. Sanvitto^{1,9}

¹CNR NANOTEC—Institute of Nanotechnology, Via Monteroni, 73100 Lecce, Italy; ²Westlake University, School of Science, 18 Shilongshan Road, Hangzhou 310024, Zhejiang Province, China; ³Westlake Institute for Advanced Study, Institute of Natural Sciences, 18 Shilongshan Road, Hangzhou 310024, Zhejiang Province, China; ⁴Vladimir State University, 600000 Vladimir, Russia; ⁵University of Salento, Via Arnesano, 73100 Lecce, Italy; ⁶PRISM, Princeton Institute for the Science and Technology of Materials, Princeton University, Princeton, New Jersey 08540, USA; ⁷Spin Optics Laboratory, St. Petersburg State University, St. Petersburg 198504, Russia; ⁸Russian Quantum Centre, 100 Novaya St., 143025 Skolkovo, Moscow Region, Russia; ⁹INFN, Sezione di Lecce, 73100 Lecce, Italy



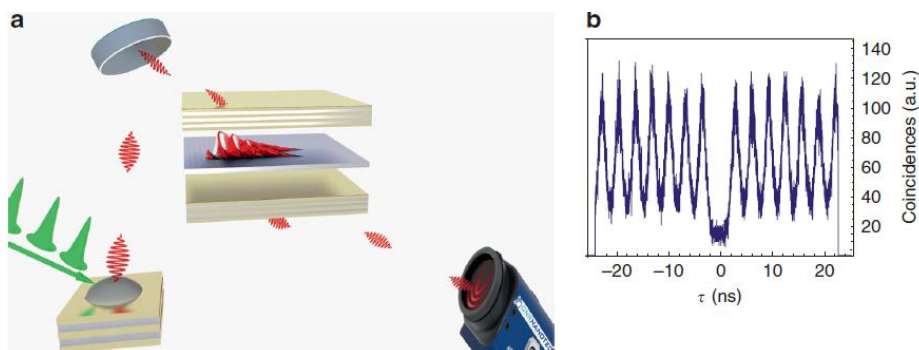
The self-trapping of exciton-polariton condensates is demonstrated and explained by the formation of a new polaronlike state. Above the polariton lasing threshold, local variation of the lattice temperature provides the mechanism for an attractive interaction between polaritons. Because of this attraction, the condensate collapses into a small bright spot. Its position and momentum variances approach the Heisenberg quantum limit. The self-trapping does not require either a resonant driving force or a presence of defects. The trapped state is stabilized by the phonon-assisted stimulated scattering of excitons into the polariton condensate. While the formation mechanism of the observed self-trapped state is similar to the Landau-Pekar polaron model, this state is populated by several thousands of quasiparticles, in a striking contrast to the conventional single-particle polaron state.

Status: published work in Physical Review Letters 2019, **123**, 047401

Quantum hydrodynamics of a single particle

Daniel Gustavo Suárez-Forero,^{1,2} Vincenzo Ardizzone,¹ Saimon Filipe Covre da Silva,³ Marcus Reindl,³ Antonio Fieramosca,^{1,4} Laura Polimeno,^{1,4} Milena De Giorgi,¹ Lorenzo Dominici,¹ Loren N. Pfeiffer,⁵ Giuseppe Gigli,⁴ Dario Ballarini,¹ Fabrice Laussy,^{6,7} Armando Rastelli,³ and Daniele Sanvitto¹

¹CNR NANOTEC, Institute of Nanotechnology, Campus Ecotekne, Via Monteroni, 73100 Lecce, Italy. ²Dipartimento di Ingegneria dell'Innovazione, Università del Salento, Campus Ecotekne, via Monteroni, 73100 Lecce, Italy. ³Institute of Semiconductor and Solid State Physics, Johannes Kepler University, Altenbergerstr. 69, Linz 4040, Austria. ⁴Dipartimento di Matematica e Fisica E. De Giorgi, Università del Salento, Campus Ecotekne, via Monteroni, Lecce 73100, Italy. ⁵PRISM, Princeton Institute for the Science and Technology of Materials, Princeton University, Princeton, NJ 08540, USA. ⁶Faculty of Science and Engineering, University of Wolverhampton, Wulfruna Street, Wolverhampton WV1 1LY, UK. ⁷Russian Quantum Center, Novaya 100, 143025 Skolkovo, Moscow Region, Russia



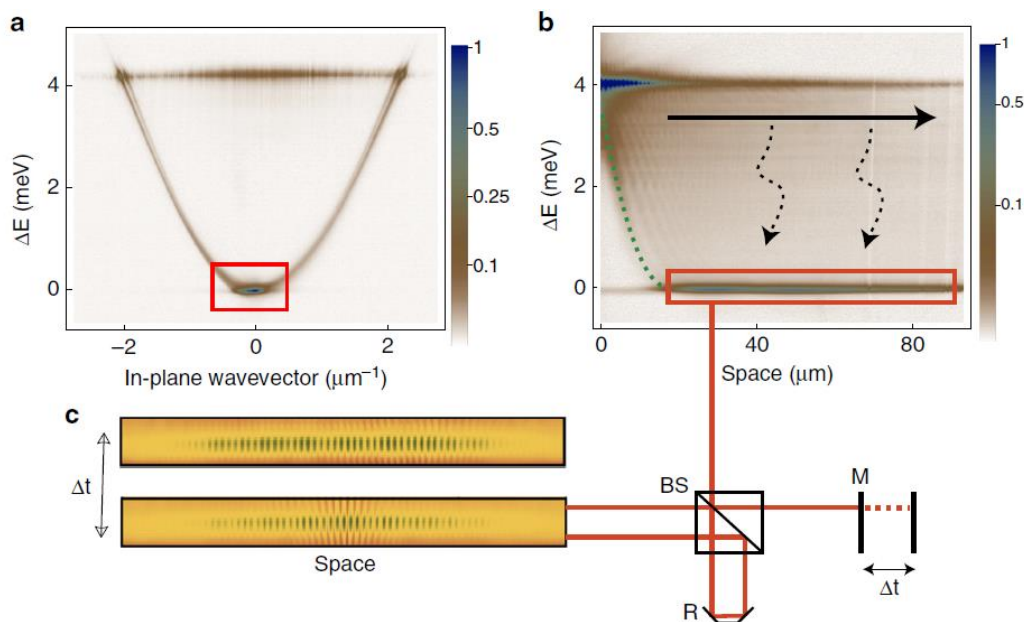
Semiconductor devices are strong competitors in the race for the development of quantum computational systems. In this work, we interface two semiconductor building blocks of different dimensionalities with complementary properties: (1) a quantum dot hosting a single exciton and acting as a nearly ideal single-photon emitter and (2) a quantum well in a 2D microcavity sustaining polaritons, which are known for their strong interactions and unique hydrodynamic properties, including ultrafast real-time monitoring of their propagation and phase mapping. In the present experiment, we can thus observe how the injected single particles propagate and evolve inside the microcavity, giving rise to hydrodynamic features typical of macroscopic systems despite their genuine intrinsic quantum nature. In the presence of a structural defect, we observe the celebrated quantum interference of a single particle that produces fringes reminiscent of wave propagation. While this behavior could be theoretically expected, our imaging of such an interference pattern, together with a measurement of antibunching, constitutes the first demonstration of spatial mapping of the self-interference of a single quantum particle impinging on an obstacle.

Status: published work in *Light: Science & Application* 2020, **9**, 85

Directional Goldstone waves in polariton condensates close to equilibrium

Dario Ballarini,¹ Davide Caputo,^{1,2} Galbadrakh Dagvadorj,^{3,4} Richard Juggins,³ Milena De Giorgi,¹ Lorenzo Dominici,¹ Kenneth West,⁵ Loren N. Pfeiffer,⁶ Giuseppe Gigli,^{1,2} Marzena H. Szymańska,³ and Daniele Sanvitto,^{1,7}

¹CNR NANOTEC—Institute of Nanotechnology, Via Monteroni, 73100 Lecce, Italy. ²University of Salento, Via Arnesano, 73100 Lecce, Italy. ³Department of Physics and Astronomy, University College London, Gower Street, London WC1E 6BT, UK. ⁴Department of Physics, University of Warwick, Coventry CV4 7AL, UK. ⁵PRISM, Princeton Institute for the Science and Technology of Materials, Princeton University, Princeton, NJ 08540, USA. ⁶Electrical Engineering Department, Princeton University, Princeton, NJ 08540, USA. ⁷INFN, Sez. Lecce, 73100 Lecce, Italy.



Quantum fluids of light are realized in semiconductor microcavities using exciton-polaritons, solid-state quasi-particles with a light mass and sizeable interactions. Here, we use the microscopic analogue of oceanographic techniques to measure the excitation spectrum of a thermalized polariton condensate. Increasing the fluid density, we demonstrate the transition from a free-particle parabolic dispersion to a linear, sound-like Goldstone mode characteristic of superfluids at equilibrium. Notably, we reveal the effect of an asymmetric pumping by showing that collective excitations are created with a definite direction with respect to the condensate. Furthermore, we measure the critical sound speed for polariton superfluids close to equilibrium.

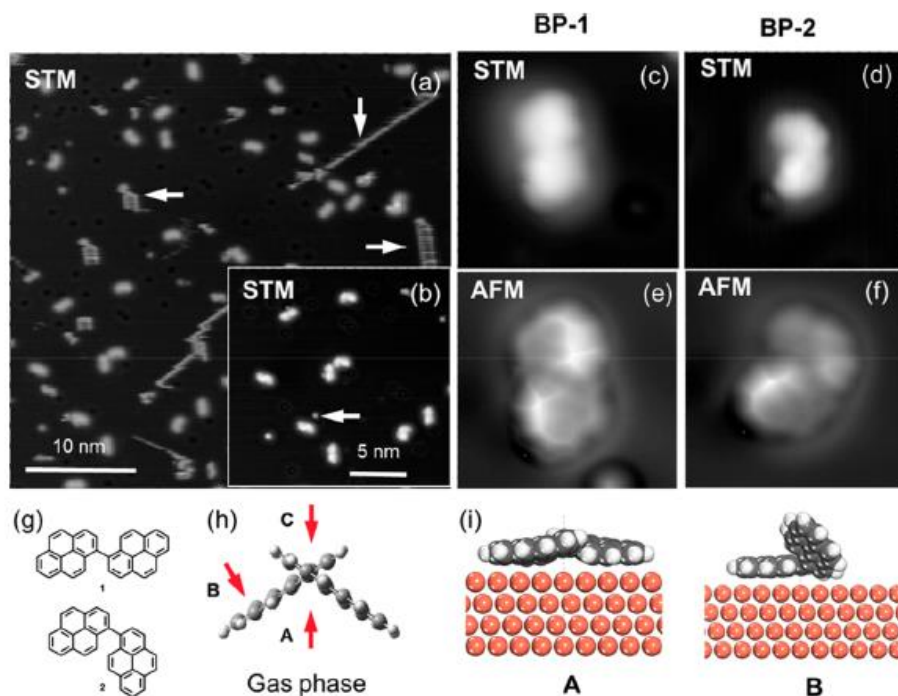
Status: published work in Nature Communications 2020, **11**, 217

Conformational Analysis of Nonplanar Archipelago Structures on a Cu (111) Surface by Molecular Imaging

Pengcheng Chen,¹ Yogesh V. Joshi,² Jordan N. Metz,² Nan Yao,¹ and Yunlong Zhang²

¹Princeton Institute for the Science and Technology of Materials, Princeton University, Princeton, NJ 08540, USA;

²ExxonMobil Research and Engineering Company, Annandale, NJ 08801, USA



We investigated some specially designed model compounds as proxies for archipelago structures in asphaltenes and heavy oils using noncontact atomic force microscopy (nc-AFM). Various adsorption conformations of three different kinds of linkers including aryl-aryl, aryl-CH₂-aryl, and aryl-(CH₂)₃-aryl were identified. By focusing on the nature of linkages or bridges between aromatic cores, this work directly addresses the long-standing question on petroleum molecular structures by validating detailed features in images and overcoming challenges of nonplanar structures and conformations, providing a foundation to apply nc-AFM to unknown structures in petroleum.

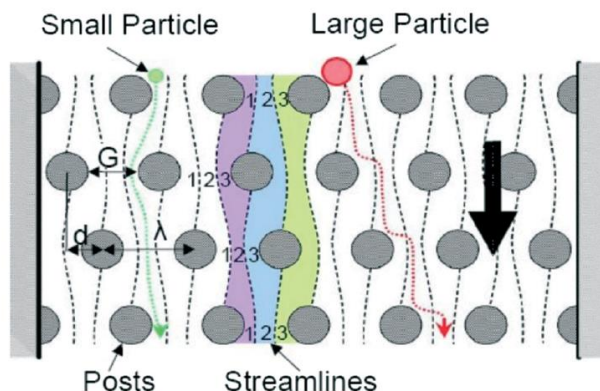
Status: published work at Energy Fuels 2020, **34**, 12135–12141

Scaling of deterministic lateral displacement devices to a single column of bumping obstacles

Weibin Liang,^{1,2} Robert H. Austin,^{1,3} and James C. Sturm^{1,2}

¹Princeton Institute for Science and Technology of Materials (PRISM), Princeton, New Jersey 08544, USA;

²Department of Electrical Engineering, Princeton University, Princeton, New Jersey 08544, USA; ³Department of Physics, Princeton University, Princeton, New Jersey 08544, USA



We describe a deterministic lateral displacement (DLD) for particle separation with only a single column of bumping features. The bifurcation of fluid streams at obstacles is not set by the “tilt” of columns with respect to macroscopic current flow, but rather by the fluidic resistances for lateral flow at each obstacle. With one column of 14 bumping features and corresponding inlet/outlet channels, the single-column DLD can separate particles with diameters of 4.8 μm and 9.9 μm at 30 $\mu\text{L min}^{-1}$, with an area of only 0.37 mm \times 1.5 mm (0.55 mm²). The large-cell output contains over 99% of the 9.9 μm particles and only 0.2% of the 4.8 μm particles. The throughput per area of 54 $\mu\text{L min}^{-1}$ per mm² represents a 10 \times increase over previous selective harvesting reports for microfluidic devices in a similar particle size range.

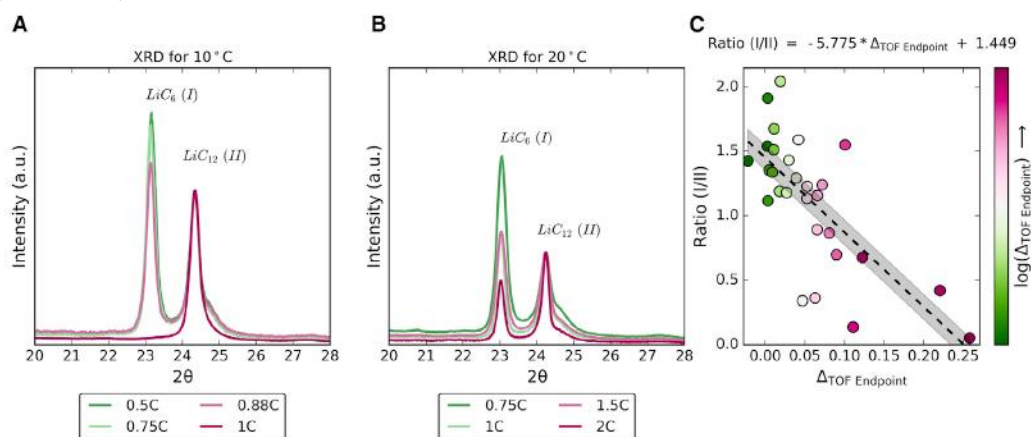
Status: published work at Lab on a Chip 2020, **20**, 3461-3467

Department of Mechanical and Aerospace Engineering

In Operando Acoustic Detection of Lithium Metal Plating in Commercial LiCoO₂/Graphite Pouch Cells

Clement Bommier,^{1,2,4} Wesley Chang,^{1,2,6} Yufang Lu,^{1,2} Justin Yeung,^{1,2} Greg Davies,^{1,2} Robert Mohr,^{5,6} Mateo Williams,^{5,6} and Daniel Steingart^{1,2,3,4,5,6}

¹Department of Mechanical and Aerospace Engineering, Princeton University, Princeton, NJ 08540, USA; ²Andlinger Center for Energy and the Environment, Princeton University, Princeton, NJ 08540, USA; ³Department of Chemical and Biological Engineering, Princeton University, Princeton, NJ 08540, USA; ⁴Department of Earth and Environmental Engineering, Columbia University, New York, NY 10027, USA; ⁵Department of Chemical Engineering, Columbia University, New York, NY 10027, USA; ⁶Columbia Electrochemical Energy Center, Columbia University, New York, NY 10027, USA



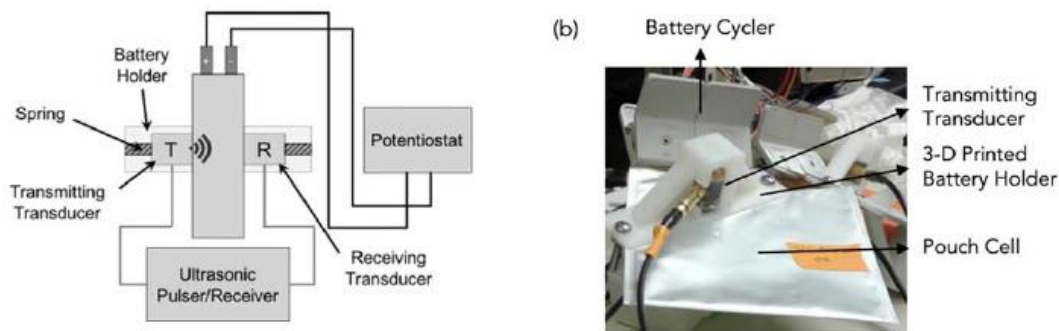
The characterization and detection of lithium metal plating during standard operation of commercial Li-ion batteries has been a long-term challenge; the nature of lithium metal plating is unpredictable and highly dependent on operating temperature and charge rate. In operando detection of lithium plating is critical for ongoing and future developments of conventional Li-ion batteries, including fast charging capabilities, extreme temperature applications, and lithium metal secondary batteries. In this study, we describe the use of acoustic ultrasound to detect lithium metal plating on commercial graphite anodes within a standard form factor. Extending from previous work on ultrasound as a battery diagnostic tool, this proof-of-concept study delineates statistically significant linear relationships between ultrasonic time-of-flight and graphite staging, and acoustic time-of-flight and postmortem electrochemical measurements to characterize the extent of lithium metal plating.

Status: published work at Cell Reports Physical Science 2020, **1**, 100035

Operando Acoustic Monitoring of SEI Formation and Long-Term Cycling in NMC/SiGr Composite Pouch Cells

Clement Bommier,^{1,2,8} Wesley Chang,^{1,2,6,8} Jianlin Li,³ Shaurjo Biswas,^{1,2} Greg Davies,² Jagjit Nanda,⁴ and Daniel Steingart^{1,2,5,6,7,8}

¹Department of Mechanical and Aerospace Engineering, Princeton University, Princeton, NJ 08540, USA; ²Andlinger Center for Energy and the Environment, Princeton University, Princeton, NJ 08540, USA; ³Energy & Transportation Science Division, Oak Ridge National Laboratory, Oak Ridge, TN 37831, USA; ⁴Chemical Science Division, Oak Ridge National Laboratory, Oak Ridge, TN 37831, USA; ⁵Department of Chemical and Biological Engineering, Princeton University, Princeton, NJ 08540, USA; ⁶Department of Earth and Environmental Engineering, Columbia University, New York NY 10027, USA; ⁷Department of Chemical Engineering, Columbia University, New York NY 10027, USA; ⁸Columbia Electrochemical Energy Center, Columbia University, New York NY 10027, USA



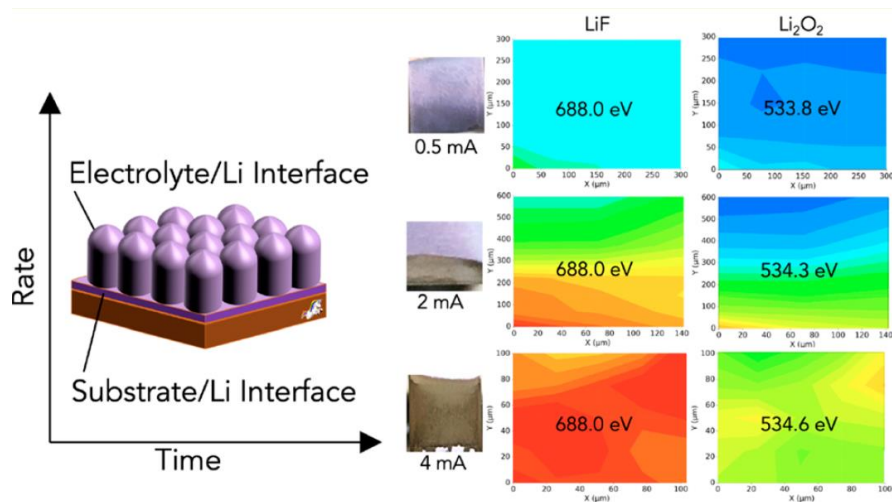
Stable long-term cycling and solid-electrolyte-interphase (SEI) formation are key challenges in the design of Si/graphite composites as Li-ion battery (LIB) anode materials. Typically, these long-term cycling properties are examined in flooded half-cell settings making use of a Li-metal counter electrode and a Si/graphite working electrode. This form factor has the advantage of offering an unlimited supply of Li-ions and electrolyte, thus isolating performance degradation to the passivation of the working electrode. However, halfcell studies are ineffective in revealing performance and degradation mechanisms of the Si/graphite composite in a more commercially realistic full cell setting. This paper outlines an operando acoustic technique that can offer insights on SEI formation and capacity degradation of Si/graphite composites in a full cell setting. Through a combination of electrochemical and chemical analyses, we show that increasing passivation of the silicon particles in the Si/graphite composite anode is correlated with an increase in the acoustic time-of-flight shift. We further show that temporary loss of the acoustic signal during the first cycle is associated with significant gassing of the cell. The operando acoustic technique outlined here is low-cost, simple to setup and has the potential for localized resolution, indicating usefulness in commercial-scale Si/graphite cell quality control and diagnosis.

Status: published work at J. Electrochem. Soc. 2020, **167**, 020517

Morphological and Chemical Mapping of Columnar Lithium Metal

Wesley Chang,^{1,2,3,4} Jeung Hun Park,^{1,2,3,5} Nikita S. Dutta,¹ Craig B. Arnold,^{1,2,5} and Daniel A. Steingart^{1,2,3,4,5,6}

¹Department of Mechanical and Aerospace Engineering, Princeton University, Princeton, NJ 08540, US; ²Andlinger Center for Energy and the Environment, Princeton University, Princeton, NJ 08540, US; ³Department of Chemical Engineering, Columbia University, New York, NY 10027, US; ⁴Columbia Electrochemical Energy Center, Columbia University, New York, NY 10027, US; ⁵Department of Chemical and Biological Engineering, Princeton University, Princeton, NJ 08540, US; ⁶Department of Earth and Environmental Engineering, Columbia University, New York, NY 10027, US



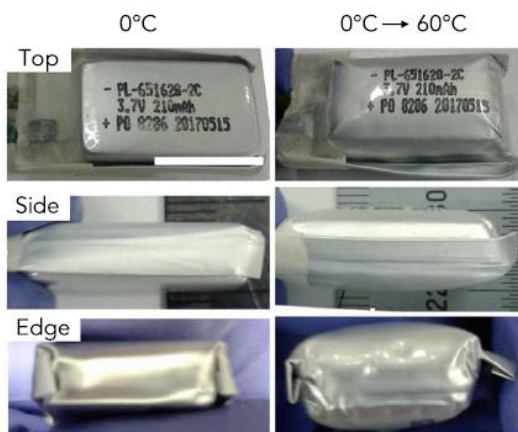
The development of high energy density lithium metal batteries requires the successful implementation of thin lithium metal anodes with limited excess lithium. Primary electrodeposition is a strategy for on-site production of thin lithium metal and avoids the costs and challenges of traditional lithium metal foil processing and transport. Herein we explore the interfacial parameters governing deposition of up to 30 μm uniform columnar lithium in LiF-rich environments, by investigating the effects of both the substrate/lithium and electrolyte/lithium interfaces for three common electrolytes: carbonate, fluorinated carbonate, and ether-based. By analyzing the transition to growth heterogeneity at higher current densities and later stage deposition, we confirm that improved growth uniformity is coupled with increasingly stable solid electrolyte interphases, but that this correlation differs for the three electrolytes. In comparison with conventional dimethyl carbonate, fluorinated carbonate and ether-based electrolytes exhibit fewer chemical shifts in the morphological transition region. We pinpoint the chemical origins of growth transitions in conventional dimethyl carbonate and show that close-packed columnar growth can be electrodeposited in ether-based electrolyte at 100-fold higher current densities.

Status: published work at Chemistry of Materials 2020, **32**, 2803–2814

Understanding Adverse Effects of Temperature Shifts on Li-Ion Batteries: An Operando Acoustic Study

Wesley Chang,^{1,2,3} Clement Bommier,^{1,2,3} Thomas Fair,^{1,2} Justin Yeung,^{1,2} Shripad Patil,⁴ and Daniel Steingart^{1,2,3,4,5,6}

¹Department of Mechanical and Aerospace Engineering, Princeton University, Princeton, NJ 08540, US; ²Andlinger Center for Energy and the Environment, Princeton University, Princeton, NJ 08540, US; ³Columbia Electrochemical Energy Center, Columbia University, New York, NY 10027, US; ⁴Department of Earth and Environmental Engineering, Columbia University, New York, NY 10027, US; ⁵Department of Chemical Engineering, Columbia University, New York, NY 10027, US; ⁶Department of Chemical and Biological Engineering, Princeton University, Princeton, NJ 08540, US



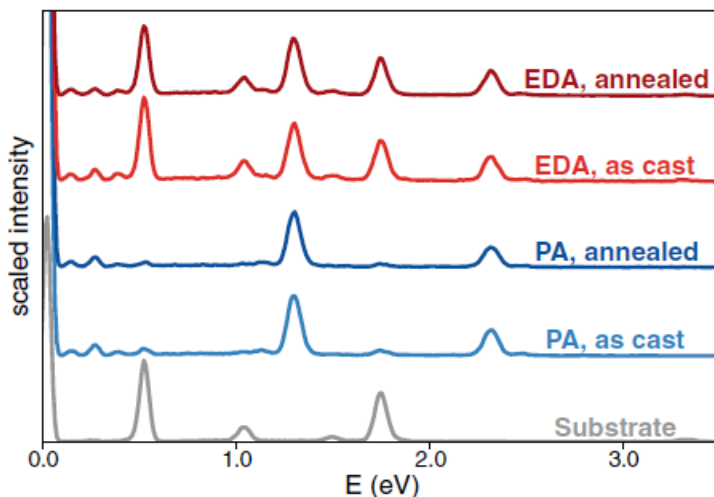
Studies related to battery performance and long-term health of commercial Li-ion batteries (LIBs) typically have a fixed temperature parameter. However, commercial LIBs are subject to temperature fluctuations due to their local environment and operating conditions, and these transient temperatures are well known to impact long-term stability. Herein, we demonstrate the adverse effects of temperature shifts, and show that transitioning from low temperature to higher temperature can lead to catastrophic failure within practical temperature ranges experienced by commercial LIBs. We show there exists an Arrhenius relationship between the rate of acoustic attenuation and the magnitude of the temperature shift. A combination of acoustic attenuation, which marks gassing occurrence during cycling, and post mortem chemical analyses provides further mechanistic insight into the Li-rich solid electrolyte interphase (SEI) formation at low temperatures and subsequent reactions with the electrolyte at higher temperatures. Further, several strategies to prevent or mitigate catastrophic failure are introduced. On a broader scale, this research further highlights the importance of temperature and current controls integration into battery management systems (BMS) for both safety and extension of cycle life as battery systems move toward fast charge (>3 C) capability.

Status: published work at Journal of The Electrochemical Society 2020, **167**, 090503

Effects of disorder on two-photon absorption in amorphous semiconductors

N. S. Dutta,¹ J. M. P. Almeida,^{2,3} C. R. Mendonca,² and C. B. Arnold,¹

¹Department of Mechanical and Aerospace Engineering, Princeton Institute for the Science and Technology of Materials, Princeton University, Princeton, New Jersey 08544, USA; ²São Carlos Institute of Physics, University of São Paulo, 13560-970, São Carlos, SP, Brazil; ³Department of Materials Engineering, São Carlos School of Engineering, University of São Paulo, 13563-120, São Carlos, SP, Brazil.



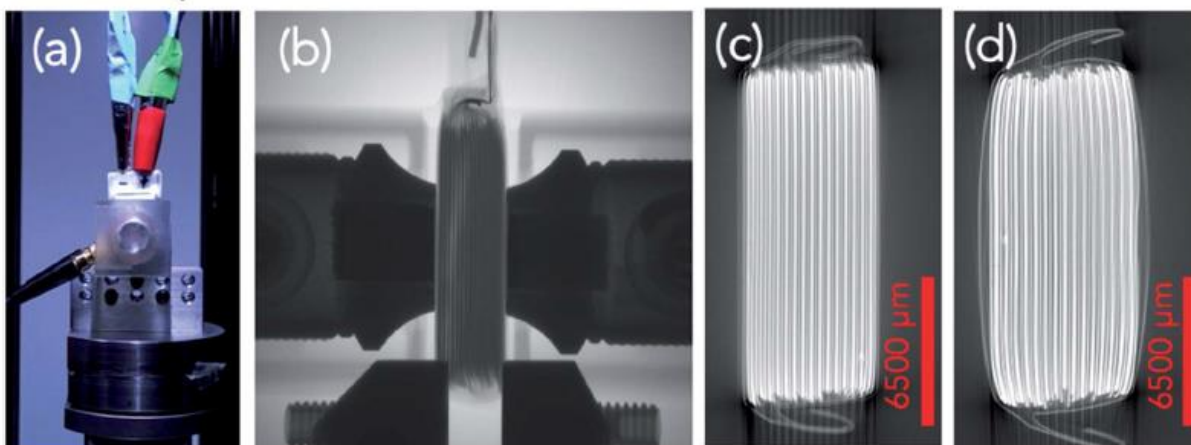
Structural disorder inherent to amorphous materials affords them unique, tailorable properties desirable for diverse applications, but our ability to exploit these phenomena is limited by a lack of understanding of complex structure-property relationships. Here we focus on nonlinear optical absorption and derive a relationship between disorder and the two-photon absorption (2PA) coefficient. We employ an open-aperture Z-scan to measure the 2PA spectra of arsenic (III) sulfide (As_2S_3) chalcogenide glass films processed with two solvents that impart different levels of structural disorder. We find that the effect of solvent choice on 2PA depends on the energy of the exciting photons and explain this as a consequence of bonding disorder and electron state localization. Our results demonstrate how optical nonlinearities in As_2S_3 can be enhanced through informed processing and present a fundamental relationship between disorder and 2PA for a generalized amorphous solid.

Status: published work in Optics Letters 2020, **45**, 3228-3231

Measuring effective stiffness of Li-ion batteries via acoustic signal processing

Wesley Chang,^{1,4,6,7} Robert Mohr,^{6,7} Andrew Kim,^{3,4} Abhi Raj,^{3,4} Greg Davies,⁴ Kate Denner,¹ Jeung Hun Park,^{1,2,4,6} and Daniel Steingart,^{1,2,4,5,6,7}

¹Department of Mechanical and Aerospace Engineering, Princeton, NJ 08540, USA; ²Department of Chemical and Biological Engineering, Princeton, NJ 08540, USA; ³Department of Electrical Engineering, Princeton, NJ 08540, USA; ⁴Andlinger Center for Energy and the Environment, Princeton University, Princeton, NJ 08540, USA; ⁵Department of Earth and Environmental Engineering, New York, NY 10027, USA; ⁶Department of Chemical Engineering, New York, NY 10027, USA; ⁷Columbia Electrochemical Energy Center, Columbia University, New York, NY 10027, USA.



In this work we build upon acoustic–electrochemical correlations to investigate the relationships between sound wave structure and chemo-mechanical properties of a pouch cell battery. Cell thickness imaging and wave detection during pouch cell cycling are conducted in parallel. Improved acoustic hardware and signal processing are used to validate the direct measurement of material stiffness, which is an intrinsic physical property. Measurement of cell thickness to micron resolution and wave transmit time to nanosecond resolution in a temperature and pressure controlled acoustic rig allows for estimation of the effective stiffness. We further explore the effects of material type and cell layering on the acoustic signal, demonstrating that the operando acoustic method can accurately measure the changes in physical state properties of a battery with high dynamic temporal and spatial range are tuned into resonance with the cavity, indicating a coherent interaction between the two spins and a cavity photon. Our results imply that microwave-frequency photons may be used to generate long-range two-qubit gates between spatially separated spins.

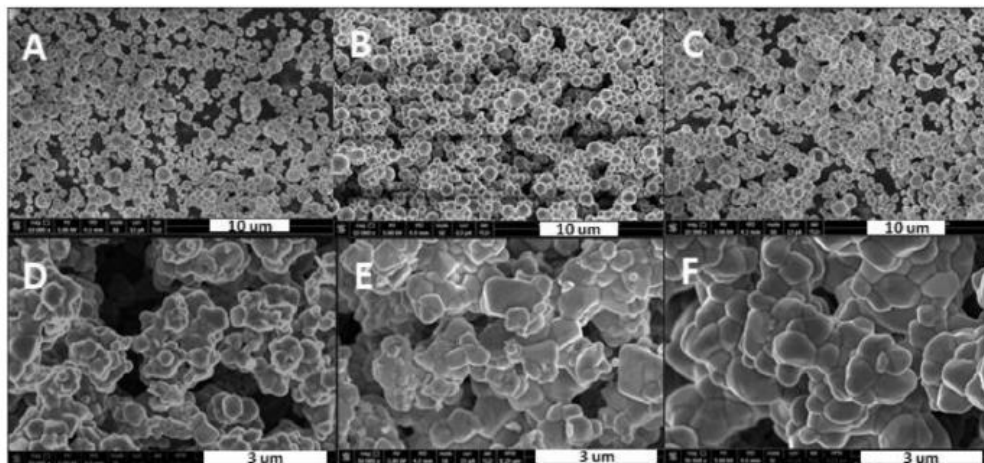
Status: published work at J. Mater. Chem. A 2020, **8**, 16624-16635

Controlled Dy-doping to nickel-rich cathode materials in high temperature aerosol synthesis

Chao Yan,¹ Xiaofang Yang,² Hao Zhao,¹ Hongtao Zhong,¹ Guoming Ma,¹ Yongfeng Qi,¹ Bruce E. Koel,² Yiguang Ju,¹

¹*Department of Mechanical and Aerospace Engineering, Princeton University, Princeton, NJ 08544, USA;*

²*Department of Chemical and Biological Engineering, Princeton University, Princeton, NJ 08544, USA*



Layered nickel-rich materials are promising next-generation cathode materials for lithium ion batteries due to their high capacity and low cost. However, the poor thermal stability and longtime cycling performance hinders the commercial applications of high nickel materials. Doping with heteroatoms has been an effective approach for improving electrochemical performance of cathode materials. In this work, controlled dysprosium (Dy) doping to NCM811 was studied in an aerosol synthesis method by controlling the precursor concentrations and heating parameters. The obtained materials were characterized by SEM, XRD, and XPS, and their electrochemical properties and thermal stability were evaluated. By controlling the doping concentration (1.5%), Dy-doped NCM811 was improved simultaneously in long-term cycling and high-rate performance. The thermal-chemical stability of the Dy-doped cathode materials was examined in a microflow reactor with a mass spectrometer. Dy-doping shifted the O₂ onset temperature to a higher temperature and reduced O₂ release by 80%, thus dramatically increasing the thermal-chemical stability and improving the fire safety of cathode materials. Since high temperature aerosol synthesis is a low-cost and scalable method, the findings in this work have broad implications for commercial synthesis of novel materials with controlled doping modification to achieve high electrochemical performance and safety in lithium ion batteries.

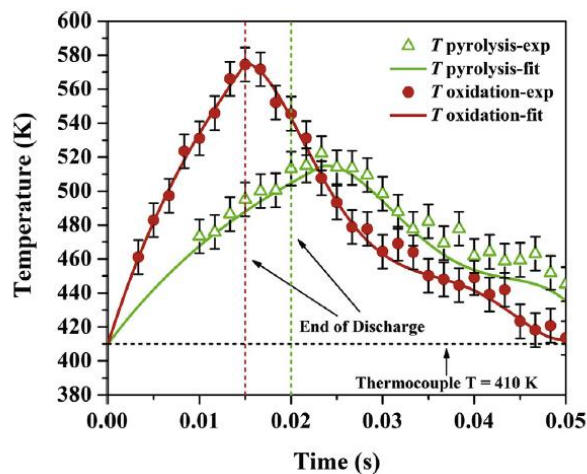
Status: published work at Proc. Combust. Inst. 2020

Kinetic study of plasma-assisted n-dodecane/O₂/N₂ pyrolysis and oxidation in a nanosecond-pulsed discharge

Hongtao Zhong,¹ Xingqian Mao,¹ Aric C Rousso,¹ Charles L Patrick,² Chao Yan,¹ Wenbin Xu,¹ Qi Chen,³ Gerard Wysocki,² Yiguang Ju,¹

¹Department of Mechanical and Aerospace Engineering, Princeton University, Princeton, NJ 08544, USA;

²Department of Electrical Engineering, Princeton University, Princeton, NJ 08544, USA; ³School of Mechanical, Electronic and Control Engineering, Beijing Jiaotong University, Beijing 100044, China



The present study investigates the kinetics of low-temperature pyrolysis and oxidation of n-dodecane/O₂/N₂ mixtures in a repetitively-pulsed nanosecond discharge experimentally and numerically. Time-resolved TDLAS measurements, steady-state gas chromatography (GC) sampling, and mid-IR dual-modulation Faraday rotation spectroscopy (DM-FRS) measurements are conducted to quantify temperature as well as species formation and evolution. A plasma-assisted n-dodecane pyrolysis and oxidation kinetic model incorporating the reactions involving electronically excited species and NO_x chemistry is developed and validated. The results show that a nanosecond discharge can dramatically accelerate n-dodecane pyrolysis and oxidation at low temperatures. The numerical model has a good agreement with experimental data for the major intermediate species. From the pathway analysis, electronically excited N₂^{*} plays an important role in n-dodecane pyrolysis and oxidation. The results also show that with addition of n-dodecane, NO concentration is reduced considerably, which suggests that there is a strong NO kinetic effect on plasma-assisted low-temperature combustion via NO-RO₂ and NO₂-fuel radical reaction pathways. This work advances the understandings of the kinetics of plasma-assisted low-temperature fuel oxidation in N₂/O₂ mixtures.

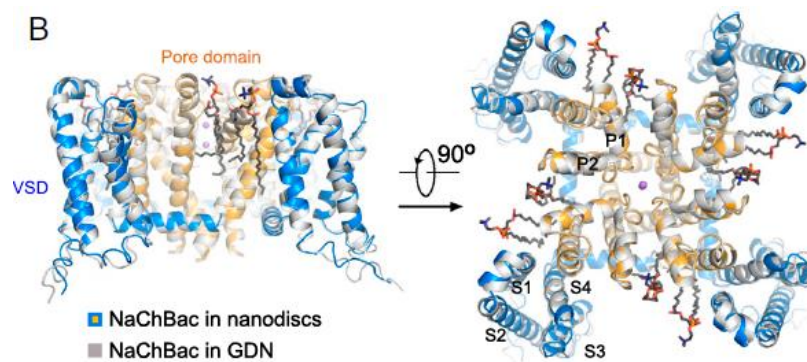
Status: published work at Proc. Combust. Inst. 2020

Department of Molecular Biology

Employing NaChBac for cryo-EM analysis of toxin action on voltage-gated Na⁺ channels in nanodisc

Shuai Gao¹, William C. Valinsky², Nguyen Cam On¹, Patrick R. Houlihan², Qian Qu³, Lei Liu³, Xiaojing Pan⁴, David E. Clapham², and Nieng Yan¹

¹Department of Molecular Biology, Princeton University, Princeton, NJ 08544; ²Janelia Research Campus, Howard Hughes Medical Institute, Ashburn, VA 20147; ³Tsinghua-Peking Joint Center for Life Sciences, Department of Chemistry, Tsinghua University, Beijing 100084, China; and ⁴Beijing Advanced Innovation Center for Structural Biology, Tsinghua-Peking Joint Center for Life Sciences, School of Life Sciences, Tsinghua University, Beijing 100084, China



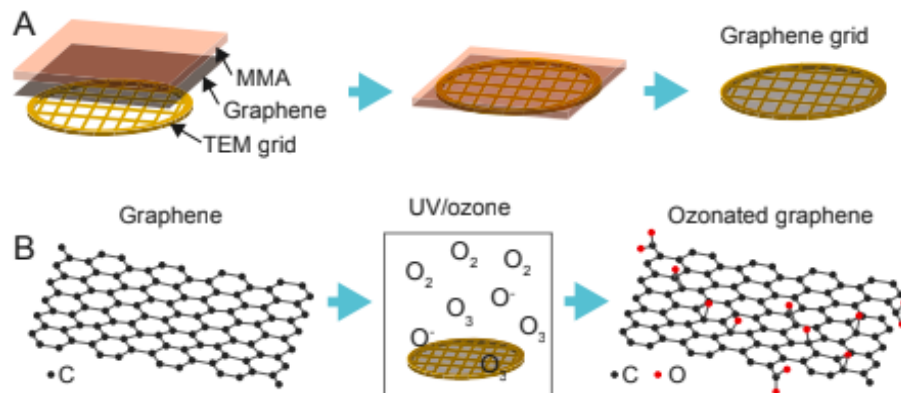
NaChBac, the first bacterial voltage-gated Na⁺ (Na_v) channel to be characterized, has been the prokaryotic prototype for studying the structure–function relationship of Na_v channels. Here we present the single particle electron cryomicroscopy (cryo-EM) analysis of NaChBac in both detergent micelles and nanodiscs. Under both conditions, the conformation of NaChBac is nearly identical to that of the potentially inactivated Na_vAb. Determining the structure of NaChBac in nanodiscs enabled us to examine gating modifier toxins (GMTs) of Nav channels in lipid bilayers. To study GMTs in mammalian Na_v channels, we generated a chimera in which the extracellular fragment of the S3 and S4 segments in the second voltage-sensing domain from Na_v1.7 replaced the corresponding sequence in NaChBac. Cryo-EM structures of the nanodisc-embedded chimera alone and in complex with HuwenToxin IV (HWTX-IV) were determined to 3.5 and 3.2 Å resolutions, respectively. Compared to the structure of HWTX-IV–bound human Na_v1.7, at an overall resolution of 3.2 Å, the local resolution of the toxin has been improved from ~6 to ~4 Å. This resolution enabled visualization of toxin docking. NaChBac can serve as a convenient surrogate for structural studies of the interactions between GMTs and Na_v channels in a membrane environment.

Status: published work at PNAS 2020, **117**, 14187-14193

High-yield monolayer graphene grids for near-atomic resolution cryoelectron microscopy

Yimo Han^a, Xiao Fan^a, Haozhe Wang^b, Fang Zhao^c, Christopher G. Tully^c, Jing Kong^b, Nan Yao^d, and Nieng Yan^a

^aDepartment of Molecular Biology, Princeton University, Princeton, NJ 08544; ^bDepartment of Electrical Engineering and Computer Science, Massachusetts Institute of Technology, Cambridge, MA 02139; ^cDepartment of Physics, Princeton University, Princeton, NJ 08544; and ^dPRISM Imaging and Analysis Center, Princeton University, Princeton, NJ 08544



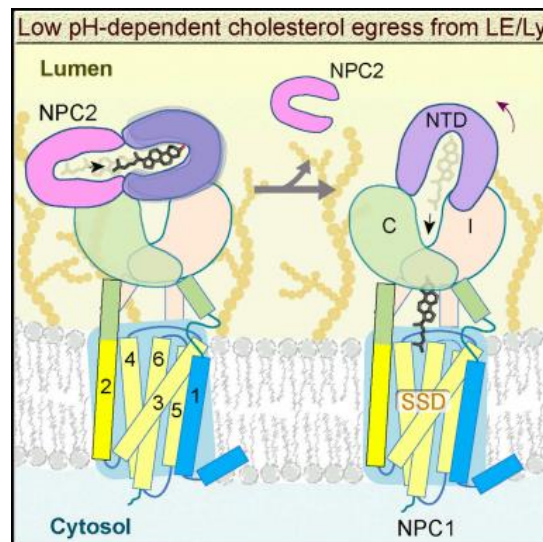
Cryogenic electron microscopy (cryo-EM) has become one of the most powerful techniques to reveal the atomic structures and working mechanisms of biological macromolecules. New designs of the cryo-EM grids—aimed at preserving thin, uniform vitrified ice and improving protein adsorption—have been considered a promising approach to achieving higher resolution with the minimal amount of materials and data. Here, we describe a method for preparing graphene cryo-EM grids with up to 99% monolayer graphene coverage that allows for more than 70% grid squares for effective data acquisition with improved image quality and protein density. Using our graphene grids, we have achieved 2.6-Å resolution for streptavidin, with a molecular weight of 52 kDa, from 11,000 particles. Our graphene grids increase the density of examined soluble, membrane, and lipoproteins by at least 5-fold, affording the opportunity for structural investigation of challenging proteins which cannot be produced in large quantity. In addition, our method employs only simple tools that most structural biology laboratories can access. Moreover, this approach supports customized grid designs targeting specific proteins, owing to its broad compatibility with a variety of nanomaterials.

Status: published work at Proc. Natl. Acad. Sci. 2020, **117**, 1009-1014

Structural Basis of Low-pH-Dependent Lysosomal Cholesterol Egress by NPC1 and NPC2

Hongwu Qian,¹ Xuelan Wu,² Ximing Du,³ Xia Yao,¹ Xin Zhao,⁴ Joyce Lee,¹ Hongyuan Yang,³ and Nieng Yan¹

¹Department of Molecular Biology, Princeton University, Princeton, NJ 08544, USA; ²Department of Chemistry, Princeton University, Princeton, NJ 08544, USA; ³School of Biotechnology and Biomolecular Science, the University of New South Wales, Sydney, NSW 2052, Australia; ⁴Beijing Advanced Innovation Center for Structural Biology, Tsinghua-Peking Joint Center for Life Sciences, School of Life Sciences, Tsinghua University, Beijing 100084, China



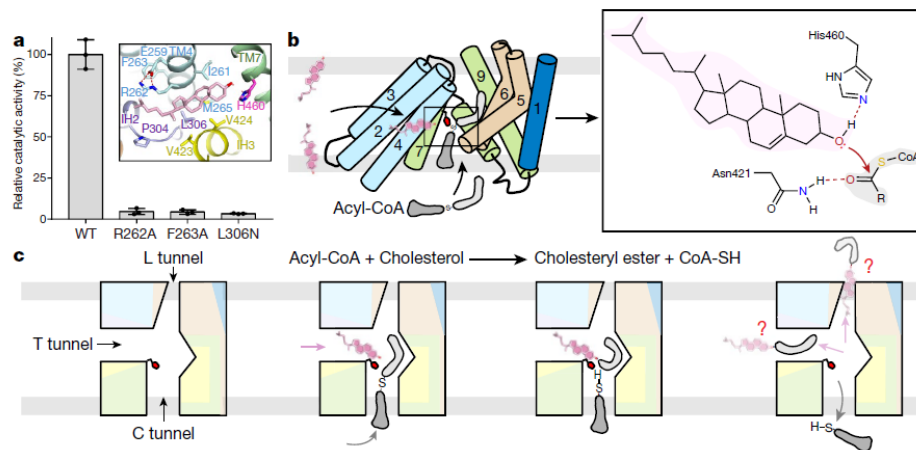
Lysosomal cholesterol egress requires two proteins, NPC1 and NPC2, whose defects are responsible for Niemann-Pick disease type C (NPC). Here, we present systematic structural characterizations that reveal the molecular basis for low-pH-dependent cholesterol delivery from NPC2 to the transmembrane (TM) domain of NPC1. At pH 8.0, similar structures of NPC1 were obtained in nanodiscs and in detergent at resolutions of 3.6 Å and 3.0 Å, respectively. A tunnel connecting the N-terminal domain (NTD) and the transmembrane sterol-sensing domain (SSD) was unveiled. At pH 5.5, the NTD exhibits two conformations, suggesting the motion for cholesterol delivery to the tunnel. A putative cholesterol molecule is found at the membrane boundary of the tunnel, and TM2 moves toward formation of a surface pocket on the SSD. Finally, the structure of the NPC1-NPC2 complex at 4.0 Å resolution was obtained at pH 5.5, elucidating the molecular basis for cholesterol handoff from NPC2 to NPC1(NTD).

Status: published work at Cell 2020, **182**, 1-14

Structural basis for catalysis and substrate specificity of human ACAT1

Hongwu Qian¹, Xin Zhao², Renhong Yan^{3,4}, Xia Yao¹, Shuai Gao¹, Xue Sun⁵, Ximing Du⁶, Hongyuan Yang⁶, Catherine C. L. Wong⁵ & Nieng Yan¹

¹Department of Molecular Biology, Princeton University, Princeton, NJ, USA. ²State Key Laboratory of Membrane Biology, Beijing Advanced Innovation Center for Structural Biology, Tsinghua-Peking Joint Center for Life Sciences, School of Life Sciences, Tsinghua University, Beijing, China. ³Key Laboratory of Structural Biology of Zhejiang Province, School of Life Sciences, Westlake University, Hangzhou, China. ⁴Institute of Biology, Westlake Institute for Advanced Study, Hangzhou, China. ⁵Center for Precision Medicine Multi-omics Research, State Key Laboratory of Natural and Biomimetic Drugs, School of Pharmaceutical Sciences, Peking-Tsinghua Center for Life Sciences, Peking University, Beijing, China. ⁶School of Biotechnology and Biomolecular Science, The University of New South Wales, Sydney, New South Wales, Australia.



As members of the membrane-bound O-acyltransferase (MBOAT) enzyme family, acyl-coenzyme A:cholesterol acyltransferases (ACATs) catalyse the transfer of an acyl group from acyl-coenzyme A to cholesterol to generate cholesteryl ester, the primary form in which cholesterol is stored in cells and transported in plasma. ACATs have gained attention as potential drug targets for the treatment of diseases such as atherosclerosis, Alzheimer's disease and cancer. Here we present the cryo-electron microscopy structure of human ACAT1 as a dimer of dimers. Each protomer consists of nine transmembrane segments, which enclose a cytosolic tunnel and a transmembrane tunnel that converge at the predicted catalytic site. Evidence from structure-guided mutational analyses suggests that acyl-coenzyme A enters the active site through the cytosolic tunnel, whereas cholesterol may enter from the side through the transmembrane tunnel. This structural and biochemical characterization helps to rationalize the preference of ACAT1 for unsaturated acyl chains, and provides insight into the catalytic mechanism of enzymes within the MBOAT family.

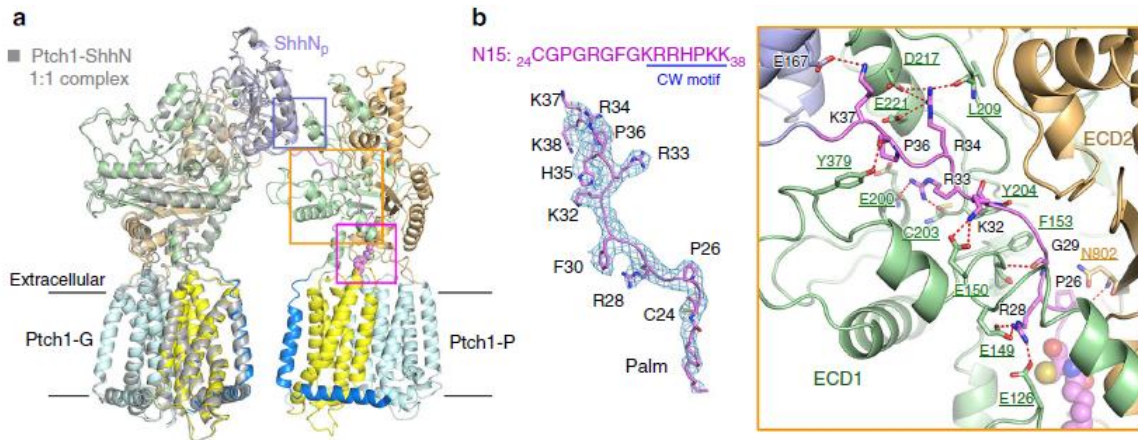
Status: published work at Nature 2020, **581**, 333-338

Inhibition of tetrameric Patched1 by Sonic Hedgehog through an asymmetric paradigm

Hongwu Qian¹, Pingping Cao², Miaohui Hu¹, Shuai Gao¹, Nieng Yan¹ & Xin Gong^{1,3}

¹Department of Molecular Biology, Princeton University, Princeton, NJ 08544, USA. ²State Key Laboratory of Membrane Biology, Beijing Advanced Innovation Center for Structural Biology, Tsinghua-Peking Joint Center for Life Sciences, School of Life Sciences and School of Medicine, Tsinghua University, Beijing 100084, China.

³Department of Biology, Southern University of Science and Technology, Shenzhen, Guangdong 518055, China.



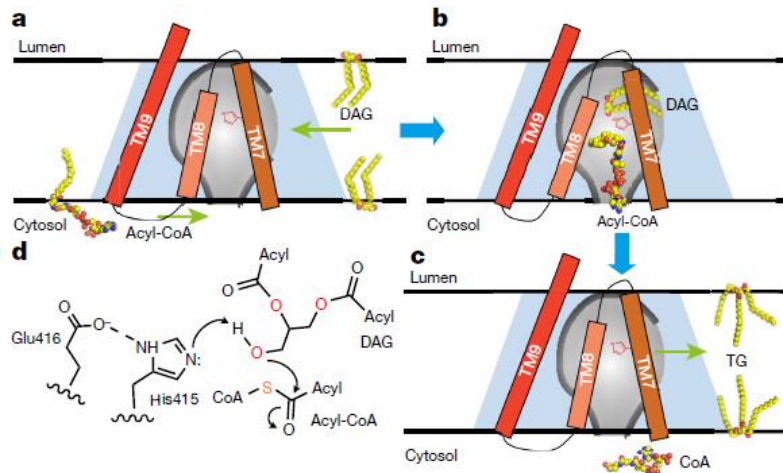
The Hedgehog (Hh) pathway controls embryonic development and postnatal tissue maintenance and regeneration. Inhibition of Hh receptor Patched (Ptch) by the Hh ligands relieves suppression of signaling cascades. Here, we report the cryo-EM structure of tetrameric Ptch1 in complex with the palmitoylated N-terminal signaling domain of human Sonic hedgehog (ShhN_p) at a 4:2 stoichiometric ratio. The structure shows that four Ptch1 protomers are organized as a loose dimer of dimers. Each dimer binds to one ShhN_p through two distinct inhibitory interfaces, one mainly through the N-terminal peptide and the palmitoyl moiety of ShhN_p and the other through the Ca²⁺-mediated interface on ShhN_p. Map comparison reveals that the cholesteryl moiety of native ShhN occupies a recently identified extracellular steroid binding pocket in Ptch1. Our structure elucidates the tetrameric assembly of Ptch1 and suggests an asymmetric mode of action of the Hh ligands for inhibiting the potential cholesterol transport activity of Ptch1.

Status: published work at Nature Communications 2019, **10**, 2320

Structural and mechanism of human diacylglycerol O-acyltransferase 1

Lie Wang,¹ Hongwu Qian,² Yin Nian,^{1,4} Yimo Han,^{2,5} Zhenning Ren,¹ Hanzhi Zhang,¹ Liya Hu,¹ B. V. Venkataram Prasad,¹ Arthur Laganowsky,³ Nieng Yan,² & Ming Zhou¹

¹Verna and Marrs McLean Department of Biochemistry and Molecular Biology, Baylor College of Medicine, Houston, TX, USA. ²Department of Molecular Biology, Princeton University, Princeton, NJ, USA. ³Department of Chemistry, Texas A&M University, College Station, TX, USA. ⁴Present address: Ion Channel Research and Drug Development Center, Kunming Institute of Zoology, Chinese Academy of Sciences, Kunming, China. ⁵Present address: Department of Material Science and Nanoengineering, Rice University, Houston, TX, USA.



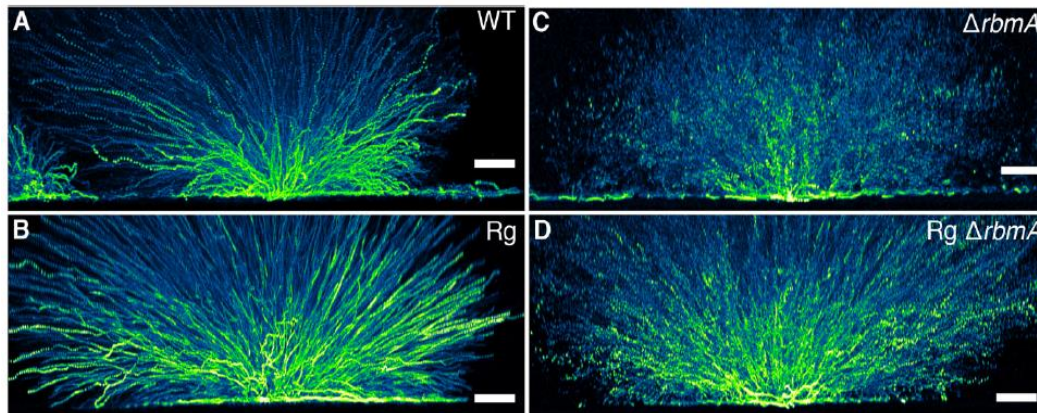
Diacylglycerol O-acyltransferase 1 (DGAT1) synthesizes triacylglycerides and is required for dietary fat absorption and fat storage in humans. DGAT1 belongs to the membrane-bound O-acyltransferase (MBOAT) superfamily, members of which are found in all kingdoms of life and are involved in the acylation of lipids and proteins. How human DGAT1 and other mammalian members of the MBOAT family recognize their substrates and catalyse their reactions is unknown. The absence of three-dimensional structures also hampers rational targeting of DGAT1 for therapeutic purposes. Here we present the cryo-electron microscopy structure of human DGAT1 in complex with an oleoyl-CoA substrate. Each DGAT1 protomer has nine transmembrane helices, eight of which form a conserved structural fold that we name the MBOAT fold. The MBOAT fold in DGAT1 forms a hollow chamber in the membrane that encloses highly conserved catalytic residues. The chamber has separate entrances for each of the two substrates, fatty acyl-CoA and diacylglycerol. DGAT1 can exist as either a homodimer or a homotetramer and the two forms have similar enzymatic activity. The N terminus of DGAT1 interacts with the neighboring protomer and these interactions are required for enzymatic activity.

Status: published work at Nature 2020, **581**, 329 - 332

Cell position fates and collective fountain flow in bacterial biofilms revealed by light-sheet microscopy

Boyang Qin,^{1,2} Chenyi Fei,^{1,3} Andrew A. Bridges,^{1,4} Ameya A. Mashruwala,^{1,4} Howard A. Stone,² Ned S. Wingreen,^{1,3,5} Bonnie L. Bassler,^{1,4}

¹Department of Molecular Biology, Princeton University, Princeton, NJ 08544, USA. ²Department of Mechanical and Aerospace Engineering, Princeton University, Princeton, NJ 08544, USA. ³Lewis-Sigler Institute for Integrative Genomics, Princeton University, Princeton, NJ 08544, USA. ⁴The Howard Hughes Medical Institute, Chevy Chase, MD 20815, USA. ⁵Princeton Center for Theoretical Science, Princeton University, Princeton, NJ 08544, USA



Bacterial biofilms represent a basic form of multicellular organization that confers survival advantages to constituent cells. The sequential stages of cell ordering during biofilm development have been studied in the pathogen and model biofilm-former *Vibrio cholerae*. How do the spatial trajectories of individual cells and the collective motions of many cells drive biofilm expansion? We developed dual-view light-sheet microscopy to investigate biofilm developmental dynamics from a founder cell to a mature three-dimensional community. Tracking of individual cells revealed two distinct fates: one set of biofilm cells expanded ballistically outward, while the other became trapped at the substrate. A collective fountain-like flow transported cells to the biofilm front, bypassing members trapped at the substrate and facilitating lateral biofilm expansion. This collective flow pattern was quantitatively captured by a continuum model of biofilm growth against substrate friction. Coordinated cell movement required the matrix protein RbmA, without which cells expanded erratically. Thus, tracking cell lineages and trajectories in space and time revealed how multicellular structures form from a single founder cell.

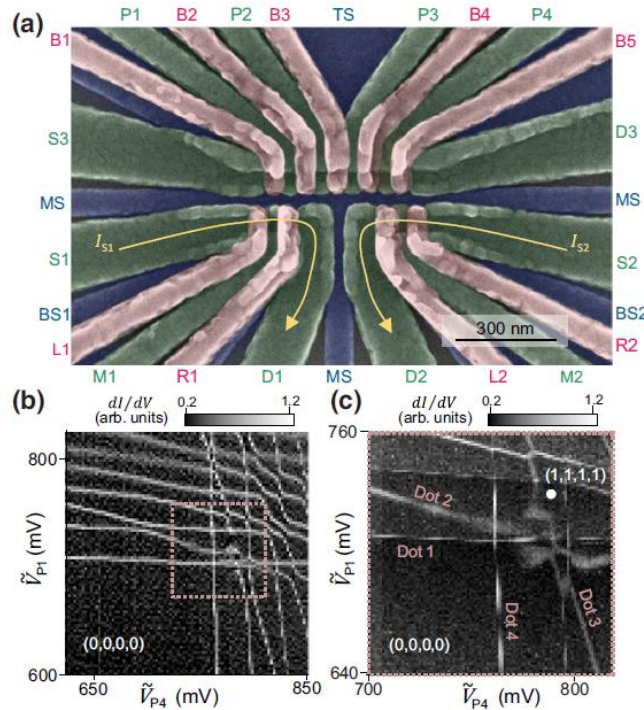
Status: published work at Science 2020, **369**, 71

Department of Physics

Site-Selective Quantum Control in an Isotopically Enriched $^{28}\text{Si}/\text{Si}_{0.7}\text{Ge}_{0.3}$ Quadruple Quantum Dot

A.J. Sigillito,¹ J.C. Loy,¹ D.M. Zajac,¹ M.J. Gullans,¹ L.F. Edge,² and J.R. Petta¹

¹Department of Physics, Princeton University, Princeton, New Jersey 08544, USA; ²HRL Laboratories LLC, 3011 Malibu Canyon Road, Malibu, California 90265, USA



Silicon spin qubits are a promising quantum-computing platform offering long coherence times, small device sizes, and compatibility with industry-backed device-fabrication techniques. In recent years, high-fidelity single-qubit and two-qubit operations have been demonstrated in Si. Here we demonstrate coherent spin control in a quadruple quantum dot fabricated from isotopically enriched ^{28}Si . We tune the ground-state charge configuration of the quadruple dot down to the single-electron regime and demonstrate tunable interdot tunnel couplings as large as 20 GHz, which enables exchange-based two-qubit gate operations. Site-selective single spin rotations are achieved with the use of electric dipole spin resonance in a magnetic field gradient. We execute a resonant controlled-NOT gate between two adjacent spins in 270 ns.

Status: published work at Physical Review Applied 2019, **11**, 061006

Pyrolytic carbon coating of fused quartz by vacuum vapor transport

Burkhant Suerfu, Michael Souza, Frank Calaprice

Department of Physics, Princeton University, Jadwin Hall, Princeton, New Jersey 08544, USA



Fused quartz has excellent thermal and chemical properties as crucible material for single crystal growth from melt, and its high purity and low cost makes it especially attractive for the growth of high-purity crystals. However, in the growth of certain types of crystals, a layer of pyrolytic carbon coating is needed between the melt and the quartz crucible. In this article, we describe a method for applying pyrolytic carbon coating by vacuum vapor transport. The method is shown to be effective in yielding relatively uniform coating on a wide range of crucible sizes and shapes. The resultant pyrolytic carbon coating is characterized by optical attenuation measurements. In each coating process, the thickness of coating is shown to approach a terminal value with an exponential tail as the duration of pyrolysis increases, and the average thickness roughly increases linearly with the ratio of the volume of available hexane vapor to the surface area of pyrolytic coating. Quartz crucibles coated by this process have been used to successfully grow up to 2-in-diameter NaI single crystals, and the surface quality of NaI crystal was found to improve as the thickness of coating increases.

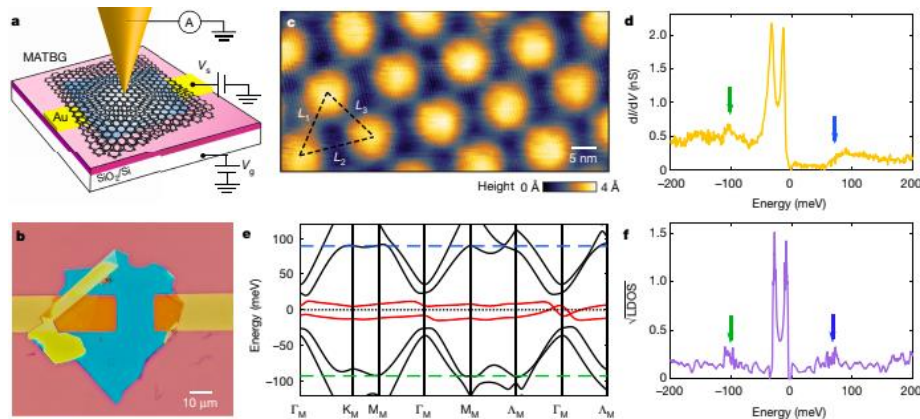
An XL30 FEG-SEM was used to obtain images of carbon coating and the beginning and the end of the calibration sample and the thickness of the entire scanned surface was found by comparing SEM measurements to the data obtained from optical attenuation measurements. A Raman Spectrometer was used to map the thickness of the carbon coating on quartz crucibles.

Status: published work at Journal of Crystal Growth 2019, **516**, 40-44

Spectroscopic signatures of many-body correlations in magic-angle twisted bilayer graphene

Yonglong Xie,¹ Biao Lian,² Berthold Jäck,¹ Xiaomeng Liu,¹ Cheng-Li Chiu,¹ Kenji Watanabe,³ Takashi Taniguchi,³ B. Andrei Bernevig,¹ & Ali Yazdani¹

¹Joseph Henry Laboratories and Department of Physics, Princeton University, Princeton, NJ, USA. ²Princeton Center for Theoretical Science, Princeton University, Princeton, NJ, USA. ³National Institute for Material Science, Tsukuba, Japan.



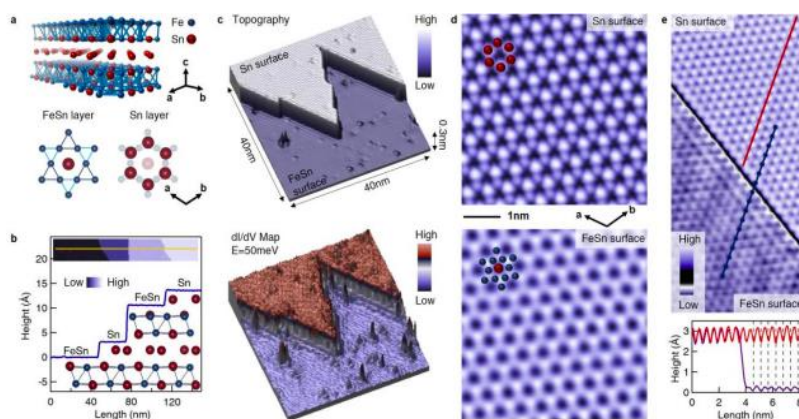
The discovery of superconducting and insulating states in magic-angle twisted bilayer graphene (MATBG) has ignited considerable interest in understanding its nature of electronic interactions. The transport properties of MATBG as a function of doping are similar to those of high-transition-temperature copper oxides and other unconventional superconductors. To our knowledge, there is no direct experimental evidence of strong many-body correlations in MATBG. Here we present high-resolution spectroscopic measurements that provide such evidence as a function of carrier density. MATBG displays unusual spectroscopic characteristics that can be attributed to electron–electron interactions over a wide range of doping levels. We show that our measurements cannot be explained with a mean-field approach for modelling electron–electron interactions in MATBG. The breakdown of a mean-field approach when applied to other correlated superconductors, such as copper oxides, has long inspired the study of the highly correlated Hubbard model. We show that a phenomenological extended-Hubbard- model cluster calculation, which is motivated by the nearly localized nature of the relevant electronic states of MATBG, produces spectroscopic features that are similar to those that we observed experimentally. Our findings demonstrate the critical role of many-body correlations in understanding the properties of MATBG.

Status: published work at Nature 2019, **572**, 101-105

Giant and anisotropic many-body spin-orbit tunability in a strongly correlated kagome magnet

Jia-Xin Yin¹, Songtian S. Zhang¹, Hang Li², Kun Jiang³, Guoqing Chang¹, Bingjing Zhang⁴, Biao Lian⁵, Cheng Xiang^{6,7}, Ilya Belopolski¹, Hao Zheng¹, Tyler A. Cochran¹, Su-Yang Xu¹, Guang Bian¹, Kai Liu⁴, Tay-Rong Chang⁸, Hsin Lin⁹, Zhong-Yi Lu⁴, Ziqiang Wang³, Shuang Jia^{6,7}, Wenhong Wang², M. Zahid Hasan^{1,10}

¹Laboratory for Topological Quantum Matter and Advanced Spectroscopy (B7), Department of Physics, Princeton University, Princeton, New Jersey 08544, USA. ²Beijing National Laboratory for Condensed Matter Physics, Institute of Physics, Chinese Academy of Sciences, Beijing 100190, China. ³Department of Physics, Boston College, Chestnut Hill, Massachusetts 02467, USA. ⁴Department of Physics and Beijing Key Laboratory of Opto-electronic Functional Materials & Micro-nano Devices, Renmin University of China, Beijing 100872, China. ⁵Princeton Center for Theoretical Science, Princeton University, Princeton, New Jersey 08544, USA. ⁶International Center for Quantum Materials and School of Physics, Peking University, Beijing 100871, China. ⁷CAS Center for Excellence in Topological Quantum Computation, University of Chinese Academy of Science, Beijing 100190, China. ⁸Department of Physics, National Cheng Kung University, Tainan 701, Taiwan. ⁹Institute of Physics, Academia Sinica, Taipei 11529, Taiwan. ¹⁰Lawrence Berkeley National Laboratory, Berkeley, California 94720, USA.



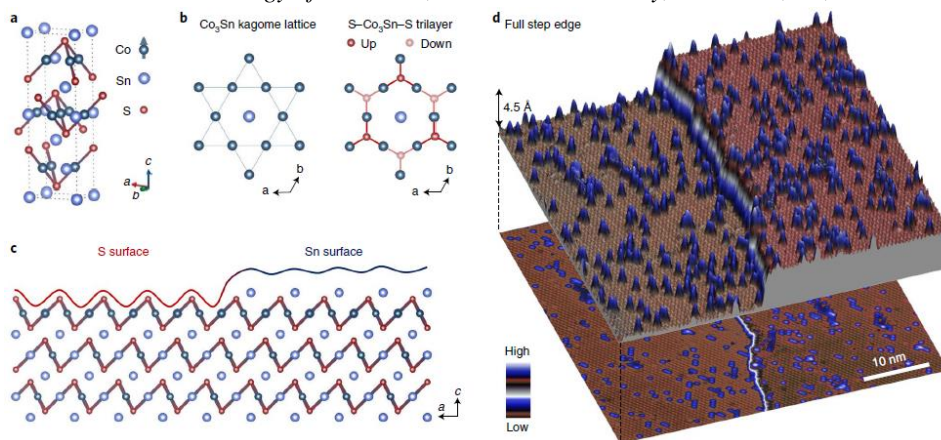
Kagome lattice electrons are useful for studying the physics of topological quantum electronic states due to their unusual geometry. In the presence of strong spin-orbit coupling, the structures of kagome lattices are entangled. We use a combination of vector-magnetic-field capability and scanning tunnelling microscopy to elucidate the spin-orbit nature of the kagome ferromagnet Fe₃Sn₂. We discover an electronic state from the kagome lattice couples strongly to the vector field with three-dimensional anisotropy. Probing the fermionic quasi-particle interference reveals consistent spontaneous nematicity and vector magnetization is capable of altering this state. Spin-driven giant electronic responses point to the realization of a correlated magnetic topological phase. The tunability of this kagome magnet provides new ways of controlling spin-orbit properties and explores phenomena in topological or quantum materials.

Status: published work at Nature 2018, **562**, 91-95

Negative flat band magnetism in a spin-orbit-coupled correlated kagome magnet

Jia-Xin Yin¹, Songtian S. Zhang¹, Guoqing Chang¹, Qi Wang², Stepan S. Tsirkin³, Zurab Guguchia^{1,4}, Biao Lian⁵, Huibin Zhou^{6,7}, Kun Jiang⁸, Ilya Belopolski¹, Nana Shumiya¹, Daniel Multer¹, Maksim Litskevich¹, Tyler A. Cochran¹, Hsin Lin⁹, Ziqiang Wang⁸, Titus Neupert³, Shuang Jia^{6,7}, Hechang Lei², and M. Zahid Hasan^{1, 10, 11}

¹Laboratory for Topological Quantum Matter and Advanced Spectroscopy (B7), Department of Physics, Princeton University, Princeton, NJ, USA. ²Department of Physics and Beijing Key Laboratory of Opto-electronic Functional Materials & Micro-nano Devices, Renmin University of China, Beijing, China. ³Department of Physics, University of Zurich, Zurich, Switzerland. ⁴Laboratory for Muon Spin Spectroscopy, Paul Scherrer Institute, Villigen PSI, Switzerland. ⁵Princeton Center for Theoretical Science, Princeton University, Princeton, NJ, USA. ⁶International Center for Quantum Materials and School of Physics, Peking University, Beijing, China. ⁷CAS Center for Excellence in Topological Quantum Computation, University of Chinese Academy of Sciences, Beijing, China. ⁸Department of Physics, Boston College, Chestnut Hill, MA, USA. ⁹Institute of Physics, Academia Sinica, Taipei, Taiwan. ¹⁰Materials Sciences Division, Lawrence Berkeley National Laboratory, Berkeley, CA, USA. ¹¹Princeton Institute for the Science and Technology of Materials, Princeton University, Princeton, NJ, USA



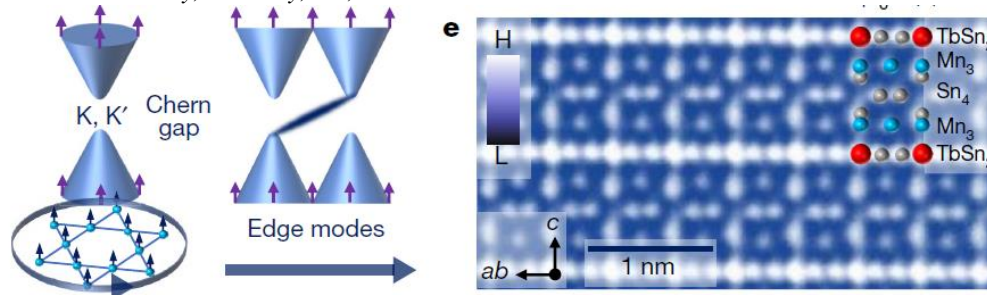
Electronic systems with flat bands are predicted to be a fertile ground for hosting emergent phenomena including unconventional magnetism and superconductivity, but materials that manifest this feature are rare. Here, we use scanning tunneling microscopy to elucidate the atomically resolved electronic states and their magnetic response in the kagome magnet $\text{Co}_3\text{Sn}_2\text{S}_2$. We observe a pronounced peak at the Fermi level, which we identify as arising from the kinetically frustrated kagome flat band. On increasing the magnetic field up to ± 8 T, this state exhibits an anomalous magnetization-polarized many-body Zeeman shift, dominated by an orbital moment that is opposite to the field direction. Such negative magnetism is induced by spin-orbit-coupling quantum phase effects tied to non-trivial flat band systems. We image the flat band peak, resolve the associated negative magnetism, showing that $\text{Co}_3\text{Sn}_2\text{S}_2$ is a rare example of a kagome magnet where the low-energy physics can be dominated by the spin-orbit coupled flat band.

Status: published work at Nature Physics 2019, **15**, 443

Quantum-limit Chern topological magnetism in TbMn₆Sn₆

J. X. Yin,^{1,15} W. Ma,^{2,15} T. A. Cochran,^{1,15} X. Xu,^{2,15} S. S. Zhang,¹ H. J. Tien,³ N. Shumiya,¹ G. Cheng,⁴ K. Jiang,⁵ B. Lian,⁶ Z. Song,⁷ G. Chang,¹ I. Belopolski,¹ D. Multer,¹ M. Litskevich,¹ Z. J. Cheng,¹ X. P. Yang,¹ B. Swidler,¹ H. Zhou,² H. Lin,⁸ T. Neupert,⁹ Z. Wang,⁵ N. Yao,⁴ T. R. Chang,^{3,10,11} S. Jia,^{2,12,13} and M. Z. Hasan,^{1,14}

¹Laboratory for Topological Quantum Matter and Advanced Spectroscopy, Department of Physics, Princeton University, Princeton, NJ, USA. ²International Center for Quantum Materials, School of Physics, Peking University, Beijing, China. ³Department of Physics, National Cheng Kung University, Tainan, Taiwan. ⁴Princeton Institute for Science and Technology of Materials, Princeton University, Princeton, NJ, USA. ⁵Department of Physics, Boston College, Chestnut Hill, MA, USA. ⁶Princeton Center for Theoretical Science, Princeton University, Princeton, NJ, USA. ⁷Department of Physics, Princeton University, Princeton, NJ, USA. ⁸Institute of Physics, Academia Sinica, Taipei, Taiwan. ⁹Department of Physics, University of Zurich, Zurich, Switzerland. ¹⁰Center for Quantum Frontiers of Research and Technology (QFort), Tainan, Taiwan. ¹¹Physics Division, National Center for Theoretical Sciences, Hsinchu, Taiwan. ¹²CAS Center for Excellence in Topological Quantum Computation, University of Chinese Academy of Sciences, Beijing, China. ¹³Beijing Academy of Quantum Information Sciences, Beijing, China. ¹⁴Lawrence Berkeley National Laboratory, Berkeley, CA, USA.

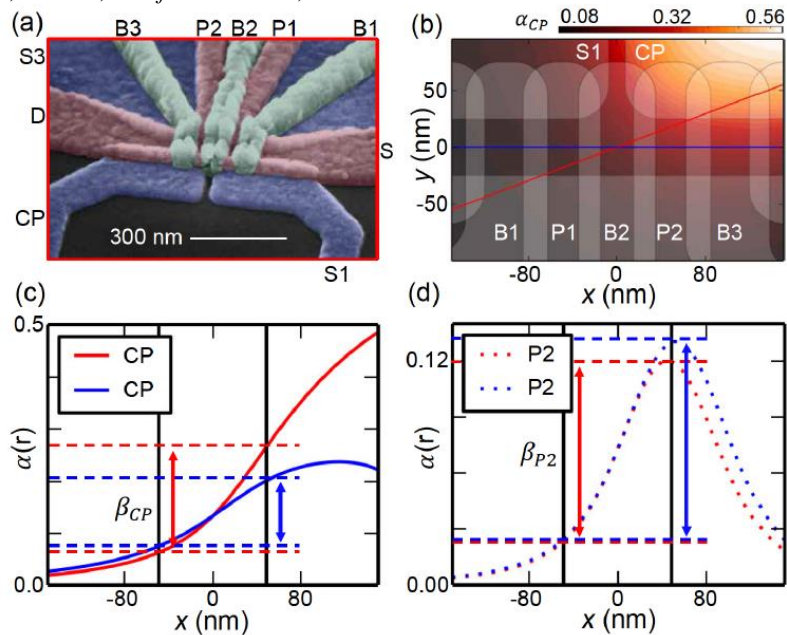


The quantum-level interplay between geometry, topology and correlation is at the forefront of fundamental physics. Kagome magnets are predicted to support intrinsic Chern quantum phases. However, quantum materials hosting ideal spin–orbit-coupled kagome lattices with strong out-of-plane magnetization are lacking. Here, using scanning tunnelling microscopy, we identify a new topological kagome magnet, TbMn₆Sn₆, that is close to satisfying these criteria. We visualize its effectively defect-free, purely manganese-based ferromagnetic kagome lattice with atomic resolution. Remarkably, its electronic state shows distinct Landau quantization on application of a magnetic field, and the quantized Landau fan structure features spin-polarized Dirac dispersion with a large Chern gap. We further demonstrate the bulk–boundary correspondence between the Chern gap and the topological edge state, as well as the Berry curvature field correspondence of Chern gapped Dirac fermions. Our results point to the realization of a quantum-limit Chern phase in TbMn₆Sn₆, and may enable the observation of topological quantum phenomena in the RMn₆Sn₆ (where R is a rare earth element) family. Our visualization of the magnetic bulk–boundary–Berry correspondence covering real space and momentum space demonstrates a proof-of-principle method for revealing topological magnets.

Status: published work in Nature 2020, **583**, 533-536

Split-Gate Cavity Coupler for Silicon Circuit Quantum Electrodynamics

F. Borjans,¹ X. Croot,¹ S. Putz,¹ X. Mi,¹ S. M. Quinn,² A. Pan,² J. Kerckho,² E. J. Pritchett,² C. A. Jackson,² L. F. Edge,² R. S. Ross,² T. D. Ladd,² M. G. Borselli,² M. F. Gyure,² and J. R. Petta¹
¹Department of Physics, Princeton University, Princeton, New Jersey 08544, USA; ²HRL Laboratories LLC, 3011 Malibu Canyon Road, Malibu, California 90265, USA



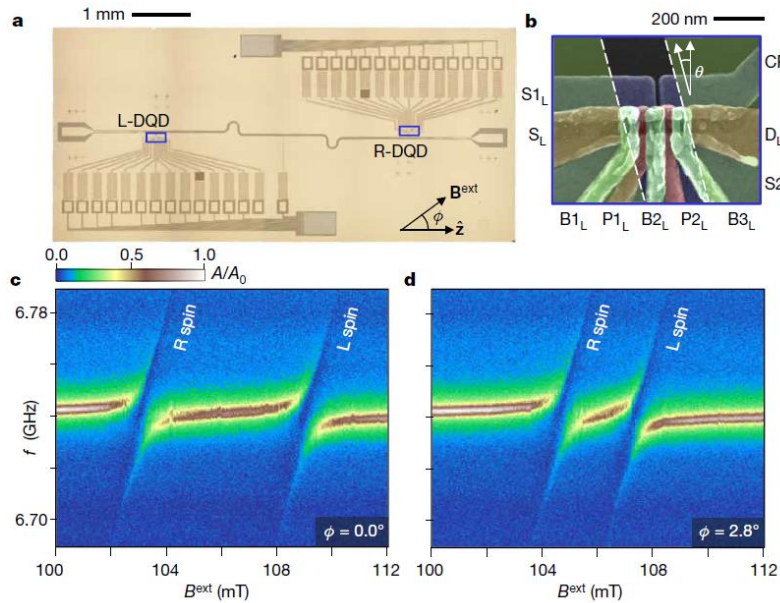
Coherent charge-photon and spin-photon coupling has recently been achieved in silicon double quantum dots (DQD). Here we demonstrate a versatile split-gate cavity-coupler that allows more than one DQD to be coupled to the same microwave cavity. Measurements of the cavity transmission as a function of level detuning yield a charge cavity coupling rate $g_c/2\pi = 58$ MHz, charge decoherence rate $\gamma_c/2\pi = 36$ MHz, and cavity decay rate $\kappa_c/2\pi = 1.2$ MHz. The charge cavity coupling rate is in good agreement with device simulations. Our coupling technique can be extended to enable simultaneous coupling of multiple DQDs to the same cavity mode, opening the door to long-range coupling of semiconductor qubits using microwave frequency photons.

Status: published work at Applied Physical Letters 2020, **116**, 234001

Resonant microwave-mediated interactions between distant electron spins

F. Borjans,¹ X. G. Croot,¹ X. Mi,^{1,2} M. J. Gullans,¹ and J. R. Petta¹

¹Department of Physics, Princeton University, Princeton, NJ, USA. ²Present address: Google Inc., Santa Barbara, CA, USA



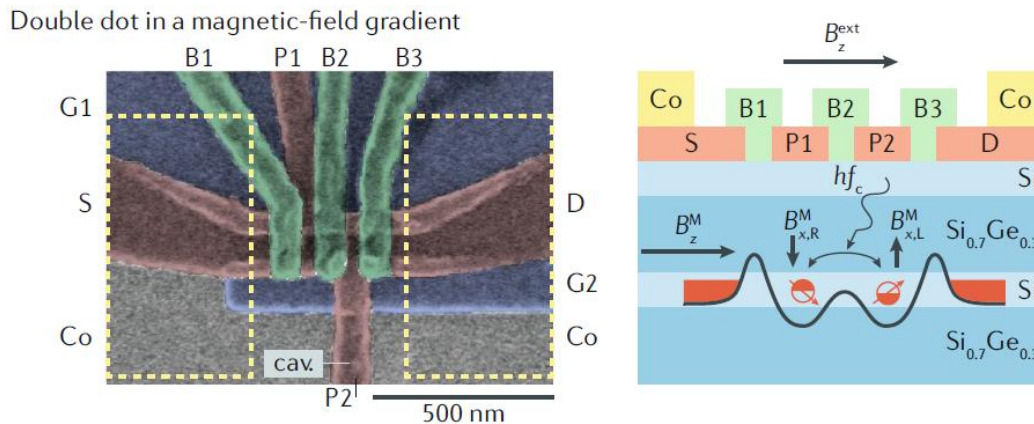
Nonlocal qubit interactions are a hallmark of advanced quantum information technologies. The ability to transfer quantum states and generate entanglement over distances much larger than qubit length scales greatly increases connectivity and is an important step towards maximal parallelism and the implementation of two-qubit gates on arbitrary pairs of qubits. Qubit-coupling schemes based on cavity quantum electrodynamics also offer the possibility of using high-quality-factor resonators as quantum memories. Extending qubit interactions beyond the nearest neighbour is particularly beneficial for spin-based quantum computing architectures, which are limited by short-range exchange interactions. Despite the rapidly maturing device technology for silicon spin qubits, experimental progress towards achieving long-range spin–spin coupling has so far been restricted to interactions between individual spins and microwave photons. Here we demonstrate resonant microwave-mediated coupling between two electron spins that are physically separated by more than four millimetres. An enhanced vacuum Rabi splitting is observed when both spins are tuned into resonance with the cavity, indicating a coherent interaction between the two spins and a cavity photon. Our results imply that microwave-frequency photons may be used to generate long-range two-qubit gates between spatially separated spins.

Status: published work at Nature 2020, **577**, 195-198

Superconductor–semiconductor hybrid-circuit quantum electrodynamics

Guido Burkard,¹ Michael J. Gullans,² Xiao Mi,^{2,3} and Jason R. Petta,²

¹Department of Physics, University of Konstanz, Konstanz, Germany; ²Department of Physics, Princeton University, Princeton, NJ, USA; ³Google Inc., Santa Barbara, CA, USA.

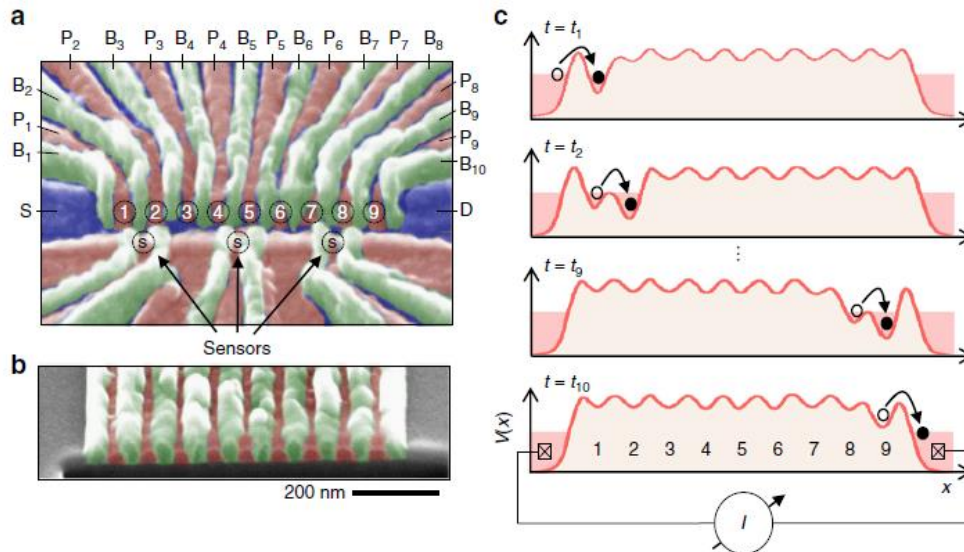


Light–matter interactions at the single-particle level have generally been explored in the context of atomic, molecular and optical physics. Recent advances motivated by quantum information science have made it possible to explore coherent interactions between photons trapped in superconducting cavities and superconducting qubits. In the context of quantum information, the study of coherent interactions between single charges and spins in semiconductors and photons trapped in superconducting cavities is very relevant, as the spin degree of freedom has a coherence time that can potentially exceed that of superconducting qubits, and cavity photons can serve to effectively overcome the limitation of short-range interaction inherent to spin qubits. Here, we review recent advances in hybrid ‘super–semi’ quantum systems, which coherently couple superconducting cavities to semiconductor quantum dots. We first present an overview of the physics governing the behaviour of superconducting cavities, semiconductor quantum dots and their modes of interaction. We then survey experimental progress in the field, focusing on recent demonstrations of cavity quantum electrodynamics in the strong-coupling regime with a single charge and a single spin. Finally, we broadly discuss promising avenues of future research, including the use of super–semi systems to investigate phenomena in condensed-matter physics.

Status: published work at Nature Reviews Physics 2020, **2**, 129-140

Shuttling a single charge across a one-dimensional array of silicon quantum dots

A.R. Mills, D.M. Zajac, M.J. Gullans, F.J. Schupp, T.M. Hazard & J.R. Petta
Department of Physics, Princeton University, Princeton, NJ 08544, USA



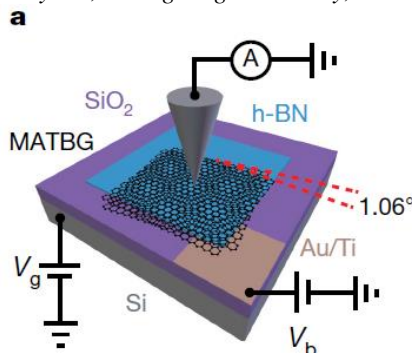
Significant advances have been made towards fault-tolerant operation of silicon spin qubits, with single qubit fidelities exceeding 99.9%, several demonstrations of two-qubit gates based on exchange coupling, and the achievement of coherent single spin-photon coupling. Coupling arbitrary pairs of spatially separated qubits in a quantum register poses a significant challenge as most qubit systems are constrained to two dimensions with nearest neighbor connectivity. For spins in silicon, new methods for quantum state transfer should be developed to achieve connectivity beyond nearest-neighbor exchange. Here we demonstrate shuttling of a single electron across a linear array of nine series-coupled silicon quantum dots in ~ 50 ns via a series of pairwise interdot charge transfers. By constructing more complex pulse sequences we perform parallel shuttling of two and three electrons at a time through the array. These experiments demonstrate a scalable approach to physically transporting single electrons across large silicon quantum dot arrays.

Status: published work at Nature Communications 2019, **10**, 1063

Cascade of electronic transitions in magic-angle twisted bilayer graphene

Dillon Wong,^{1,2} Kevin P. Nuckolls,^{1,2} Myungchul Oh,^{1,2} Biao Lian,³ Yonglong Xie,^{1,2,5,6} Sangjun Jeon,^{1,2,7} Kenji Watanabe,⁴ Takashi Taniguchi,⁴ B. Andrei Bernevig,² and Ali Yazdani^{1,2}

¹Joseph Henry Laboratories, Jadwin Hall, Princeton University, Princeton, NJ, USA. ²Department of Physics, Princeton University, Princeton, NJ, USA. ³Princeton Center for Theoretical Science, Princeton University, Princeton, NJ, USA. ⁴National Institute for Material Science, Tsukuba, Japan. ⁵Department of Physics, Harvard University, Cambridge, MA, USA. ⁶Department of Physics, Massachusetts Institute of Technology, Cambridge, MA, USA. ⁷Present address: Department of Physics, Chung-Ang University, Seoul, Republic of Korea.



Magic-angle twisted bilayer graphene exhibits a variety of electronic states, including correlated insulators, superconductors and topological phases. Understanding the microscopic mechanisms responsible for these phases requires determination of the interplay between electron–electron interactions and quantum degeneracy. Signatures of strong electron–electron correlations have been observed at partial fillings of the flat electronic bands in recent spectroscopic measurements, and transport experiments have shown changes in the Landau level degeneracy at fillings corresponding to an integer number of electrons per moiré unit cell. However, the interplay between interaction effects and the degeneracy of the system is currently unclear. Here we report a cascade of transitions in the spectroscopic properties of magic-angle twisted bilayer graphene as a function of electron filling, determined using high-resolution scanning tunneling microscopy. We find distinct changes in the chemical potential and a rearrangement of the low-energy excitations at each integer filling of the moiré flat bands. These spectroscopic features are a direct consequence of Coulomb interactions, which split the degenerate flat bands into Hubbard subbands. We find these interactions, the strength of which we can extract experimentally, to be surprisingly sensitive to the presence of a perpendicular magnetic field, which strongly modifies the spectroscopic transitions. The cascade of transitions that we report here characterizes the correlated high-temperature parent phase, from which various insulating and superconducting ground-state phases emerge at low temperatures in magic-angle twisted bilayer graphene.

Status: published work at Nature 2020, **582**, 198